Variations by degrees: Western European paleoenvironmental fluctuations across MIS 13–11

Journal of Human Evolution 169 (2022) 103213

Contents lists available at ScienceDirect

Journal of Human Evolution

journal homepage: www.elsevier.com/locate/jhevol

Variations by degrees: Western European paleoenvironmental fluctuations across MIS 13–11

Robert Hosfield

Department of Archaeology, University of Reading, Whiteknights Campus, Reading, RG6 6AB, United Kingdom

ARTICLE INFO

Article history:
Received 30 March 2021
Accepted 28 April 2022
Available online xxx

Keywords:
Lower Paleolithic
Middle Pleistocene
Oscillayers
MIS 11c
MIS 11a

ABSTRACT

Marine Isotope Stages (MIS) 13–11 saw a major transformation in the hominin occupation of Europe, with an expansion in the scale and geographical distribution of sites and artifact assemblages. That expansion is explored here in the context of paleoenvironmental variability, focusing on geographical and chronological trends in climatic and habitat conditions at and between key Lower Paleolithic sites in Western Europe. Climatic conditions at British sites are compared across MIS 13–11, and used to test predicted values from the Oscillayers data set. Conditions at hominin and nonhominin sites are compared to explore possible limitations in hominin tolerances during MIS 13–11. Trends in conditions are explored with reference to long-term global patterns, short-term substage events, and seasonal variations. The apparent increase in the scale of hominin activity in north-western Europe during MIS 13 is surprising in light of the relatively harsh conditions of late MIS 13, and is likely to reflect significant physiological and/or behavioral adaptations, a mild south-north temperature gradient in western Europe during MIS 13, and the relatively mild, sustained conditions spanning MIS 15–13. The expanded occupation of north-western Europe during MIS 11 probably reflects the extended mild conditions of MIS 11c, since marked seasonal temperature differences and substantial behavioral changes between hominin sites in MIS 13 and 11 are not clearly evident. Site-specific conditions in south-western Europe during MIS 11 suggest milder winters, warmer summers, and reduced seasonal variability compared to north-western Europe. Some or all of these conditions may have supported larger, core populations, as may the relatively mild conditions associated with south-western European sites during MIS 12. Finally, comparisons between north-western and north-central European sites indicate relatively small differences in seasonal temperatures, suggesting that climate may only be a partial factor behind the smaller-scale occupations of north-central Europe during MIS 13–11.

1. Introduction

Since the turn of the century, there has been an increasing consensus that Neanderthal and Middle Paleolithic origins are deeply rooted in the European Middle Pleistocene. This is evident in terms of skeletal morphology (e.g., Rightmire, 1997; Martinón-Torres et al., 2012; Stringer, 2012; Arsuaga et al., 2014), genetic signatures (e.g., Meyer et al., 2014), and material culture (e.g., White and Ashton, 2003; Moncel et al., 2011, 2020; de Lombera-Hermida et al., 2020). Yet a further characteristic of the 'Neanderthalization' process is evidence of biocultural adaptation to an increasingly wide range of climates, habitats, and landscapes, including cold environments (e.g., Ashton and Lewis, 2002; Ocobock et al., 2021). It is true that the seasonal timings of specific Neanderthal occupations are often uncertain, and that not all Neanderthals lived in cold environments (e.g., Davies and Gollop, 2003; Hardy, 2010). Nonetheless, site-specific evidence (e.g., Lynford: Boismier et al., 2012; Pech de l'Azé IV [Layers 4–5] and Roc de Marsal [Layers 2–4]: Dibble et al., 2017) and regional occupations (e.g., Britain in Marine Isotope Stage [MIS] 3: White, 2006; White and Pettitt, 2011) indicate the climatic resilience of selected Late Pleistocene Neanderthals. But when did these expansions in climatic adaptations start to appear?

With some notable exceptions (e.g., Happisburgh 3; Parfitt et al., 2010), Early and early Middle Pleistocene hominin occupations of Europe were predominantly concentrated below 45°N, in Gamble's (1986, fig. 3.1) 'Mediterranean' province (Hosfield and Cole, 2018). In both north-western and north-central Europe, this began to change significantly from MIS 15 onwards (Fig. 1), with the interval

E-mail address: r.hosfield@reading.ac.uk.

https://doi.org/10.1016/j.jhevol.2022.103213

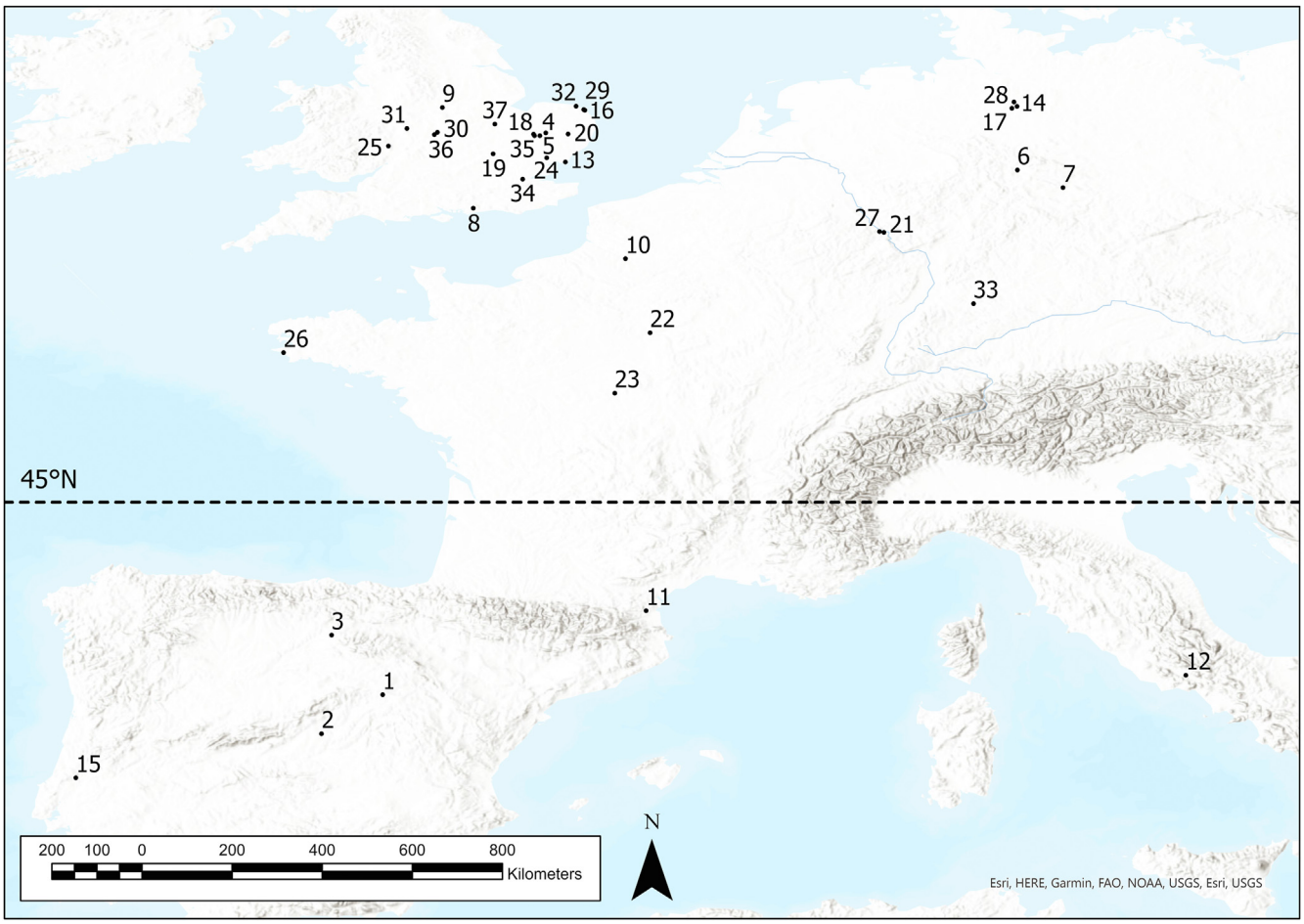

Figure 1. Key western European Lower Paleolithic and Middle Pleistocene sites discussed in the text. 1: Ambrona and Torralba; 2: Áridos; 3: Atapuerca (Trinchera Dolina and Sima de los Huesos); 4: Barnham; 5: Beeches Pit; 6: Bilshausen; 7: Bilzingsleben; 8: Boxgrove; 9: Brooksby; 10: Cagny-la-Garenne; 11: Caune de l'Arago; 12: Ceprano; 13: Clacton; 14: Dethlingen; 15: Gruta da Aroeira; 16: Happisburgh 1; 17: Hetendorf; 18: High Lodge; 19: Hitchin; 20: Hoxne; 21: Kärlich; 22: La Celle; 23: La Noira; 24: Marks Tey; 25: Mathon; 26: Menez-Dregan; 27: Miesenheim; 28: Munster-Breloh; 29: Ostend; 30: Pools Farm Pit; 31: Quinton; 32: Sidestrand; 33: Steinheim; 34: Swanscombe; 35: Warren Hill; 36: Waverley Wood; 37: Woodston. Figure created in ArcGIS Pro v. 2.6.1 (map projection: World Geodetic System [WGS] 1984).

between ca. 600 and 400 ka (MIS 15–11) representing a key phase in European hominin evolution (Ashton and Davis, 2021). This is reflected initially in flagship sites (e.g., Boxgrove, Happisburgh 1, High Lodge, La Noira [Upper Layer], Miesenheim I, Warren Hill; Wymer et al., 1991; Ashton et al., 1992; Roberts and Parfitt, 1999; Turner, 1999; Iovita et al., 2017; Lewis et al., 2019), and during and after MIS 12 in both flagship sites (e.g., Barnham, Bilzingsleben, Cagny-la-Garenne I and II, Clacton, Hoxne, La Celle, Swanscombe; Singer et al., 1973, 1993; Conway et al., 1996; Ashton et al., 1998; Mania and Mania, 2005; Limondin-Lozouet et al., 2010; Moncel et al., 2015; Ashton, 2016; Lamotte and Tuffreau, 2016) and the artifact accumulations of major rivers (e.g., the Thames, Solent, and Seine; Tuffreau and Antoine, 1995; Wymer, 1999; Santonja and Villa, 2006). An expanding rather than relocating hominin geographical range is indicated by the continuing richness of the site and artifact record in southern Europe at this time, both in flagship sites (e.g., Ambrona, Caune de l'Arago, Aroeira, Áridos, Ceprano, Trinchera Dolina TD-10, Torralba; Howell and Freeman, 1982; Villa, 1990; de Lumley et al., 2004; Manzi et al., 2010; Daura et al., 2017; Saladié et al., 2018) and across river landscapes (e.g., the Manzanares, Jarama, and Tagus valleys; Rubio-Jara et al., 2016; Rubio-Jara and Panera, 2019).

These transformations in the scales of the European site and artifact record have been linked to hominin behavioral changes. For example, during MIS 13–11 (533–374 ka), there is a widespread appearance of handaxe technology across western Europe (e.g., Moncel et al., 2015; Ashton and Davis, 2021), although core and flake assemblages also persist (e.g., White, 2000; McNabb, 2007, 2020). Direct subsistence evidence is more limited, but the available data suggest hunting abilities throughout this period (e.g., Parfitt and Roberts, 1999; Rodriguez-Hidalgo et al., 2017). Handaxes may also be a proxy for a wider suite of behavioral changes (e.g., Ashton, 2015; Hosfield and Cole, 2018). These may have included adaptations to cold climates (e.g., sleeping under fur coverings; Rodríguez et al., 2021). However, the changing site and artifact record across MIS 13–11 may also reflect changing paleoenvironmental conditions (see also Blain et al., 2021). Here I suggest two, mutually exclusive, testable hypotheses to explore the nature of the potential relationships between paleoclimatic conditions and the expanding hominin occupation record across MIS 13–11:

Hypothesis 1. The range of paleoclimatic conditions associated with hominin occupations expanded across MIS 13–11. This would suggest that hominins expanded into and tolerated a wider range of

climatic niches over time through novel biocultural adaptations, leading to the demonstrated increase in the scale of the archaeological record (as discussed above; e.g., Hosfield and Cole, 2018).

Hypothesis 2. The range of paleoclimatic conditions associated with hominin occupations remained stable or narrowed across MIS 13–11. This would suggest that hominins continued to occupy the same range of climatic niches over time, using pre-existing biocultural adaptations. The demonstrated expansion in the hominin record, especially from MIS 11 onwards (e.g., Hosfield and Cole, 2018), would then suggest that these conditions became available over a wider geographical extent and/or a longer chronological duration.

The paleoclimate of MIS 13–11 is well documented in 'global' isotope records such as SPECMAP and EPICA Dome C (Imbrie et al., 1984; Jouzel et al., 2007; although isotopic oscillations in these records have been linked to, for example, changes in the global volume of glacial ice, different global data sets are also variably impacted by regionally specific factors). The interval is marked by differences in the timing and duration of peak warmth in MIS 13 and 11 (e.g., Candy et al., 2010) and it incorporates the Mid-Brunhes Event (MBE), which is associated with an increase in the amplitude of glacial–interglacial cycles. These trends are broadly consistent in both global and regional data sets, although there are some discrepancies between them. A key question concerns the relevance of such large-scale records for understanding hominin occupations and their lived experiences. Although ice-core and benthic records are of sufficient resolution to detect centennial-scale fluctuations (e.g., Pol et al., 2011), dating of Lower Paleolithic sites operates at much lower resolution, making integration of the records difficult. Moreover, conditions at individual sites will reflect microclimates and habitats as well as global and regional trends. Assessing hominin environmental tolerances and/or preferences is therefore ultimately dependent on site-specific reconstructions and patterns.

To explore the changing European Lower Paleolithic site and artifact record across MIS 13–11 from a climatic perspective, I addressed five questions in this paper. I used the answers to these questions to evaluate the two hypotheses proposed earlier:

Question 1. Are there significant differences between the temperature estimates at occupied British sites in MIS 13 and in MIS 11?

Question 2. Are there significant differences between the temperature estimates at occupied and non-occupied British sites in MIS 13?

Question 3. Are there significant differences between the temperature estimates at occupied and non-occupied British sites in MIS 11?

Question 4. Are there significant differences between western European climate transects in MIS 13 compared to MIS 11?

Question 5. Are there greater proportions of north-western European landscapes with tolerated temperatures (as defined by hominin-occupied sites) in MIS 11 compared to MIS 13?

The issues of both changing climatic tolerances and 'Neanderthalization' cannot be explored without some consideration of the identity of European hominins during MIS 13–11. Unfortunately, this continues to be an area of considerable debate, with diverse taxonomies (e.g., Thoma, 1972; Stringer and Hublin, 1999; Prossinger et al., 2003; Bruner and Manzi, 2005; Mounier et al., 2009; de Lumley, 2015; Roksandic et al., 2018, their table 1), considerable morphological variability (e.g., Rightmire, 1998, 2008; Dennell et al., 2011; Martinón-Torres et al., 2012; Stringer, 2012), and difficulties arising from the limited number of large samples (Sima de los Huesos and Caune de l'Arago) and the original definition of *Homo heidelbergensis* on the Mauer mandible. In particular, it is possible that there were broadly contemporary lineages of *H. heidelbergensis* and early Neanderthals in the European later Middle Pleistocene, based on dental variation between the Sima de los Huesos and Caune de l'Arago samples (Martinón-Torres et al., 2012). For simplicity, however, this paper follows the approach of Dennell et al. (2011:1513): "The term '*H. heidelbergensis*' is thus a convenient abbreviation for a longer statement along the lines that whilst most European Middle Pleistocene hominin specimens share some features with *H. erectus*, *H. neanderthalensis* and even some specimens regarded as 'archaic *H. sapiens*' — leaving aside for the moment how each is or can be defined — they seem nonetheless to be sufficiently distinct to be placed in a separate category that was ancestral in Europe to Neanderthals."

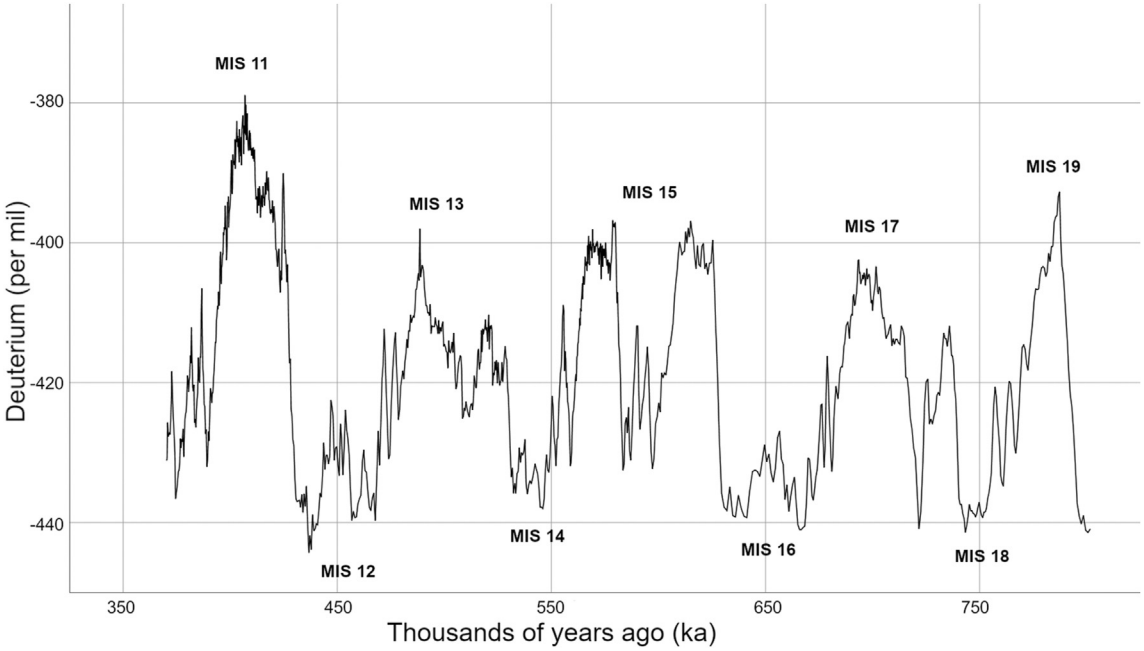

Figure 2. Global isotopic data sets for MIS 19–11 (ice core data from Jouzel et al., 2007). The Y axis plots deuterium (^{2}H isotope) values and is a temperature proxy, with higher values indicating higher temperatures).

1.1. Global and regional climates during MIS 13–11

Global data sets such as the SPECMAP, LR04, and EPICA Dome C records (e.g., Imbrie et al., 1984; Bassinot et al., 1994; Lisiecki and Raymo, 2005; Jouzel et al., 2007) provide the general paleoclimatic context for the changes in the western European Lower Paleolithic record around 500 ka (see also Ashton, 2015; Moncel et al., 2015; Hosfield and Cole, 2018): a general trend toward longer climate cycles of increased magnitude over the course of the last one million years (EPICA-Community et al., 2004; Lisiecki and Raymo, 2005); a transition from cool interglacials and moderate glacials to warm interglacials and severe glacials, marked by the MBE (see Candy and Alonso-Garcia, 2018, their fig. 1), with considerably milder peak warm stage conditions in MIS 11 compared to earlier warm stages, and markedly cooler peak cold stage conditions in MIS 12 compared to earlier cold stages (Fig. 2); the contrasting timings and degree of stability of the peak interglacial conditions in MIS 13 (late peak) and MIS 11 (early peak); milder conditions associated with MIS 11c relative to MIS 13; similarities in the late stage interstadials of MIS 13 and 11 (Fig. 3a); and high-resolution variability (Fig. 3b).

Of particular note in the MIS 13–11 interval are the δD (deuterium) levels in MIS 13, barely exceeding −403‰ (Fig. 3b), leading Spahni et al. (2005) to describe the stage as an 'intermediate warm

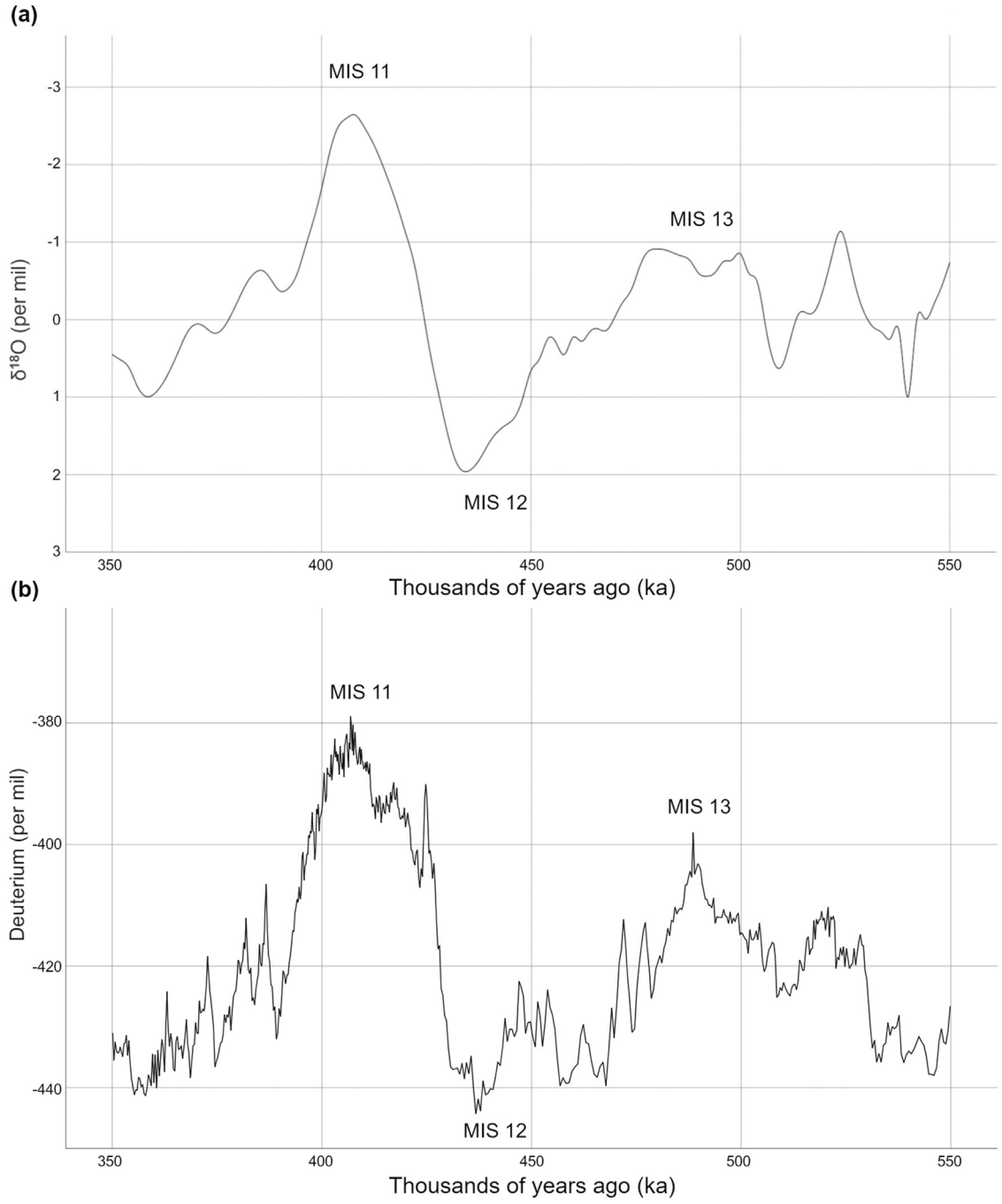

Figure 3. Global isotopic data sets for MIS 13–11. a) Lower resolution (stable oxygen isotope [deep-sea core] data from Bassinot et al., 1994). The Y axis plots ^{18}O isotope values and is a temperature proxy, with lower values indicating higher temperatures. b) Higher resolution (ice core data from Jouzel et al., 2007). The Y axis plots deuterium (^{2}H isotope) values and is a temperature proxy, with higher values indicating higher temperatures.

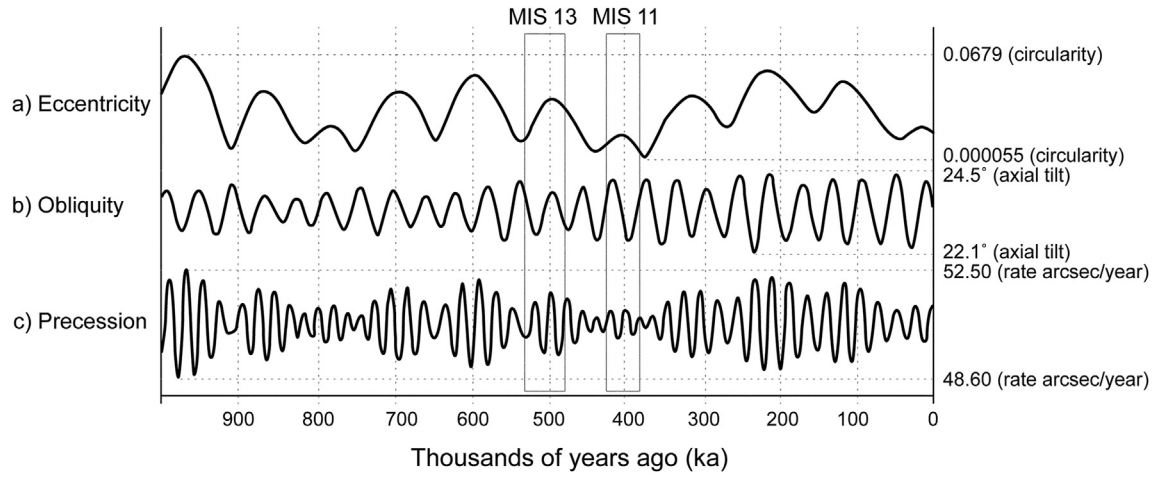

Figure 4. Contrasting patterns in Croll–Milankovitch cycles for MIS 13 and MIS 11 (modified from Wikipedia Commons [© Pablo Carlos Budassi and Creative Commons [CC BY-SA 4.0; https://creativecommons.org/licenses/by-sa/4.0/deed.en]). Note the higher values for eccentricity and precession in late MIS 13 compared to MIS 11 (axial precession has a greater impact on seasonal extremes during periods of high eccentricity), with higher values for obliquity occurring in early MIS 11 (seasonality becomes stronger during phases of greater obliquity).

period' (comparable, although more sustained, conditions also existed in MIS 15; Fig. 2). The other marked contrast between MIS 13 and 11 concerns the timing and duration of the periods of peak warmth. In MIS 13, this occurs relatively briefly and late in the stage, whereas the long peak of MIS 11c, lasting ca. 30 kyr, occurs in the first half of the warm stage (Candy et al., 2014). This sustained warmth is also evident in site-specific isotope records, with evidence from Marks Tey (Tye et al., 2016) and Hitchin (Sherriff et al., 2021) suggesting long-term thermal stability in southern Britain for much of MIS 11c (Ho I–III). Lag times between warming trends and Middle Pleistocene hominin range expansions are currently uncertain, but the timing of peak warmth periods relative to the start and end of a warm stage would only have significant implications for range expansion in the north-western limits of Lower Paleolithic Europe during MIS 11, reflecting the complexities of sea-level fluctuations after the breaching of the Weald–Artois anticline in MIS 12 (Gupta et al., 2017). However, the longer peak of MIS 11c may well have supported sustained occupations by hominins and other members of the biological communities, in areas of western Europe that were not permanently occupied (Candy et al., 2014). Yet these peak conditions also suffered significant and abrupt disruptions at regional scales. The MIS 11 Non-Arboreal Pollen (NAP)/Older Holsteinian Oscillation (OHO) event may have lasted for 250–300 years, based on varve data (laminated deposits, reflecting annual processes such as finer and coarser sediment accumulation on lake beds; e.g., Whittow, 2000), with a possible 2–3 °C temperature decrease and more open conditions (Candy et al., 2014). Such intervals may have disrupted or ended local occupations, potentially resulting in technological and/or typological differences in the artifact record on either side of the occupation breaks (e.g., Ashton et al., 2016; Davis and Ashton, 2019). Site-specific data also indicate changing hydrological conditions at regional scales during MIS 11c. Sedimentology, $\delta^{13}C$, trace element, and molluscan evidence from the Hitchin tufa suggest increasing rainfall during Ho III (associated with tufa formation) and wetter conditions than those in southern Britain today, followed by a subsequent reduction (and a break in tufa formation; Sherriff et al., 2021). Sherriff et al. (2021) suggest that the rainfall patterns may have been regional, based on rises and falls in Hoxnian lake levels (e.g., Gibbard et al., 1977), around the Ho II–III and IIIb–IV transitions, respectively.

Marine Isotope Stage 11 is also characterized by late substage variability, with a stadial (MIS 11b?) followed by a late interstadial (MIS 11a?). If the correlation of the British site of Quinton (Faunal Unit 2) to MIS 11b is correct, the temperature estimates from that site highlight the challenges for hominins in the northern portions of western Europe at this time, as they are broadly comparable with the data for the early MIS 12 Ostend Arctic Bed in East Anglia. The δD levels in later MIS 11 rarely exceed −410‰ and are frequently −420‰ or lower (Fig. 3b). This is especially notable if the associations of the occupations at the British sites of Hoxne and Beeches Pit (Bed 7) to MIS 11a and 11b, respectively, are correct

Table 1
British MIS 13 and MIS 11 site samples for questions 1–3 (as discussed in the text).

Britain	Question 1	Question 2	Question 3
Sample 1	MIS 13 hominin sites	MIS 13 hominin sites	MIS 11 hominin sites
Sites	Boxgrove (Unit 4c and Freshwater Silt Bed)	Boxgrove (Unit 4c and Freshwater Silt Bed)	Barnham (Unit 5c)
	Brooksby (Redland's Brooksby Channel)	Brooksby (Redland's Brooksby Channel)	Beeches Pit (Bed 7)
	Happisburgh 1 (Organic Mud)	Happisburgh 1 (Organic Mud)	Swanscombe (Lower Loam)
	High Lodge (Bed C1)	High Lodge (Bed C1)	Swanscombe (Lower Middle Gravel)
	Waverley Wood (Channel 2, Organic Mud)	Waverley Wood (Channel 2, Organic Mud)	
Sample 2	MIS 11 hominin sites	MIS 13 nonhominin sites	MIS 11 nonhominin sites
Sites	Barnham (Unit 5c)	Mathon (Brays Bed)	Hoxne (Bed D)
	Beeches Pit (Bed 7)	Pools Farm Pit (Brandon Lower Organic Sands and Silts)	Quinton (Faunal Unit 1)
	Swanscombe (Lower Loam)	Sidestrand[a] (*Unio* bed)	Quinton (Faunal Unit 2)
	Swanscombe (Lower Middle Gravel)		Quinton (Faunal Unit 3)
			Woodston

[a] In light of the uncertainty of the provenance of the handaxe reported from the Sidestrand till (Preece et al., 2009) this site is classified here as lacking hominin evidence.

Table 2
Mean air temperature of the coldest month values (T_{min}), mean air temperature of the warmest month values (T_{max}), differences between T_{min} and T_{max} values (T_{range}), ages, and provisional chronological correlations with the Oscillayers 10 kyr-stepped outputs (Gamisch, 2019) for selected Middle Pleistocene sites (hominin—artifacts and/or fossils—and nonhiminin).

Sites	T_{min} (°C)	T_{max} (°C)	T_{range} (°C)[a]	Method (data)[b]	Age[c]	Oscillayers output[c]	Source[d]
MIS 13							
Bilshausen[e]	−7	+15	22.0	PIT-PDF (pollen)	Early MIS 13	530 ka	Szymanek and Julien (2018)
Bilshausen[e]	(−3) – (−2)	>+17	19.5	PIT-PDF (pollen)	Peak MIS 13	490 ka	Szymanek and Julien (2018)
Bilshausen[e]	−8	+14	22.0	PIT-PDF (pollen)	Late MIS 13	480 ka	Szymanek and Julien (2018)
Boxgrove (Unit 4c and Freshwater Silt Bed ≈ Units 4b and 4c)[f]	(−4) – (+4)	(+15) – (+20)	17.5	MCR (herpetofauna) and MOTR (ostracoda)	MIS 13 (temperate)	490 ka	Holmes et al. (2010)
Brooksby (Redland's Brooksby Channel)[f]	(−10) – (+2)	(+15) – (+16)	19.5	MCR (coleoptera)	Late MIS 13	480 ka[g]	Coope (2006)
Happisburgh 1 (Organic Mud)[f]	(−11) – (−3)	(+12) – (+15)	20.5	MCR (coleoptera)	Late MIS 13	480 ka[g]	Coope (2006)
High Lodge (Bed C1)[f]	(−4) – (+1)	(+15) – (+16)	17.0	MCR (coleoptera)	Late MIS 13	480 ka[g]	Coope (2006)
Mathon (Brays Bed)[e]	(−1.5) – (+1)	(+15) – (+17)	16.3	MCR (coleoptera)	Late MIS 13	480 ka[g]	Coope et al. (2002)
Pools Farm Pit (Brandon Lower Organic Sands and Silts)[e]	(−5) – (+1)	(+15) – (+16)	17.5	MCR (coleoptera)	Late MIS 13	480 ka[g]	Maddy et al. (1994)
Sidestrand (*Unio* Bed)[e]	(−9) – (+9)	(+16) – (+24)	20.0	MCR (coleoptera)	MIS 13 (temperate)	490 ka	Preece et al. (2009)
Waverley Wood (Channel 2, Organic Mud)[f]	NA	(+10) – (+15)	NA	MCR (coleoptera)	Late MIS 13	480 ka[g]	Coope (2006)
MIS 12							
Caune de l'Arago (G1 and G2)[f]	−1.8	+17.1	18.9	BM (rodentia)	MIS 12	NA[h]	López-García et al. (2021)
Caune de l'Arago (G3 and G4)[f]	−1.5	+18.5	20.0	BM (rodentia)	MIS 12	NA[h]	López-García et al. (2021)
Ostend (Arctic Bed; MCR data)[e]	(−36) – (−10)	(+9) – (+11)	33.0	MCR (coleoptera)	Early MIS 12	470 ka	Candy et al. (2015)
Ostend (Arctic Bed; MOTR data)[e]	(−21) – (−20)	(+10) – (+13)	32.0	MOTR (ostracoda)	Early MIS 12	470 ka	Candy et al. (2015)
Sima de los Huesos (LU 6)[f]	+2.3	+19.3	17.0	BM (rodentia)	MIS 12	450 ka	López-García et al. (2021)
Trinchera Dolina (TD-10.4, Level T21)[f]	+3.8	+20.3	16.5	MER (herpetofauna)	MIS 12−11	NA[i]	Blain et al. (2021)
MIS 11							
Ambrona (AS4/3)[f]	+3.2	+21.3	18.1	MER (herpetofauna)	MIS 11a	370 ka	Blain et al. (2021)
Áridos 1[f]	+8.8	+24.9	16.1	MER (herpetofauna)	MIS 11b	380 ka	Blain et al. (2021)
Barnham (Unit 5c, HoII)[f]	NA	(+17) – (+18)	NA	NS (herpetofauna)	MIS 11c	410 ka	Holman (1998)
Beeches Pit (Bed 7)[f]	(−7) – (−1)	(+15) – (+21)	22.0	MOTR (ostracoda)	MIS 11b	380 ka	Benardout (2015)
Bilzingsleben II[f]	(−0.5) – (+1)	(+19) – (+22)	20.3	NS (mollusca and paleobotany)	MIS 11	NA[j]	Mania and Mai (2001) in Szymanek and Julien (2018)
Bilzingsleben II[f]	(−7) – (+4)	(+16) – (+20)	19.5	NS (ostracoda)	MIS 11	NA[j]	Müller and Pasda (2011)
Dethlingen, Hetendorf and Munster-Breloh[e]	−14	+16	30.0	PIT-PDF (pollen)	Early MIS 11	420 ka	Szymanek and Julien (2018)
Dethlingen, Hetendorf and Munster-Breloh[e]	(−2) – (+2)	(+20) – (+21)	20.5	PIT-PDF (pollen)	Peak MIS 11	410 ka	Szymanek and Julien (2018)
Dethlingen, Hetendorf and Munster-Breloh[e]	−10	+17	27.0	PIT-PDF (pollen)	Late MIS 11	370 ka	Szymanek and Julien (2018)
Gruta da Aroeira[f]	+7.1	+22.1	15.0	BM (rodentia)	MIS 11	NA[k]	López-García et al. (2021)
Hoxne (Bed D, HoIIIa)[e]	(−10) – (+6)	(+15) – (+19)	19.0	NS (coleoptera)	MIS 11c	410 ka	Coope (1993)
Quinton (Faunal Unit 1)[e]	(−10) – (+8)	(+15) – (+22)	19.5	MCR (coleoptera)	MIS 11c	410 ka	Coope and Kenward (2007)
Quinton (Faunal Unit 2)[e,l]	(−27) – (−10)	(+9) – (+11)	28.5	MCR (coleoptera)	MIS 11b	380 ka	Coope and Kenward (2007)
Quinton (Faunal Unit 3)[e,l]	(−12) – (+4)	(+15) – (+19)	21.0	MCR (coleoptera)	MIS 11a	370 ka	Coope and Kenward (2007)
Swanscombe (Lower Loam)[f]	(−3) – (+4)	(+15) – (+19)	16.5	MOTR (ostracoda)	MIS 11c	420 ka	White et al. (2013)
Swanscombe (Lower Middle Gravel)[f]	(−7) – (+3)	(+15) – (+21)	20.0	MOTR (ostracoda)	MIS 11c	410 ka	White et al. (2013)

Table 2 (*continued*)

Sites	T_{min} (°C)	T_{max} (°C)	T_{range} (°C)[a]	Method (data)[b]	Age[c]	Oscillayers output[c]	Source[d]
Trinchera Dolina (TD-10.3, Level T17)[f]	+5.7	+20.0	14.3	MER (herpetofauna)	MIS 11c	NA[i]	Blain et al. (2021)
Woodston[e]	(−3) – (0)	(+16) – (+19)	19.0	MOTR (ostracoda)	MIS 11c	410 ka	Horne (2007)

[a] T_{range} based on midpoint T_{min} and T_{max} values (e.g., 0 °C and +17.5 °C for Boxgrove).
[b] BM = bioclimatic model (López-García et al., 2021); MCR = mutual climatic range (Atkinson et al., 1987); MER = mutual ecogeographic range (Blain et al., 2016); MOTR = mutual ostracod temperature range (Horne, 2007); NS = not specified; PIT-PDF = probabilistic indicator taxon approach, using a probability density function (Kühl and Gobet, 2010).
[c] Ages and correlations with Oscillayers outputs based on sources in table, Ashton et al. (2016), and Candy et al. (2014).
[d] Sources of T_{min} and T_{max} data.
[e] Nonhominin sites.
[f] Hominin sites.
[g] Coope (2006) has suggested that Happisburgh 1, Mathon, Pools Farm Pit, Waverley Wood, Brooksby, and High Lodge may be contemporary, because of specific beetle species (e.g., *Micropeplus hoogendorni*) being restricted in Britain to the first four of those sites, and stratigraphical similarities between the last five of those sites within the Bytham River valley (see also Preece et al., 2009).
[h] Correlation with Oscillayers was not attempted because of the general assignment of level G to MIS 12 by Falguères et al. (2015).
[i] Correlation with Oscillayers was not attempted because of the wide age estimate (350–450 ka) suggested by Moreno et al. (2015) for the TD10 layer.
[j] Correlation with Oscillayers was not attempted because of the general assignment of Bilzingsleben to MIS 11 (Mania and Mania, 2005).
[k] Correlation with Oscillayers was not attempted because of the wide age estimate (390–436 ka) suggested by Daura et al. (2017) for unit 2.
[l] Faunal Unit 2 at Quinton represents a major cooling episode, whereas Faunal Unit 3 is characterized by climatic conditions that are 'not inconsistent with those of the preceding interglacial [i.e. MIS 11c]' (Candy et al., 2014:34). They are tentatively correlated here with the 380 ka and 370 ka Oscillayers outputs, respectively, while recognizing that the correlations of the MIS 11 cold stadial event and subsequent interstadial event to MIS 11b and 11a, respectively, as per Ashton et al. (2008a), remains uncertain.

(Ashton et al., 2008a; Benardout, 2015), as it suggests late MIS 11 occupations during cooler conditions than those characteristic of late MIS 13.

However, the contributions of global-scale records to our understanding of hominin environmental tolerances in regions such as western Europe are ultimately limited for two reasons. Firstly, global data sets partly reflect regionally specific settings and processes, such as those of high-latitude Antarctica (EPICA) and the western North Atlantic (SPECMAP; Candy et al., 2011a). They also ignore regional and local factors that impact climatic and paleoenvironmental conditions, such as the effects of topography and soil conditions (e.g., Zellweger et al., 2015).

Fortunately, regional data sets are also available and these both reinforce and challenge global perspectives. Sea-surface temperature data from the north-east Atlantic (Candy et al., 2015) highlight relative stability across MIS 15–13 (Fig. 2), with sustained mild conditions of either fully interglacial or interstadial character and minimal evidence for glacial environments (Candy and Alonso-Garcia, 2018, their fig. 6). This indicates the potential for sustained hominin dispersals and/or expanding populations immediately before, and at the beginning of, the MIS 13–11 interval. Core samples also indicate a relatively mild south-north transect temperature range of ca. 4 °C, based on mean annual sea-surface temperatures for the MIS 13 peak at ca. 490 ka. This range contrasts with the value of 6.3 °C for the MIS 5e peak (and is also weak relative to other later Middle and Late Pleistocene interglacials) and may have facilitated the late MIS 13 range expansions represented in northern Europe by sites such as Boxgrove and Miesenheim I. The sea-surface temperature records from the north-east Atlantic also highlight regional trends that differ from global records, such as limited evidence for the MBE (i.e., the extremes of interglacial/glacial cycles are comparable on either side of MIS 12; Candy and Alonso-Garcia, 2018). This is further supported by plant and animal-based reconstructions from terrestrial British sites, which also suggest no evidence for an MIS 12 MBE in north-western Europe, as interglacial climates of the early Middle Pleistocene are comparable with, or warmer than, those of the later Middle and Late Pleistocene (Candy et al., 2010). Similar regional trends are also suggested by pollen records from southern Europe (Tzedakis et al., 2006; Schreve and Candy, 2010).

A different global data set, the Croll–Milankovitch cycles (e.g., Berger, 1988; Muller and MacDonald, 1997), offers a perspective on seasonality. Seasonality becomes stronger during phases of greater obliquity (tilt), whereas axial precession (wobble) has a greater

Table 3
Bioclim variables modeled in the Oscillayers data set (WorldClim, 2020).

Bioclim variable	Summary
Bio1	Mean annual temperature (°C)
Bio2	Mean diurnal range (mean of monthly [maximum temperature − minimum temperature] value; °C)
Bio3	Isothermality ([Bio2/Bio7] × 100)
Bio4	Temperature seasonality (standard deviation × 100)
Bio5	Maximum temperature of the warmest month (°C)
Bio6	Minimum temperature of the coldest month (°C)
Bio7	Annual temperature range (Bio5–Bio6; °C)
Bio8	Mean temperature of the wettest quarter (°C)
Bio9	Mean temperature of the driest quarter (°C)
Bio10	Mean temperature of the warmest quarter (°C)
Bio11	Mean temperature of the coldest quarter (°C)
Bio12	Annual precipitation (mm)
Bio13	Precipitation of the wettest month (mm)
Bio14	Precipitation of the driest month (mm)
Bio15	Precipitation seasonality (coefficient of variability)
Bio16	Precipitation of the wettest quarter (mm)
Bio17	Precipitation of the driest quarter (mm)
Bio18	Precipitation of the warmest quarter (mm)
Bio19	Precipitation of the coldest quarter (mm)

Table 4
Mean Deuterium values by 10 kyr block.

10 kyr-stepped output[a]	n[b]	Mean Deuterium value[b]	10 kyr-stepped output[a]	n[b]	Mean Deuterium value[b]
530 ka[c]	20	−422.4540	440 ka	18	−437.7267
	(24)	(−424.1617)	430 ka[d]	27	−417.4652
520 ka	30	−414.8430		(24)	(−420.4317)
510 ka	27	−421.3778	420 ka[d]	34	−396.6853
500 ka	26	−413.6577		(37)	(−396.4459)
490 ka	26	−407.5431	410 ka	50	−387.5056
480 ka[d]	15	−417.0733	400 ka	51	−393.0745
	(21)	(−417.1381)	390 ka	35	−418.4569
470 ka[d]	22	−424.8136	380 ka	34	−424.3324
	(16)	(−427.6312)	370 ka[c]	3	−434.1000
460 ka	15	−435.4600		(33)	(−430.1470)
450 ka	18	−428.5167			

[a] 10 kyr-stepped outputs relate to Oscillayers data (Gamisch, 2019).
[b] Deuterium values from Jouzel et al. (2007; n = number of values from which the mean Deuterium value was calculated); means generated from values falling within 10 kyr of the stepped outputs (i.e., within 445 ka–435 ka for the 440 ka output), based on the ages in Jouzel et al. (2007). Smaller negative values (e.g., −390) indicate warmer conditions; larger negative values (e.g., −430) indicate colder conditions.
[c] Where the 10 kyr range for a stepped output incorporates the upper or lower boundary of the MIS 13–11 range (e.g., 533 ka [MIS 14/13 boundary] and the 530 ka output), the mean value is generated from values falling within the MIS of interest (e.g., 533–525 ka in the case of the 530 ka output and MIS 13; the value and sample size based on the full 10 kyr range of values are shown in parenthesis, e.g., 535–525 ka in the case of the 530 ka output).
[d] Where the 10 kyr range for a stepped output incorporates an internal MIS boundary within the MIS 13–11 range (e.g., 478 ka [MIS 13/12 boundary] and the 480 ka output), the mean values for the adjacent outputs are generated according to revised ranges defined by the boundary (e.g., 485–478 ka for the 480 ka output and 478–465 ka for the 470 ka output; the value and sample size based on the full 10 kyr range of values are shown in parenthesis, e.g., 485–475 ka in the case of the 480 ka output).

impact on seasonal extremes during periods of high or maximum eccentricity (orbital shape; Berger, 1988; Bell and Walker, 2005; Woodward, 2014). The Croll–Milankovitch cycles indicate higher values for eccentricity and precession in late MIS 13 compared to MIS 11, but this pattern is reversed for obliquity, with higher values occurring in early MIS 11 (Fig. 4), suggesting differing seasonality regimes. This has potential significance for the changing hominin record and can be explored with reference to site-specific summer and winter temperature contrasts.

Overall, both global and regional data sets are broadly consistent, although with some notable discrepancies (e.g., the evidence for the MBE; Candy et al., 2010, 2014). These data sets suggest warmer peak interglacial climatic conditions in MIS 11 compared to MIS 13, but broadly similar late-stage conditions in both MIS 13 and 11. How do the conditions at hominin sites compare with these general trends?

2. Materials and methods

Microfauna assemblages offer on-site perspectives on winter and summer temperatures and, in some cases, annual precipitation patterns (e.g., Blain et al., 2014). These data provide point-specific descriptions of local conditions, but also a partial insight into geographical patterns, although precise temporal comparisons between sites are difficult as absolute ages of individual sites are either unknown or carry a larger error margin than the resolution of substage variations within isotope stages. It is impossible, for example, to state whether the occupations at Barnham (MIS 11c) are exactly contemporary with the Lower Loam occupations at Swanscombe (also MIS 11c), although pollen stages permit a degree of correlation at regional scales (e.g., White et al., 2013, their fig. 8; Ashton et al., 2016, their fig. 3).

2.1. Questions 1–3

To address whether temperatures differed at occupied British sites in MIS 13 and MIS 11, and whether temperatures differed between occupied and nonoccupied British sites in MIS 13 and MIS 11, I compared climatic conditions using published paleotemperature estimates derived from microfauna assemblages (i.e., herpetofauna, coleoptera, and ostracods). Although species' distributions are influenced by factors in addition to temperature, such as bedrock, hydrology, and soil chemistry (Candy et al., 2010, 2011a), the distributional limits of a range of plant and animal species nonetheless appear to be primarily governed by temperature (Candy et al., 2010:188).

However, the published paleotemperature values for British sites that were used in this paper were generated using two methods: mutual climatic range (MCR; Atkinson et al., 1987), and mutual ostracod temperature range (MOTR; Horne, 2007). It is recognized that methodological differences may influence specific estimates (see discussions in Birks et al., 2010 and Farjon et al., 2020), but previous preliminary testing has demonstrated good matches between paleotemperatures generated by the MOTR and MCR methods (Horne, 2007). A mixture of methods was therefore considered acceptable in this case, and enabled the samples to be increased in size. Site-specific temperature estimates, that is, minimum temperature (T_{min}), maximum temperature (T_{max}), and temperature range (T_{range}) were statistically compared for MIS 13 and MIS 11 British sites (Question 1), MIS 13 hominin and

Table 5
10 kyr-stepped outputs with the smallest (warmest) and largest (coldest) mean Deuterium values for MIS 13, MIS 12, and MIS 11.

MIS	Description	10 kyr-stepped output[a]	Span of Deuterium values[b]	Mean Deuterium value[b]
13	Warmest 10 kyr interval	490 ka	495–485 ka	−407.5431
	Coldest 10 kyr interval	530 ka	533–525 ka	−422.4540
12	Warmest 10 kyr interval	430 ka	435–424 ka	−417.4652
	Coldest 10 kyr interval	440 ka	445–435 ka	−437.7267
11	Warmest 10 kyr interval	410 ka	415–405 ka	−387.5056
	Coldest 10 kyr interval[c]	380 ka	385–375 ka	−424.3324

[a] 10 kyr-stepped outputs relate to Oscillayers data (Gamisch, 2019).
[b] Deuterium values from Jouzel et al. (2007).
[c] The 380 ka output was selected as the coldest interval for MIS 11 because of the very small MIS 11 sample size for the 370 ka output (n = 3; see Table 4).

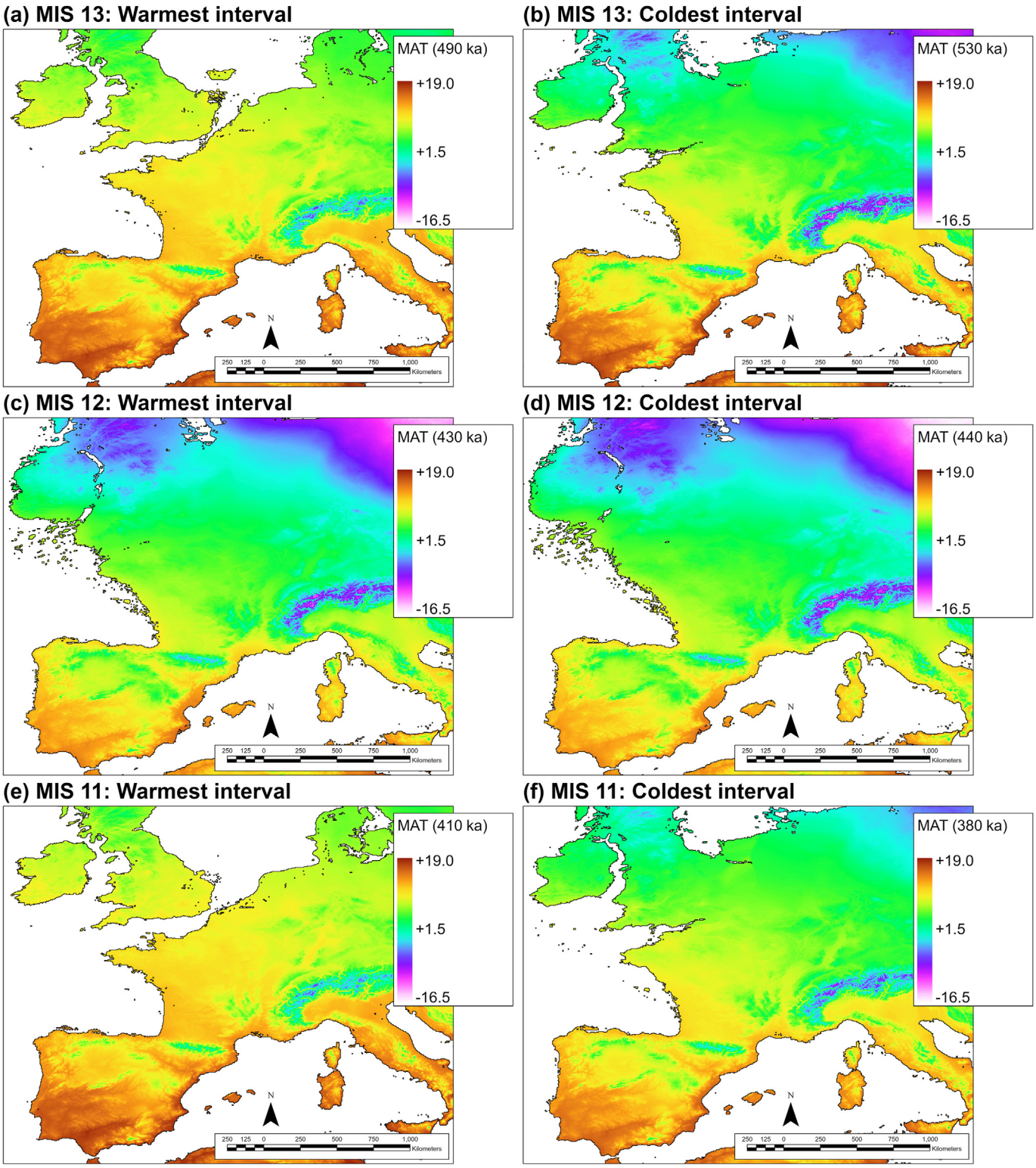

Figure 5. Reconstructed paleocoastlines and mean annual temperature (MAT; °C; Bio1) estimates for the warmest (a, c, and e) and coldest intervals (b, d, and f) in MIS 13 (a and b), MIS 12 (c and d) and MIS 11 (e and f), using the 10 kyr-stepped outputs from Gamisch (2019). Color scale based on minimum (−16.5 °C, pink) and maximum values (+19.0 °C, brown) across all six maps. Created in ArcGIS Pro v. 2.6.1 (map projection: WGS, 1984). Note that the Oscillayers mapping for the warmest MIS 13 interval (a) does not represent the Weald–Artois ridge. (For interpretation of the references to color in this figure legend, the reader is referred to the Web version of this article).

nonhominin British sites (Question 2), and MIS 11 hominin and nonhominin British sites (Question 3). Minimum temperature, T_{max}, and T_{range}, respectively, measure the mean air temperature of the coldest month (i.e., January in the northern hemisphere), the mean air temperature of the warmest month (i.e., July in the northern hemisphere), and the difference between T_{min} and T_{max}, a measure of seasonality (definitions as per Farjon et al., 2020; it is important to note that where a span of values is reported, e.g., a

T_{min} of −4 to +4 °C for Boxgrove, it indicates that the mean monthly temperature lay somewhere between those limits, not that the temperatures ranged between those limits; Coope et al., 2002). The site samples for questions 1–3 were limited to British sites between 50.87°N–52.91°N and 2.38°W–1.53°E (Table 1; Fig. 1) to minimize the impacts of interregional variability. Site temperature values were extracted from previous publications (values, methods, and source details in Table 2). All statistical comparisons were made using the nonparametric Mann–Whitney U test because of the impact of small sample sizes on data distributions. Midpoint values were used for statistical comparison (e.g., +17.5 °C for the T_{max} value for Boxgrove; Table 2). The test level of significance (α) for all tests was 0.05. Test results were reported as follows: U = Mann–Whitney test statistic [sample size], p = significance (two-sided test). Data distributions were visualized using boxplots.

2.2. Questions 4 and 5

Modeling climatic transects across MIS 13–11 (Question 4) and defining the proportions of western European landscapes with tolerated or preferred temperatures (as defined by occupied sites) in MIS 11 and MIS 13 (Question 5) requires a continuous model. The majority of existing global paleoclimate reconstructions are based on general circulation models (GCMs). However, many of these models cover the Late Pleistocene (e.g., Singarayer and Valdes, 2010) or the Pliocene or earlier periods (e.g., Sloan and Rea, 1996; Haywood et al., 2013). General circulation model approaches have started to be applied to earlier periods of the Pleistocene (e.g., PaleoClim and the 2Ma simulation; Brown et al., 2018; Timmermann et al., 2022), but are characterized by relatively large spatial resolution (e.g., 3.75° for the 2Ma simulation; Timmermann et al., 2022) or are limited to specific time intervals: the PaleoClim database covers MIS 19 (ca. 787 ka), as well as the mid-Pliocene Warm Period (ca. 3.264–3.025 Ma), and MIS M2 in the Late Pliocene (ca. 3.3 Ma; Brown et al., 2018). However, the recently published Oscillayers data set (Gamisch, 2019; https://datadryad.org/stash/dataset/doi:10.5061/dryad.27f8s90) offers a potential means of assessing geographical and temporal variations in western European paleoclimates across MIS 13–11. Oscillayers modeled 19 bioclim variables for the Plio-Pleistocene, at 10 kyr intervals and with a spatial resolution of 2.5 arc-minutes (approximately 3.55 km × 3.55 km = 12.6 km^2 at 40°N; Table 3). The Oscillayers data for each bioclim variable and each 10 kyr step (.asc format) were converted into raster layers (ASCII to Raster) and mapped in ArcGIS Pro v. 2.6.1 (map projection: WGS, 1984).

The Oscillayers outputs for each 10 kyr interval were derived from interpolated anomalies between the bioclim layers of the present and the Last Glacial Maximum (LGM), scaled relative to the Plio-Pleistocene global mean temperature curve (Gamisch, 2019). The temperature curve was based on benthic stable oxygen isotope ratios (Hansen et al., 2013). The Oscillayers data set, therefore, offers a continuous rather than point-specific perspective on paleoclimatic variability in western Europe across MIS 13–11, although the underlying spatial patterns of each modeled period are driven by the scaled differences between the LGM and the present.

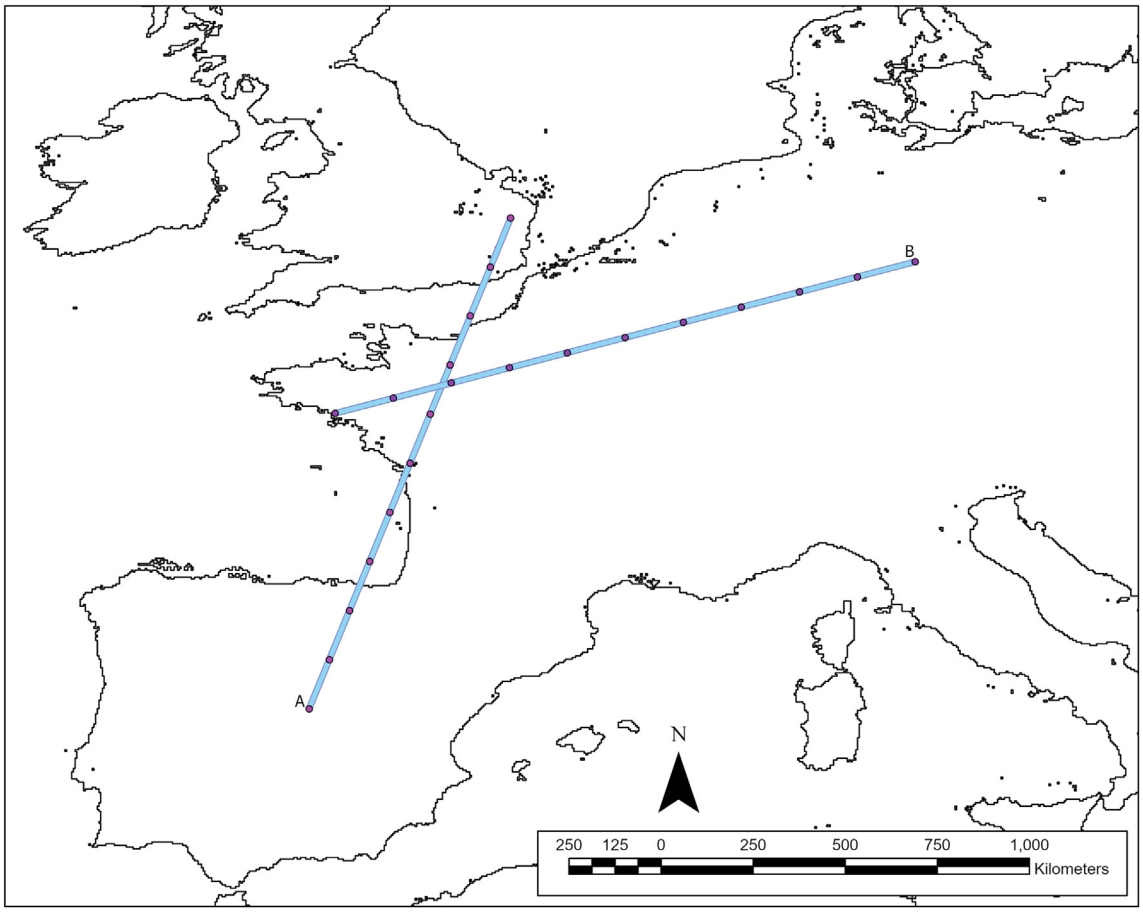

Figure 6. Paleoclimatic transect locations and sampling intervals (plotted against a 410 ka paleocoastlines reconstruction; from Gamisch, 2019). Figure created in ArcGIS Pro v. 2.6.1 (map projection: WGS, 1984). A) Áridos–Hoxne transect, B) Bilzingsleben–Saint-Colomban transect.

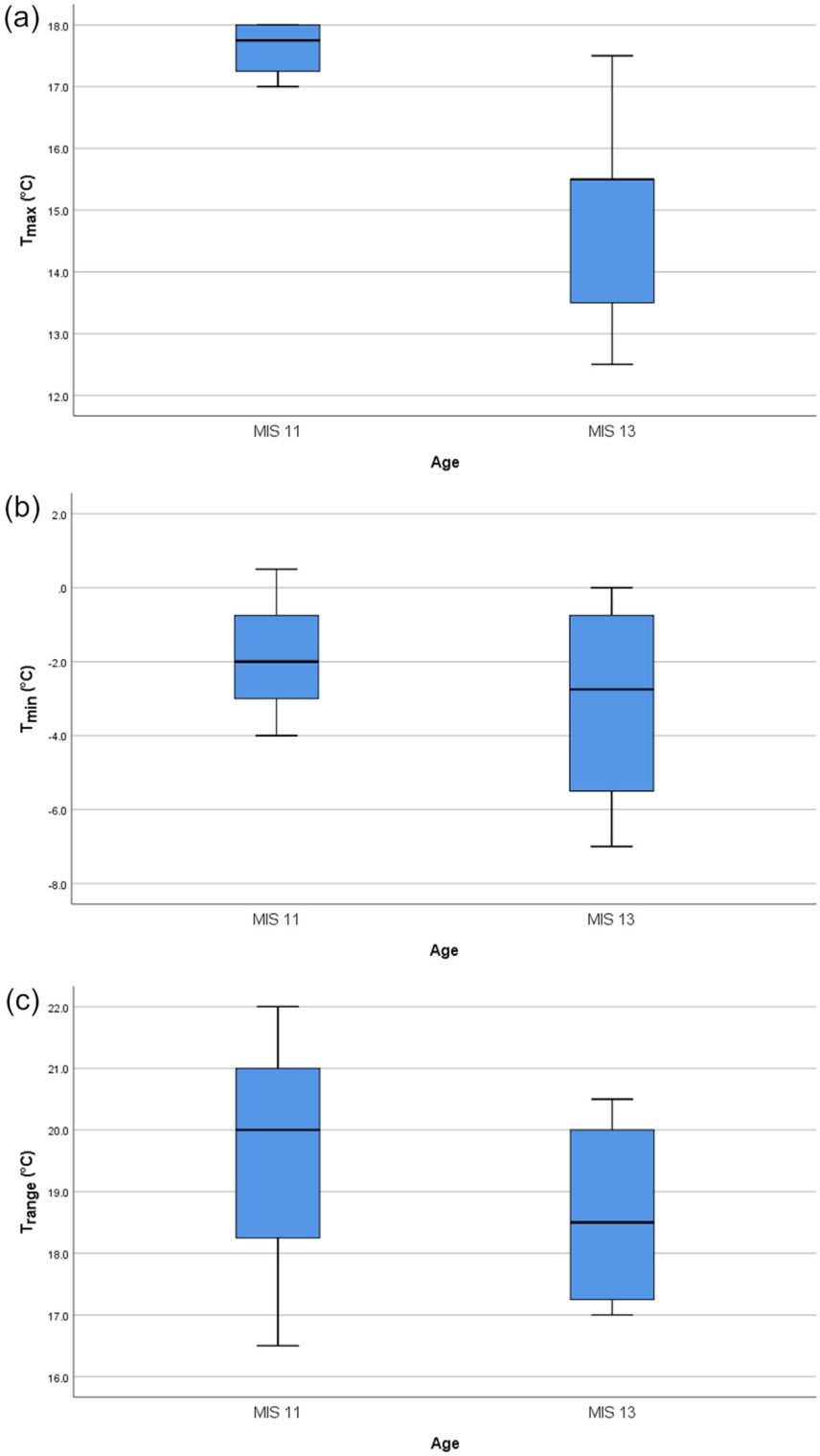

Figure 7. Boxplots of estimates for British MIS 13 and MIS 11 hominin sites of a) maximum temperature (T_{max}; °C), b) minimum temperature (T_{min}; °C), and c) temperature range (T_{range}; °C). Significant differences between MIS 13 and MIS 11 hominin sites for T_{max} only. Sample sizes: T_{max}: $n = 5$ (MIS 13) and $n = 4$ (MIS 11); T_{min} and T_{range}: $n = 4$ (MIS 13) and $n = 3$ (MIS 11). See Table 1 for list of individual sites. Note that Waverley Wood (MIS 13) and Barnham (MIS 11) were excluded from the T_{min} and T_{range} samples, as there were no T_{min} estimates for those sites (see Table 2). The solid black line within each box represents the median. The box represents the interquartile range (IQR). The lower and upper whiskers represent values no more than 1.5 IQR below the first quartile and no more than 1.5 IQR above the third quartile, respectively.

Brown et al. (2020) have raised both theoretical and methodological concerns with regard to the Oscillayers data set. Their theoretical concerns are two-fold: 1) that the Oscillayers method does not allow climate to vary spatiotemporally and 2) that the method cannot incorporate important changes in paleoclimatic forcing mechanisms, such as orbital-forcing changes in

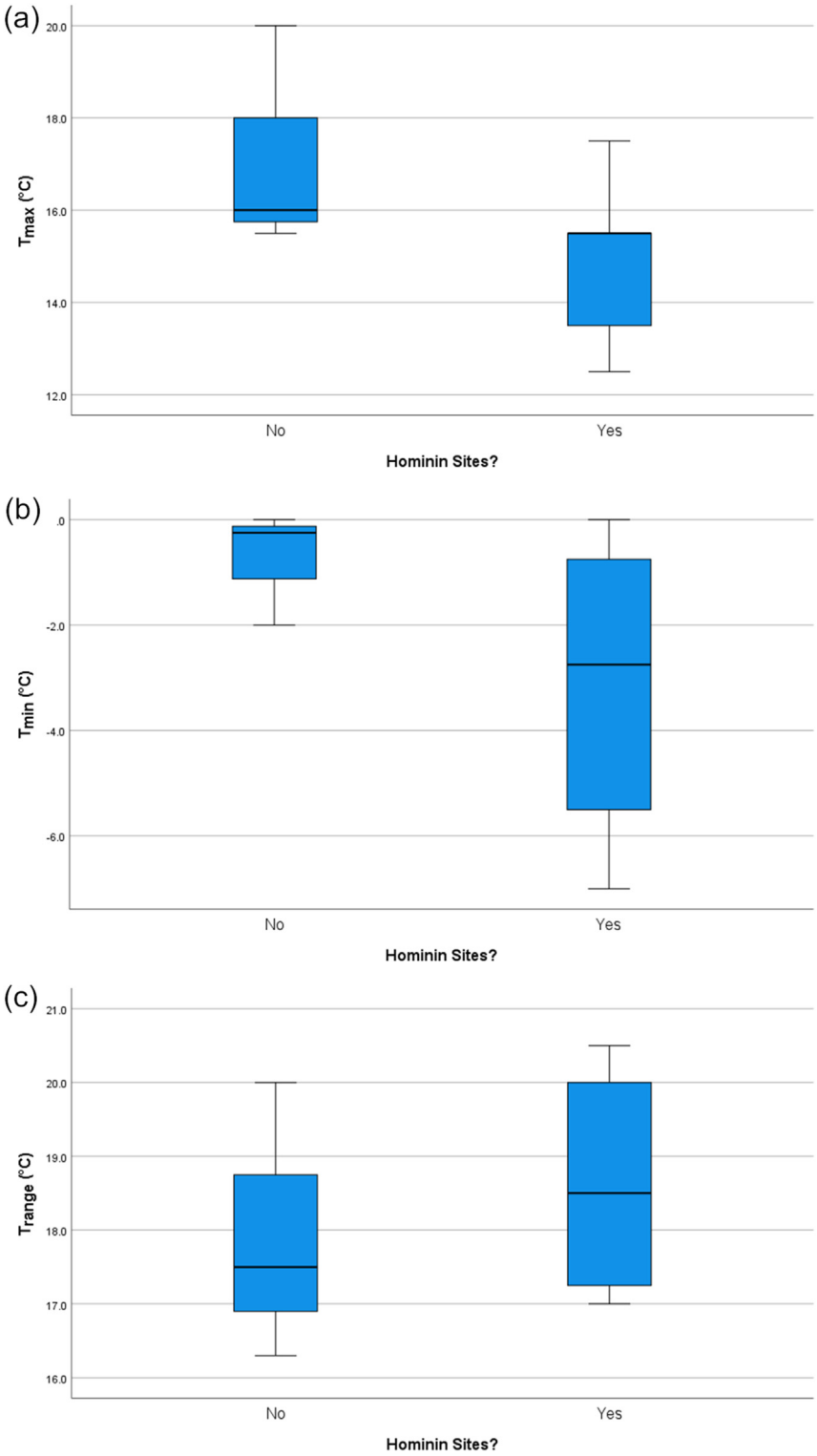

Figure 8. Boxplots of estimates for British hominin and nonhominin MIS 13 sites of a) maximum temperature (T_{max}; °C), b) minimum temperature (T_{min}; °C), and c) temperature range (T_{range}; °C). No significant differences between hominin and nonhominin MIS 13 sites. Sample sizes: T_{max}: $n = 5$ (hominin) and $n = 3$ (nonhominin); T_{min} and T_{range}: $n = 4$ (hominin) and $n = 3$ (nonhominin). See Table 1 for list of individual sites. Note that Waverley Wood [MIS 13] was excluded from the T_{min} and T_{range} samples, as no T_{min} estimate was available for that site (see Table 2). The solid black line within each box represents the median. The box represents the interquartile range (IQR). The lower and upper whiskers represent values no more than 1.5 IQR below the first quartile and no more than 1.5 IQR above the third quartile, respectively.

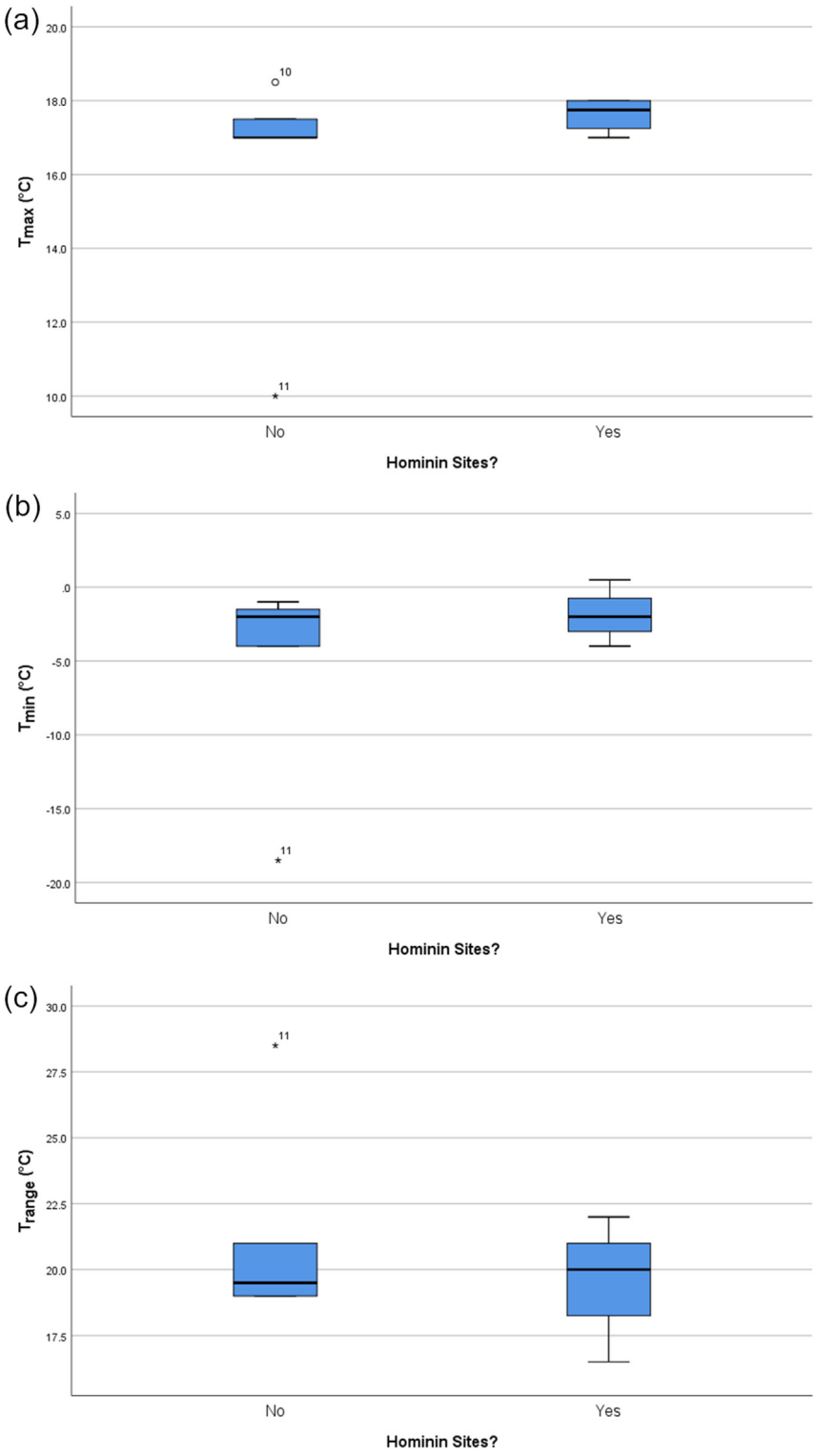

Figure 9. Boxplots of estimates for British hominin and nonhominin MIS 11 sites of a) maximum temperature (T_{max}; °C), b) minimum temperature (T_{min}; °C), and c) temperature range (T_{range}; °C). No significant differences between hominin and nonhominin MIS 11 sites. Sample sizes: T_{max}: $n = 4$ (hominin) and $n = 5$ (nonhominin); T_{min} and T_{range}: $n = 3$ (hominin) and $n = 5$ (nonhominin). Site 10 (potential outlier) is from Quinton (Faunal Unit 1); site 11 (extreme value) is from Quinton (Faunal Unit 2). See Table 1 for list of individual sites. Note that Barnham [MIS 11] was excluded from the T_{min} and T_{range} samples, as no T_{min} estimate was available for that site; see Table 2). The solid black line within each box represents the median. The box represents the interquartile range (IQR). The lower and upper whiskers represent values no more than 1.5 IQR below the first quartile and no more than 1.5 IQR above the third quartile, respectively. Potential outliers (circles) are between 1.5 and 3 IQR below the first quartile or above the third quartile. Extreme values (stars) are more than 3 IQR below the first quartile or above the third quartile.

Table 6
Mean annual temperature values (°C; see also Figs. 5 and 10) for warmest and coldest intervals in MIS 13, MIS 12, and MIS 11, derived from Oscillayers outputs for the Bio1 variable (Gamisch, 2019).

	MIS 13		MIS 12		MIS 11	
	Warmest interval (490 ka)	Coldest interval (530 ka)	Warmest interval (430 ka)	Coldest interval (440 ka)	Warmest interval (410 ka)	Coldest interval (380 ka)
Transect A (south-north)[a]						
Maximum	13.3	11.6	9.9	9.5	13.7	11.8
Minimum	8.3	5.1	1.9	1.1	9.1	5.5
Range	5.0	6.5	8.0	8.4	4.6	6.3
Transect range[b]	−5.0	−6.5	−8.0	−8.4	−4.6	−6.3
Transect B (east-west)[a]						
Maximum	10.8	8.8	6.7	6.2	11.3	9.0
Minimum	6.7	4.0	0.8	0.0	7.4	4.4
Range	4.1	4.8	5.9	6.2	3.9	4.6
Transect range[c]	+3.6	+4.8	+5.9	+6.2	+3.4	+4.6

[a] Values were sampled at 10% intervals along the transects. Maximum, minimum, range, and transect range values were calculated from these samples. Range values are the difference between the minimum and maximum values along the entire transect. Transect range values are the difference between the two values at either end of the transect.
[b] Positive signs indicate values increasing from south to north; negative signs indicate values decreasing from south to north.
[c] Positive signs indicate values increasing from east to west; negative signs indicate values decreasing from east to west.

paleogeography. With regard to methodology, Brown et al. (2020) expressed concern over the generation of precipitation estimates using a linear relationship between temperature and precipitation. They also noted that areas characterized by limited change between the LGM and the present will inevitably also show limited change in the deeper past and were critical of the Bio8–11 and Bio16–19 measures because they are based on scaling of the delta layer (Brown et al. [2020] argued that they represent joint relationships between temperature and precipitation). The authors also questioned the Bio2 (mean diurnal range) and Bio3 (isothermality) bioclim layers because of concerns about the underlying assumptions that diurnal range should increase as mean global temperatures increase (Bio2) and that warming is associated with much larger increases in maximum rather than minimum temperatures (Bio3). As part of their critique, Brown et al. (2020, their fig. 2) compared the Oscillayers reconstructions with GCMs and noted that GCM models reconstructed warmer conditions than Oscillayers, on the order of 1–5 °C in mainland western Europe. With regard to precipitation, the GCM models reconstructed both wetter and drier conditions than Oscillayers, with marked local variability.

In response, Gamisch (2020:1443) acknowledged the spatial limitations of Oscillayers: "the underlying spatial pattern of each modelled time period is driven by the scaled differences between the LGM [Last Glacial Maximum] and the present"—while noting that these limitations were recognized in the original paper (Gamisch, 2019). Overall, Gamisch (2020:1444) defended Oscillayers while acknowledging aspects of Brown et al.'s (2020) criticisms, arguing "that describing past climates with a single scaling factor might result in oversimplified models of past climate change; however, in lieu of better data products, I would contend that, despite its limitations, the Oscillayers framework (Gamisch, 2019) works as reasonably well as similar approaches." In light of Brown et al.'s (2020) concerns and Gamisch's (2020) responses, addressing Questions 4 and 5 of this paper involved a 'prestage', in which I tested the Oscillayers model against site-specific paleotemperature estimates from the MIS 13–11 interval. The mechanics of this testing along with the results are outlined in Supplementary Online Material (SOM) S1.

Results of this analysis indicated significant, positive, and moderately strong correlations between the Oscillayers temperature values and the site-specific temperature estimates (SOM Table S1) when using the midpoint values of T_{max} and T_{min}, and significant though slightly weaker positive correlations when using the highest T_{max} and the lowest T_{min} values. In light of these correlation results, the Oscillayers data were used with caution to model climatic transects across MIS 13–11 (Question 4) and to explore the proportions of western European landscapes with tolerated or preferred temperatures (as defined by occupied sites) in MIS 11 and 13 (Question 5).

Question 4—climatic transects Gamisch's original modeling created outputs at 10 kyr steps, spanning the Pliocene and Pleistocene and ending at the LGM (i.e., outputs at 20 ka, 30 ka, 40 ka, etc.). For the current paper, 10 kyr interval output maps were initially generated for the period spanning 530–370 ka, using the data published by Gamisch (2019). A subset of six 10 kyr time intervals, representing the warmest and coldest conditions in MIS 13 (533–478 ka), 12 (478–424 ka), and 11 (424–374 ka; MIS boundary dates after Lisiecki and Raymo, 2005), were then identified. These intervals were defined based on the Deuterium values in Jouzel et al. (2007). To best integrate the Deuterium data in Jouzel et al. (2007) and the 10 kyr-stepped outputs in Gamisch (2019), mean Deuterium values were calculated for the 10 kyr bounding each output (e.g., the Deuterium values from 445 to 435 ka, based on the ages in Jouzel et al. (2007), were averaged to characterize the 440 ka output). The mean Deuterium values for the 10 kyr-stepped outputs relating to the MIS 13–11 interval (533–374 ka) are summarized in Table 4 and the 10 kyr-stepped outputs with the warmest and coldest mean Deuterium values for MIS 13, 12, and 11 are identified in Table 5 and mapped in Figure 5 (mean annual temperature [MAT] values). These 10 kyr-stepped outputs are inevitably insensitive to sub-10 kyr fluctuations (e.g., the MIS 11 NAP/OHO event) known from ice core and terrestrial records, and to the specific impacts of local microclimates, for example, due to topography, during MIS 13–11.

Two arbitrary transects were created in ArcGIS Pro v. 2.6.1 (map projection: WGS 1984; Fig. 6): Transect A (south-north): Áridos (40°23′N, 3°43′W) to Hoxne (52°21′N, 1°12′E): geodesic length = 1382 km and Transect B (east-west): Bilzingsleben (51°17′N, 11°4′E) to Saint-Colomban (47°35′N, 3°5′W): geodesic length = 1105 km.

Across the six specific 10 kyr time intervals falling within MIS 13–11 (Table 5), maximum, minimum, range, and transect range values were generated for each of the 19 bioclim variables, for both transects (values were sampled at 10% intervals). Range values are the difference between the minimum and maximum values along the entire transect. Transect range values are the difference between the two values at either end of the transect (i.e., the values at Áridos and Hoxne for transect A, and the values at Bilzingsleben and Saint-Colomban for transect B). Values for bioclim variables Bio1 (MAT), Bio5 (maximum temperature of the warmest month), Bio6 (minimum temperature of the coldest month), and Bio12 (annual precipitation) are listed in Tables 6–9. Values for the

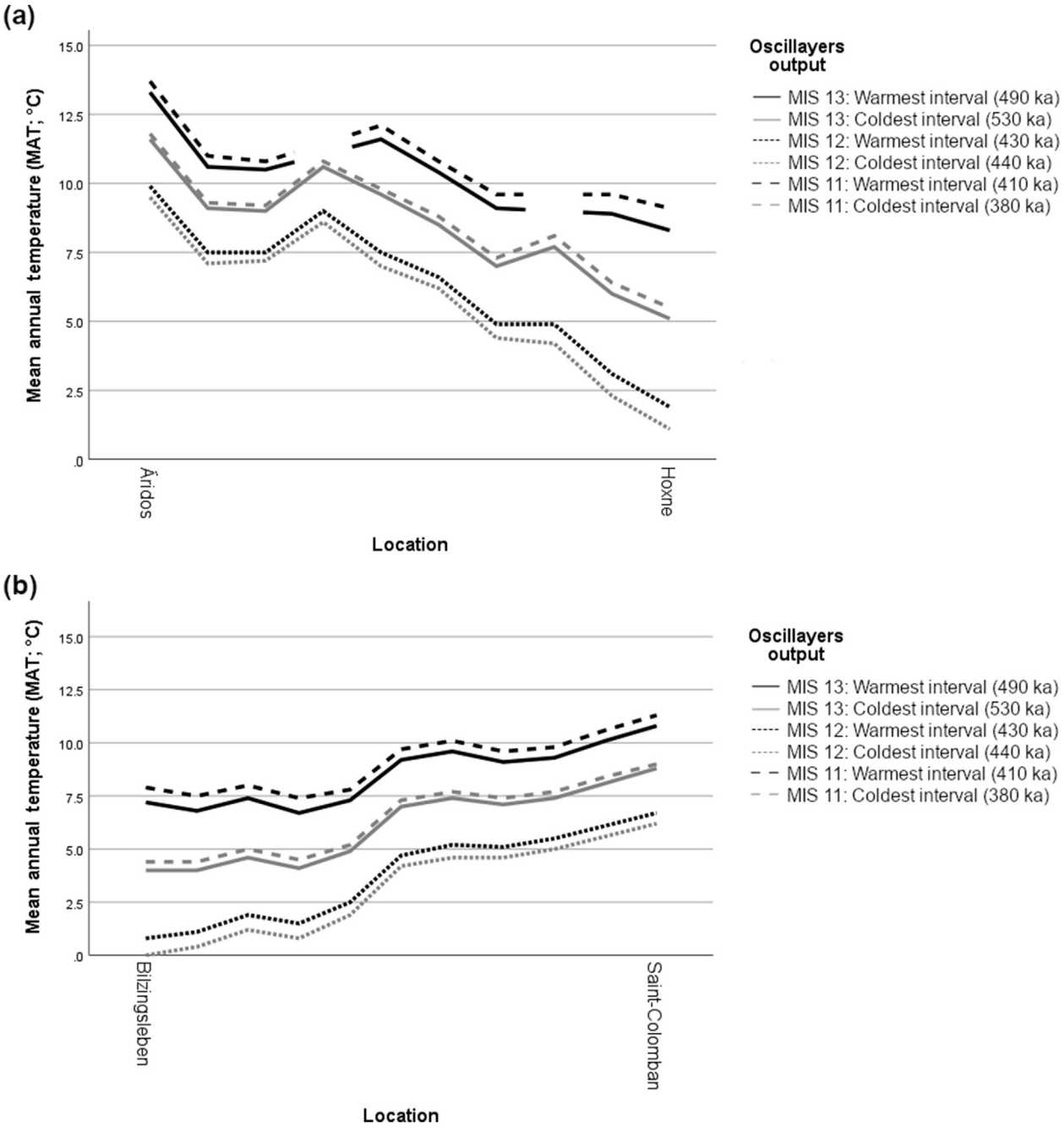

Figure 10. Mean annual temperature values (°C; see also Fig. 5 and Table 6) along south-north transect (a) and east-west transect (b), for warmest and coldest intervals in MIS 13, 12, and 11, derived from Oscillayers outputs for the Bio1 variable (Gamisch, 2019). Solid lines: MIS 13; dotted lines: MIS 12; dashed lines: MIS 11; black lines: warmest interval within individual MIS; grey lines: coldest interval within individual MIS. Data gaps occur where sample transect points fall in maritime zones during specific periods.

remaining bioclim variables are listed in SOM Tables S2–S16. Statistical comparisons were conducted on climate transect data for the 490 ka and 410 ka intervals, as these represent peak conditions in MIS 13 and 11 and therefore offered a 'like-with-like' comparison. Statistical comparisons were made using the nonparametric Mann–Whitney U test because of the impact of small sample sizes on data distributions.

Question 5—mapping potential hominin landscapes Using the combined T_{min} and T_{max} values from hominin sites assigned to MIS 13 (i.e., Boxgrove, Brooksby, Happisburgh 1, High Lodge, and Waverley Wood: T_{min}: [−11] − [+4]°C; T_{max}: [+10] − [+20]°C) and MIS 11 (i.e., Ambrona, Áridos 1, Barnham, Beeches Pit, Bilzingsleben, Gruta da Aroeira, Swanscombe [Lower Loam and Lower Middle Gravel], and Trinchera Dolina [TD-10.3]: T_{min}: [−7] − [+8.8]°C; T_{max}: [+15] − [+25]°C) and the Oscillayers Bio5 and Bio6 data for the 490 ka and 410 ka intervals (i.e., late MIS 13 and MIS 11c), maps of potential hominin landscapes were generated for north-west Europe. For each time interval, the Oscillayers Bio5 and Bio6 maps were separately reclassified into 'suitable' (defined as values falling within the collective T_{min}/T_{max} ranges across the selected hominin sites) and 'unsuitable' categories (defined as values falling below or above the T_{min}/T_{max} range). For each time interval, the reclassified Bio5 and Bio6 maps were multiplied together, with 'suitable' locations in the resulting map of potential hominin landscapes requiring the co-occurrence of suitable categories in both source maps. Temperature ranges from MIS 13 and MIS 11

Table 7
Minimum temperature of the coldest month values (°C; see also Figs. 11 and 12) for warmest and coldest intervals in MIS 13, MIS 12, and MIS 11, derived from Oscillayers outputs for the Bio6 variable (Gamisch, 2019).

	MIS 13		MIS 12		MIS 11	
	Warmest interval (490 ka)	Coldest interval (530 ka)	Warmest interval (430 ka)	Coldest interval (440 ka)	Warmest interval (410 ka)	Coldest interval (380 ka)
Transect A (south-north)[a]						
Maximum	1.9	0.7	−0.6	−0.8	2.6	0.9
Minimum	−2.4	−8.1	−13.8	−15.3	−1.1	−7.3
Range	4.3	8.8	13.2	14.5	3.7	8.2
Transect range[b]	−3.6	−8.4	−13.2	−14.5	−2.5	−7.7
Transect B (east-west)[a]						
Maximum	2.2	−0.7	−3.5	−4.3	−4.5	−0.3
Minimum	−5.4	−10.8	−16.3	−17.7	2.9	−10.1
Range	7.6	10.1	12.8	13.4	7.4	9.8
Transect range[c]	+7.6	+10.1	+12.8	+13.4	+7.0	+9.8

[a] Values were sampled at 10% intervals along the transects. Maximum, minimum, range, and transect range values were calculated from these samples. Range values are the difference between the minimum and maximum values along the entire transect. Transect range values are the difference between the two values at either end of the transect.
[b] Positive signs indicate values increasing from south to north; negative signs indicate values decreasing from south to north.
[c] Positive signs indicate values increasing from east to west; negative signs indicate values decreasing from east to west.

sites across western Europe were used (i.e., Boxgrove, Brooksby, Happisburgh 1, High Lodge, and Waverley Wood for MIS 13; Ambrona, Áridos 1, Barnham, Beeches Pit, Bilzingsleben, Gruta da Aroeira, Swanscombe [Lower Loam and Lower Middle Gravel], and Trinchera Dolina for MIS 11) to capture the range of hominin tolerances, if not necessarily preferences, during MIS 13 and 11. The mapping is exploratory and recognizes the potential discrepancy between the temperatures measured by the Bio5/Bio6 bioclim variables and the T_{min}/T_{max} estimates (as discussed in SOM S1).

3. Results

3.1. Question 1: Are there significant differences between the temperature estimates at occupied British sites in Marine Isotope Stage 13 and in Marine Isotope Stage 11?

Statistical analysis of the site-specific temperature estimates for British MIS 13 and MIS 11 sites suggests significantly warmer summer conditions (T_{max}) in MIS 11 ($U = 1.5$ [$n = 9$], $p = 0.032$; Fig. 7a). There are no significant differences between either the winter temperatures (T_{min}; $U = 4.5$ [$n = 7$], $p = 0.629$; Fig. 7b) or the temperature ranges (T_{range}; $U = 5.0$ [$n = 7$], $p = 0.857$; Fig. 7c), although the MIS 11 winter temperatures are slightly warmer, and the MIS 11 temperature ranges are slightly wider. The significant difference in summer temperature is in line with global records (Fig. 2) and also reflects the association of the majority of the MIS 11 occupations with the optimal interglacial conditions of substage MIS 11c (e.g., Barnham and Swanscombe [Lower Loam and Lower Middle Gravels]).

3.2. Question 2: Are there significant differences between the temperature estimates at occupied and non-occupied British sites in Marine Isotope Stage 13?

Statistical analysis of the site-specific T_{min}, T_{max}, and T_{range} estimates for hominin and nonhominin British MIS 13 sites indicates no significant differences between the summer ($U = 3.0$ [$n = 8$], $p = 0.250$; Fig. 8a), winter ($U = 3.5$ [$n = 7$], $p = 0.400$; Fig. 8b), or range temperatures ($U = 7.5$ [$n = 7$], $p = 0.629$; Fig. 8c), although the boxplots suggest slightly warmer summer and winter temperatures at the nonhominin sites. While the sample is small (and the provenance of a handaxe reported from the Sidestrand till has been debated; Preece et al., 2009), the results suggest that there was not a habitual preference toward the warmest conditions in MIS 13, and that 'cold adaptations' suitable for the subfreezing winter and cool summer conditions at sites such as Happisburgh 1 and Waverley Wood were already in place by late MIS 13 (Fig. 8a, b).

3.3. Question 3: Are there significant differences between the temperature estimates at occupied and non-occupied British sites in Marine Isotope Stage 11?

Statistical analysis of the site-specific T_{min}, T_{max}, and T_{range} estimates for hominin and nonhominin British MIS 11 sites indicates no significant differences between the summer ($U = 13.5$ [$n = 9$], $p = 0.413$; Fig. 9a), winter ($U = 9.0$ [$n = 8$], $p = 0.786$; Fig. 9b), or range temperatures ($U = 7.0$ [$n = 8$], $p > 0.999$; Fig. 9c). The similarities in paleotemperatures, for example, between Quinton (Faunal Units 1 and 3), Woodston, and the MIS 11c hominin sites, suggest that other factors, such as sampling bias and/or specific landscape preferences, are more likely to explain the absence of hominin evidence at the former sites. The extreme outliers for the nonhominin sites (Fig. 9) reflect the sampling of a cold substage, possibly MIS 11b, at Quinton (Faunal Unit 2; Table 2).

3.4. Question 4: Are there significant differences between western European climate transects in Marine Isotope Stage 13 compared to Marine Isotope Stage 11?

The Oscillayers maps (Figs. 5, 11, 13 and 15) provide regional-scale models of the paleoclimatic conditions that were the context for changing hominin distributions in western Europe during MIS 13–11. The mean, minimum, and maximum temperature and annual precipitation values from the Oscillayers data for the modeled warmest and coldest intervals in MIS 13, 12, and 11 suggest various patterns as outlined below (Tables 6–9; Figs. 5 and 10–16).

Mean annual temperature (Bio1) Large MAT ranges occur during both MIS 12 (warmest and coldest intervals) and the coldest intervals of MIS 13 and 11, on both transects (Table 6; Figs. 5 and 10). The largest MAT ranges (8.0–8.4 °C) occurred in MIS 12 on the south-north transect, with MAT ranges in MIS 11 and MIS 13 varying between 3.9 and 6.5 °C (Table 6). In all cases, MAT ranges were larger along the south-north transect, with temperatures decreasing to the north (transect A; Fig. 10) and increasing to the west (transect B; Fig. 10). However, the data also highlight local geographical variations along the transects. For example, where the range in the values measured at both ends of the transect (i.e.,

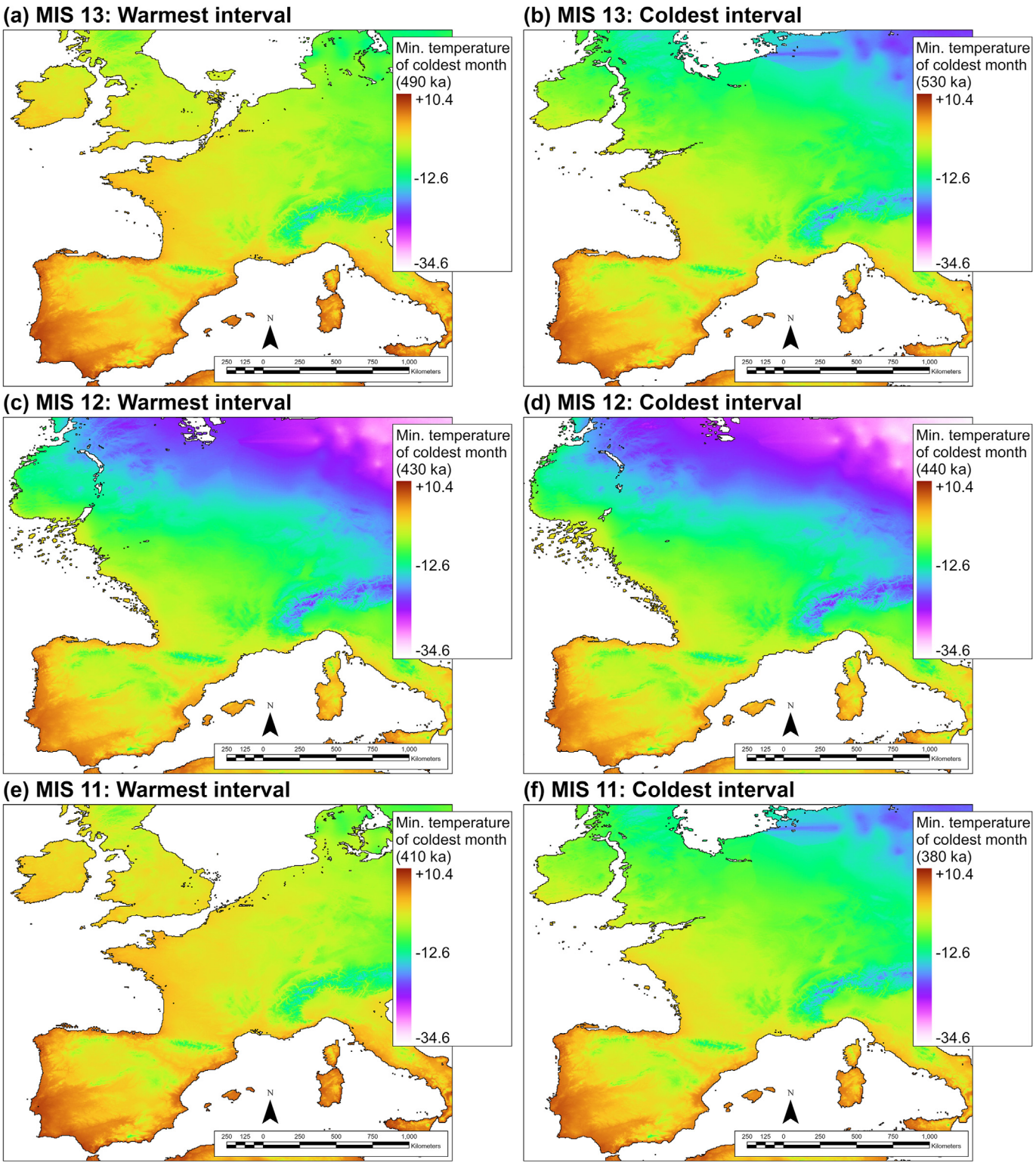

Figure 11. Reconstructed paleocoastlines and minimum temperature of the coldest month (°C; Bio6) estimates for the warmest (a, c, and e) and coldest intervals (b, d, and f) in MIS 13 (a and b), 12 (c and d), and 11 (e and f), using the 10 kyr-stepped outputs from Gamisch (2019). Color scale based on minimum (−34.6 °C, pink) and maximum values (+10.4 °C, brown) across all six maps. Figure created in ArcGIS Pro v. 2.6.1 (map projection: WGS, 1984). Note that the Oscillayers mapping for the warmest MIS 13 interval (a) does not represent the Weald–Artois ridge. (For interpretation of the references to color in this figure legend, the reader is referred to the Web version of this article).

transect range) is narrower than the total range of all the transect values (i.e., range), as in the MAT values for the MIS 11 Warmest Interval on transect B (transect range: 3.4 °C; range: 3.9 °C; Table 6; Fig. 10), where the lowest values occur in western Germany (Fig. 5e). Statistical comparison of the MAT data for the 490 ka and 410 ka intervals indicated no significant differences on either

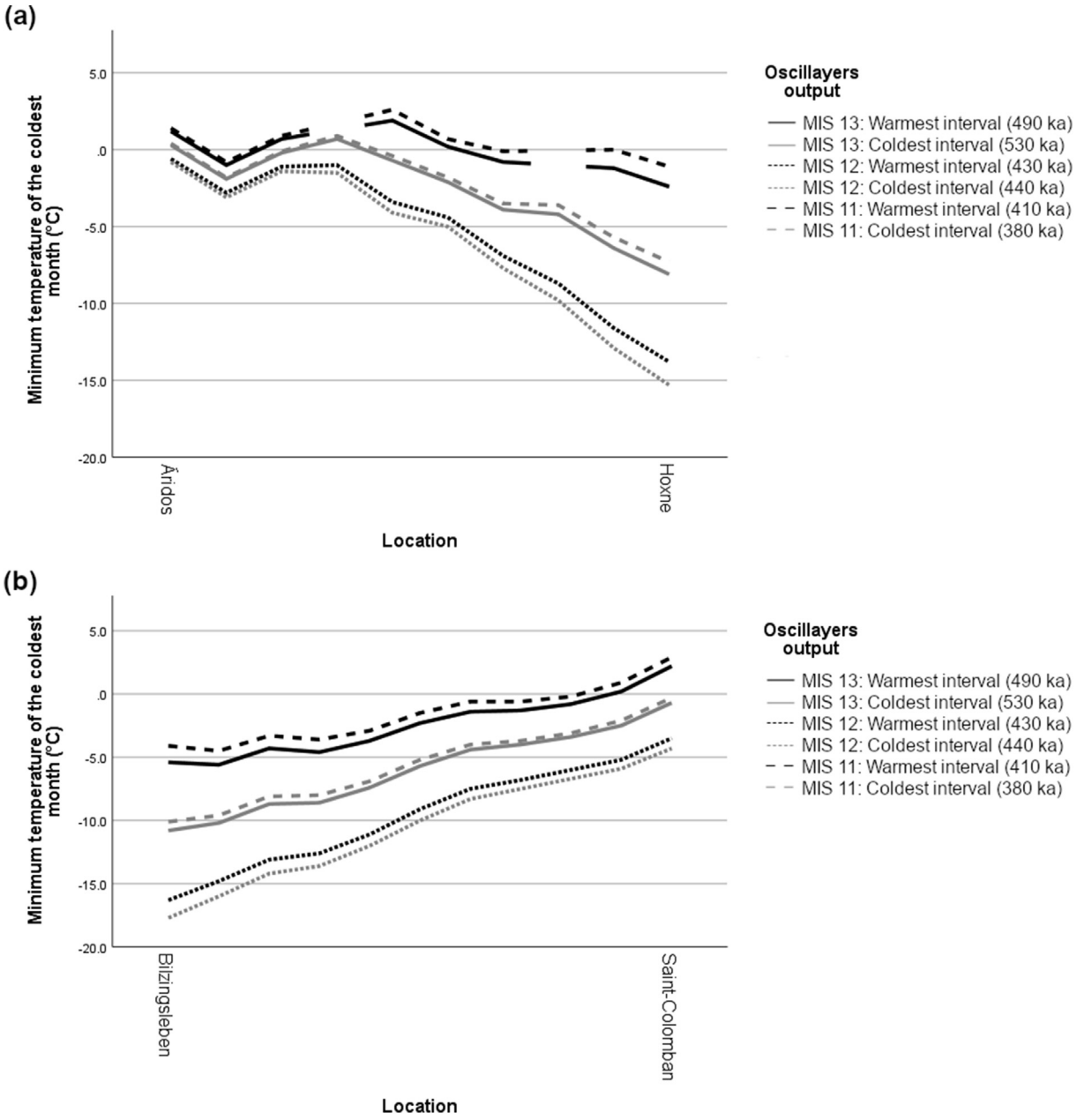

Figure 12. Minimum temperature of the coldest month values (°C; see also Fig. 11 and Table 7) along south-north transect (a) and east-west transect (b), for warmest and coldest intervals in MIS 13, MIS 12, and MIS 11, derived from Oscillayers outputs for the Bio6 variable (Gamisch, 2019). Solid lines: MIS 13; dotted lines: MIS 12; dashed lines: MIS 11; black lines: warmest interval within individual MIS; grey lines: coldest interval within individual MIS. Data gaps occur where sample transect points fall in maritime zones during specific periods.

transect (Transect A [south-north]: U = 22.5 [n = 16], p = 0.238; Transect B [east-west]: U = 39.5 [n = 22], p = 0.171.

Minimum temperature of the coldest month (Bio6) The MAT trends are exacerbated in the case of the minimum temperatures of the coldest month. These values are also at their largest during MIS 12 (warmest and coldest intervals), with the largest ranges occurring during MIS 12 on the south-north transect (13.2–14.5 °C; Table 7; Figs. 11 and 12). However, in MIS 13 and 11 (warmest and coldest intervals) there is greater variability on the east-west transect (e.g., range values of 7.6 °C and 10.1 °C in the MIS 13 warmest and coldest intervals, respectively; Table 7). There is also reduced variability in the Bio6 variable along the south-north transect during the MIS 13 and 11 warmest intervals when compared to the MAT data (e.g., a range value of 4.3 °C compared to 5.0 °C for the MIS 13 warmest interval; Tables 6 and 7). This reduction in Bio6 variability relative to MAT is not apparent on the east-west transect (e.g., a range value of 7.4 °C compared to 3.9 °C for the MIS 11 warmest interval; Tables 6 and 7). In all cases, Bio6 values decreased to the north (Transect A; Fig. 12) and increased to the west (Transect B; Fig. 12). Statistical comparison of the Bio6 data for the 490 ka and 410 ka intervals indicated no significant differences on either transect (Transect A [south-north]: U = 24.0 [n = 16], p = 0.442; Transect B [east-west]: U = 45.0 [n = 22], p = 0.332).

The mean temperatures of the coldest quarters (Bio11; SOM Table S2) similarly vary along the south-north and east-west transects (with highest values in the south and the west), offering a climatic perspective on the contrasting Lower Paleolithic record east and west of the Rhine. The Bio11 variable also emphasizes the

Table 8
Maximum temperature of the warmest month values (°C; see also Figs. 13 and 14) for warmest and coldest intervals in MIS 13, MIS 12, and MIS 11, derived from Oscillayers outputs for the Bio5 variable (Gamisch, 2019).

	MIS 13		MIS 12		MIS 11	
	Warmest interval (490 ka)	Coldest interval (530 ka)	Warmest interval (430 ka)	Coldest interval (440 ka)	Warmest interval (410 ka)	Coldest interval (380 ka)
Transect A (south-north)[a]						
Maximum	30.0	24.0	24.7	24.0	30.6	27.7
Minimum	19.9	15.8	16.3	15.8	20.3	18.3
Range	10.1	8.2	8.4	8.2	10.3	9.4
Transect range[b]	−10.1	−8.2	−8.4	−8.2	−10.3	−9.4
Transect B (east-west)[a]						
Maximum	22.9	17.9	18.4	17.9	23.4	20.8
Minimum	19.1	13.4	14.1	13.4	19.7	16.9
Range	3.8	4.5	4.3	4.5	3.7	3.9
Transect range[c]	−0.6	+2.0	+1.8	+2.0	−0.9	+0.4

[a] Values were sampled at 10% intervals along the transects. Maximum, minimum, range, and transect range values were calculated from these samples. Range values are the difference between the minimum and maximum values along the entire transect. Transect range values are the difference between the two values at either end of the transect.
[b] Positive signs indicate values increasing from south to north; negative signs indicate values decreasing from south to north.
[c] Positive signs indicate values increasing from east to west; negative signs indicate values decreasing from east to west.

potentially significant difference between minimum annual temperatures (which may only need to be tolerated for a few days each year) and the general conditions associated with the coldest periods of the year (e.g., in south-east Britain during late MIS 13 [490 ka model], the latter values are just above, rather than below, freezing).

Maximum temperature of the warmest month (Bio5) These estimates range most widely along the south-north transect (varying up to 10.3 °C during the MIS 13 and 11 warmest intervals), with ranges broadly comparable (spanning 8.2–10.3 °C) across the entire MIS 13–11 period (Table 8; Figs. 13 and 14). In contrast, the east-west transect temperature ranges are much lower, spanning 3.7–4.5 °C, but are again comparable across all six intervals (Table 8). There is also evidence of greater local geographical variability along the east-west transect (Fig. 14): in all cases, the transect ranges were narrower than the ranges (Table 8). During the MIS 13 and 11 warmest intervals maximum temperatures of the warmest month decreased to the west, whereas in the MIS 13 and 11 coldest intervals and in MIS 12 those temperatures increased to the west (Table 8; Fig. 14). In all cases on the south-north transect, maximum temperatures of the warmest month were lower in the north (Table 8; Fig. 14). Statistical comparison of the Bio5 data for the 490 ka and 410 ka intervals indicated no significant differences on either transect (Transect A [south-north]: $U = 26.5$ [$n = 16$], $p = 0.574$; Transect B [east-west]: $U = 43.5$ [$n = 22$], $p = 0.270$).

These trends are broadly mirrored in the mean temperatures of the warmest quarter (Bio10; SOM Table S3). However, the mean temperatures of the driest quarter (Bio9; SOM Table S4) vary substantially along both transects: the highest values occur in the south and west, with implications for water access during these dry periods given the associated trends in Bio14 (precipitation of the driest month; SOM Table S5), Bio17 (precipitation of the driest quarter; SOM Table S6), and Bio18 (precipitation of the warmest quarter; SOM Table S7).

Seasonality and diurnal variability Temperature seasonality (Bio4; SOM Table S8) and annual temperature range (Bio7; SOM Table S9) have implications for the feasibility of year-round occupations. Both show greater variation on the east-west transect, with higher values occurring in the east and at the northern (Britain) and southern (Iberian interior) ends of the south-north transect. Mean diurnal ranges (Bio2; SOM Table S10) have implications for the maintenance of core temperature at nights and show greater variation along the south-north transect, with larger values tending to occur in the south during MIS 13 and 11, although there is considerable local variability and no clear pattern in MIS 12. Finally, isothermality values (Bio3; SOM Table S11), which quantify day–night temperature oscillations relative to summer–winter oscillations, indicate broadly comparable variability on both transects, with higher values (i.e., greater relative day–night oscillations) occurring in the south and the west.

Precipitation (Bio12) Precipitation variability is more marked along the east-west transect (580–602 mm), with higher values in the west and only small variations between the warmest and coldest intervals (Table 9; Figs. 15 and 16). The ranges on the south-north transect are generally lower (338–375 mm in MIS 13 and 11), with the exception of MIS 12 (798–827 mm), with consistently higher values in the north (Table 9). In all cases, the impact of local factors, for example, topography, is clear, with transect ranges narrower than the range (Table 9; Fig. 16). Statistical comparison of the precipitation data for the 490 ka and 410 ka intervals indicated no significant differences on either transect (Transect A [south-north]: $U = 33.0$ [$n = 16$], $p > 0.999$; Transect B [east-west]: $U = 61.0$ [$n = 22$], $p > 0.999$).

The east-west trends are broadly mirrored in the precipitation of the wettest month (Bio13; SOM Table S12), precipitation of the wettest quarter (Bio16; SOM Table S13), and the precipitation of the coldest quarter (Bio19; SOM Table S14), with the greatest variations occurring on the east-west transect (with the exception of MIS 12) and the highest values associated with the coastal west. Variability on the south-north transect was less marked and more localized for Bio13, 16, and 19 (SOM Tables S12–S14). The mean temperatures of the wettest quarter (Bio8; SOM Table S15) vary markedly, partly reflecting the impacts of topography, but do highlight potential regional challenges such as lower temperatures in the west, resulting in several months of relatively cool, wet conditions (White, 2006).

By contrast, precipitation of the driest month (Bio14; SOM Table S5) varies on both the south-north and east-west transects, with very dry conditions in Iberia (and more localized variability elsewhere). The south-north trend is also evident in the precipitation of the warmest quarter (Bio18; SOM Table S7) and the precipitation of the driest quarter (Bio17; SOM Table S6), although the latter measure also varies clearly along the east-west transect, with wetter conditions in the north and the east (precipitation of the warmest quarter) and in the north and the west (precipitation of the driest quarter). Reflecting these trends, precipitation seasonality (Bio15; SOM Table S16) varies most clearly on the south-north transect, with the highest values in the south, where these conditions may have formed a significant seasonal challenge to the water-finding strategies of hominins and other species.

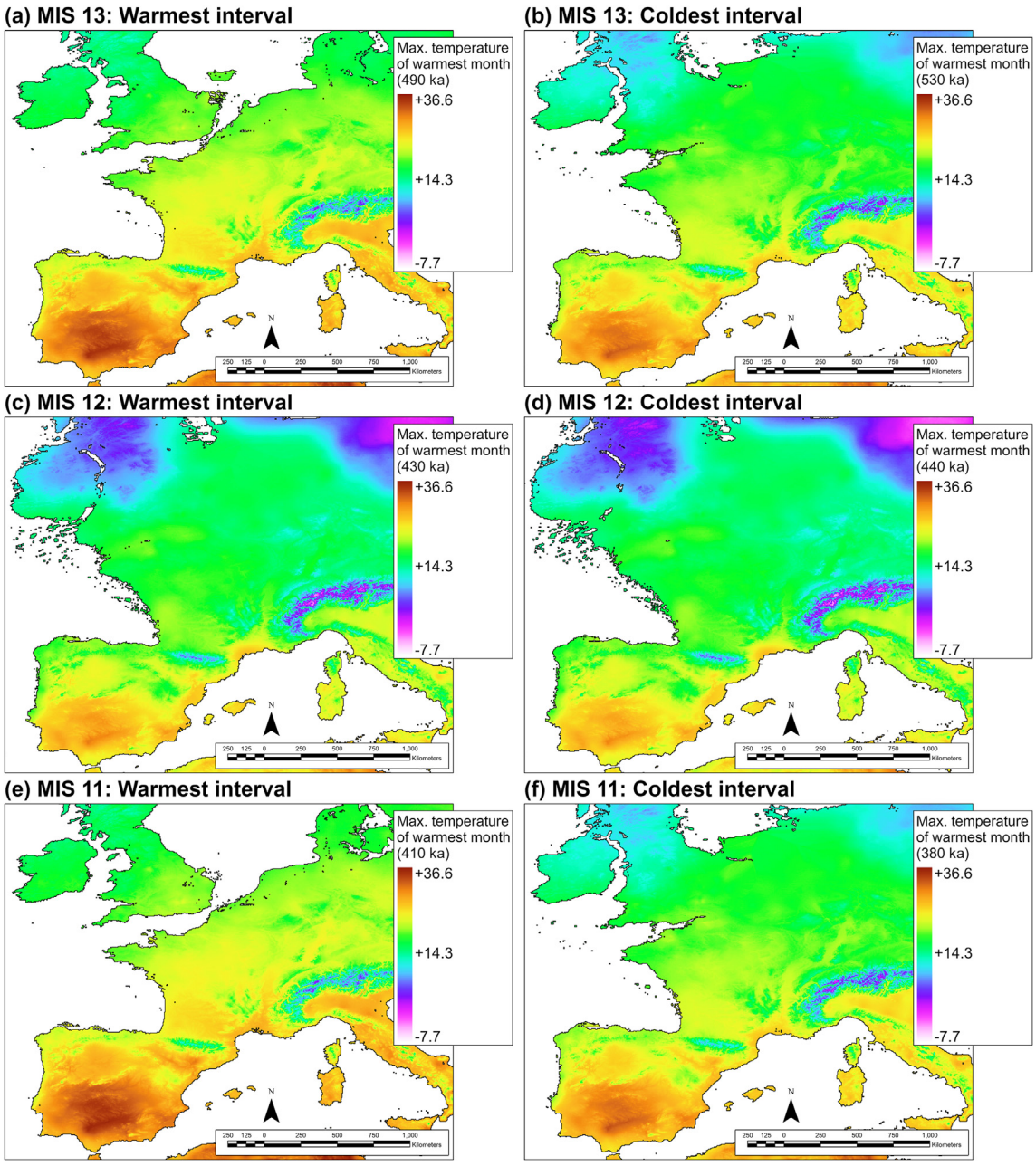

Figure 13. Reconstructed paleocoastlines and maximum temperature of the warmest month (°C; Bio5) estimates for the warmest (a, c, and e) and coldest intervals (b, d, and f) in MIS 13 (a and b), MIS 12 (c and d), and MIS 11 (e and f), using the 10 kyr-stepped outputs from Gamisch (2019). Color scale based on minimum (−7.7 °C, pink) and maximum values (+36.6 °C, brown) across all six maps. Figure created in ArcGIS Pro v. 2.6.1 (map projection: WGS, 1984). Note that the Oscillayers mapping for the warmest MIS 13 interval (a) does not represent the Weald–Artois ridge. (For interpretation of the references to color in this figure legend, the reader is referred to the Web version of this article).

In summary, statistical comparisons of the transect data for MAT (Bio1), maximum temperature (Bio5), minimum temperature (Bio6), and annual precipitation (Bio12) for the 490 ka and 410 ka intervals suggest no significant differences.

3.5. Question 5: Are there greater proportions of north-western European landscapes with tolerated temperatures—as defined by hominin-occupied sites—in Marine Isotope Stage 11 compared to Marine Isotope Stage 13?

The maps of potential hominin landscapes in north-west Europe (Fig. 17) highlight the wide geographical scope of landscapes potentially suitable, on paleoclimatic grounds (T_{max} and T_{min}) for hominins, including the increasing availability of more continental areas in MIS 11c (Fig. 17a). The percentage of suitable areas increases from 35% (late MIS 13) to 63% (MIS 11c). However, the late MIS 13 mapping (Fig. 17b) is partially restricted by limitations in the number, distribution, and dating precision of sites with T_{max} and T_{min} values. The sites that generated the T_{min} and T_{max} ranges for the late MIS 13 map were all located in southern Britain, with the result that the upper limit for T_{max} was constrained in comparison to the sample for the MIS 11c map. This is reflected in areas of the MIS 13 mapping, for example, in northern France, being mapped as unsuitable (Fig. 17b). Nonetheless, and in combination with the

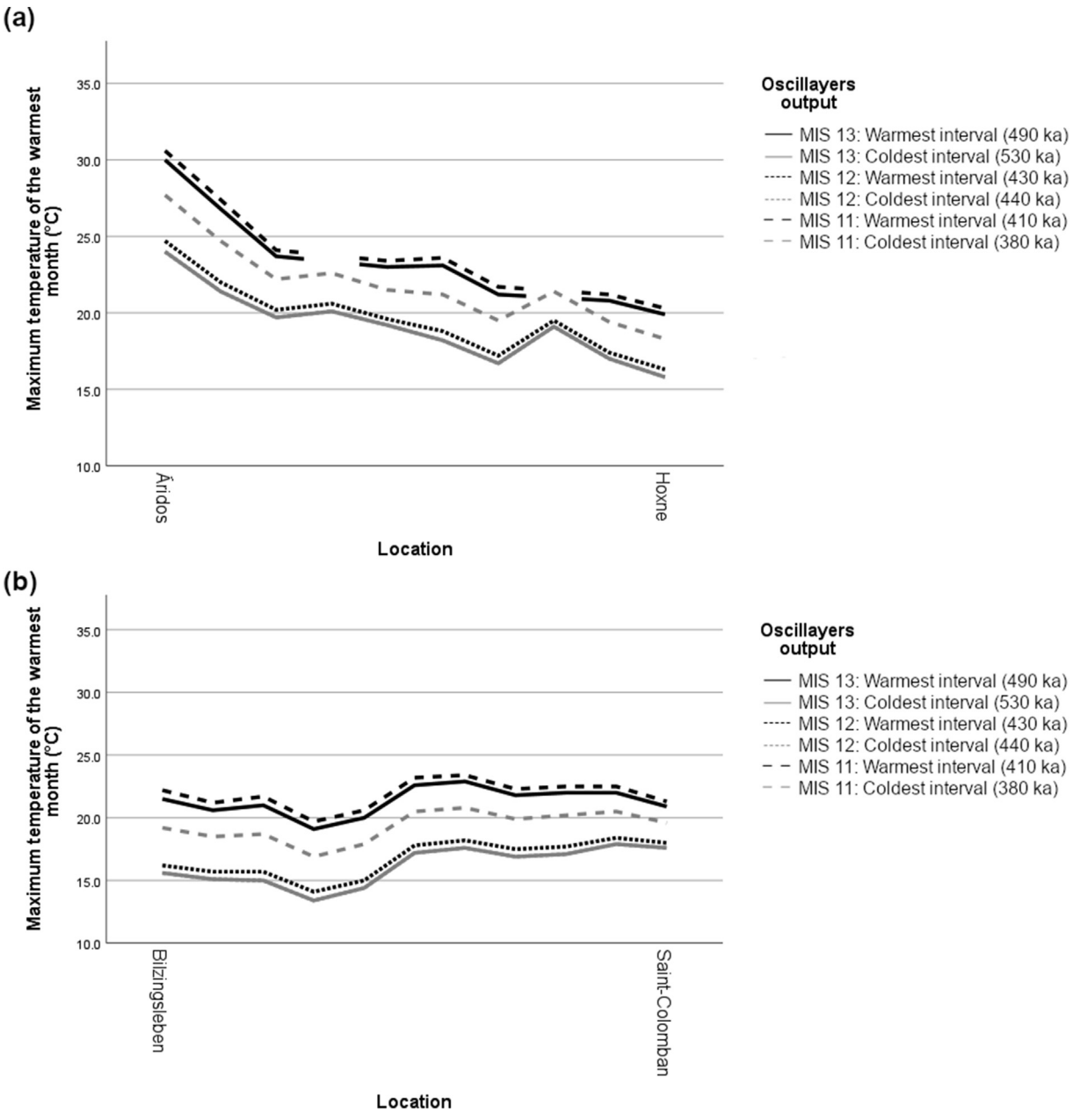

Figure 14. Maximum temperature of the warmest month values (°C; see also Fig. 13 and Table 8) along south-north transect (a) and east-west transect (b), for warmest and coldest intervals in MIS 13, MIS 12, and MIS 11, derived from Oscillayers outputs for the Bio5 variable (Gamisch, 2019). Solid lines: MIS 13; dotted lines: MIS 12; dashed lines: MIS 11; black lines: warmest interval within individual MIS; grey lines: coldest interval within individual MIS. Data gaps occur where sample transect points fall in maritime zones during specific periods.

transect data (Question 4), Figure 17 highlights that tolerable, if not necessarily preferable, climates were available to hominins across wide areas of north-western Europe (see also Blain et al., 2021, fig. 5). If the coastal zone was a preferred habitat, then it seems likely that its particular attractions were a combination of milder climates and favorable dietary and raw material resources (see also Cohen et al., 2012; Lewis et al., 2019).

4. Discussion

Although MIS 13–11 site distributions in time and space are uneven, site-specific temperature and environmental reconstructions for both hominin and nonhominin sites (Tables 2 and 10), combined with global isotopic data sets (Figs. 2 and 3) and Oscillayers data (Figs. 5 and 10–16; Tables 6–9; SOM Figs. S2–S16) permit an assessment of western European paleoclimatic and paleoenvironmental fluctuations across MIS 13–11. Site-specific temperatures broadly mirror modern European climatic trends (Fig. 18a, b), suggesting that modern ecosystem trends (e.g., in net primary productivity; Fig. 18c) may also have parallels in MIS 13–11. These fluctuations are the context for regular hominin extirpations and/or range expansions and contractions, at both MI stage and substage scales, with the latter increasingly suggested by distinctive artifact patterning (Ashton et al., 2016; Davis and Ashton, 2019).

Table 9
Annual precipitation values (mm; see also Figs. 15 and 16) for warmest and coldest intervals in MIS 13, MIS 12, and MIS 11, derived from Oscillayers outputs for the Bio12 variable (Gamisch, 2019).

	MIS 13		MIS 12		MIS 11	
	Warmest interval (490 ka)	Coldest interval (530 ka)	Warmest interval (430 ka)	Coldest interval (440 ka)	Warmest interval (410 ka)	Coldest interval (380 ka)
Transect A (south-north)[a]						
Maximum	824	833	1331	1366	823	829
Minimum	457	495	533	539	448	490
Range	367	338	798	827	375	339
Transect range[b]	+148	+127	+107	+102	+153	+130
Transect B (east-west)[a]						
Maximum	1114	1099	1084	1080	1118	1101
Minimum	514	508	501	500	516	509
Range	600	591	583	580	602	592
Transect range[c]	+395	+438	+483	+494	+385	+433

[a] Values were sampled at 10% intervals along the transects. Minimum, maximum, range, and transect range values were calculated from these samples. Range values are the difference between the minimum and maximum values along the entire transect. Transect range values are the difference between the two values at either end of the transect.
[b] Positive signs indicate values increasing from south to north; negative signs indicate values decreasing from south to north.
[c] Positive signs indicate values increasing from east to west; negative signs indicate values decreasing from east to west.

4.1. Marine Isotope Stages 13–11: Site-specific perspectives

Winter and summer temperatures on British MIS 13 sites were colder than the majority of MIS 11 sites, and generally fell below those of the present day, with more marked discrepancies in the summer data (Table 2; Fig. 7). For reference, T_{min} (January) and T_{max} (July) temperatures for present day eastern England are ca. 3–4 °C and ca. 16–17 °C, respectively (Candy et al., 2010, 2011b, 2015). Marine Isotope Stage 13 habitats predominantly consist of boreal woodland (Table 10), with implications for primary productivity and primary and secondary biomass, and potentially for hominin mobility: extant hunter-gatherers tend to move frequently in high biomass areas such as boreal forests, which are characterized by relatively inaccessible plants and animals (see Kelly, 1983, table 6).

Marine Isotope Stage 12 occupations are predominantly associated with south-western Europe (e.g., Caune de l'Arago and Atapuerca [Trinchera Dolina 10.4]), where conditions were relatively stable (López-García et al., 2021). This is in marked contrast to northern sites associated with MIS 12 (e.g., Ostend) or MIS 11 cold substages (e.g., Quinton Faunal Unit 2). Habitats at Atapuerca predominantly consisted of Mediterranean open woodland, with steppe occurring in the coldest and driest periods (Rodríguez et al., 2011).

Marine Isotope Stage 11c conditions on British sites were similar to those of the Mid-Holocene, with summer temperatures 1 or 2 °C warmer than the present day (Candy et al., 2010), although winter estimates tend to be slightly below present-day equivalents (Candy et al., 2014). The associated greater seasonality may in part reflect greater obliquity in early MIS 11 (Fig. 4). While climates may have been warmer than the present, they were not exceptionally warm in comparison with other interglacials (e.g., MIS 5e or the Mediterranean-type conditions at Pakefield in MIS 17 or 19; Candy et al., 2011b). The southern British vegetation succession for MIS 11 is also well known (overall the dominant arboreal pollen shifts from birch/pine to alder/oak to fir, and back to birch/pine; Candy et al., 2014, their fig. 5), and both specific sites and regional correlations across north-western Europe suggest the repeated association of MIS 11c archaeological sites with peak forest conditions (Limondin-Lozouet et al., 2015; Ashton, 2016). The summer temperatures associated with those MIS 11c occupations (e.g., at Barnham and Swanscombe) were generally warmer than those at MIS 13 sites (e.g., at High Lodge and Happisburgh 1), with the exception of Boxgrove. These latter differences may reflect variations in the specific ages of Boxgrove, High Lodge and Happisburgh 1 in late MIS 13 (Table 2), or possibly the coastal plain setting of Boxgrove (and its south-facing Chalk cliff-line).

Post-MIS 11c conditions were cooler, however, significantly so during MIS 11b, although estimates vary between sites (e.g., contrast Quinton [Faunal Units 2 and 3], Beeches Pit [Bed 7] and Hoxne [Stratum A and B] in Tables 2 and 10). The coolest of these estimates highlight the significance of Ashton et al.'s (2008a) reinterpretation of the timing of the Hoxne occupations, and raise the possibility of a step-change in hominin 'over-wintering' solutions between MIS 11c and 11a. The overall evidence is ambiguous, however, as some of the estimates, for example for Beeches Pit (Bed 7), are broadly comparable with late MIS 13 sites (e.g., Happisburgh 1).

Climatic and environmental similarities between nonhominin and hominin sites, especially in MIS 11 (e.g., Marks Tey/Hoxne [Stratum D] and Barnham; Tables 2 and 10), suggest that the apparent human absence at the former is due to factors other than climatic tolerances or preferences (Fig. 19). These may include taphonomic and sampling issues, as previously discussed by Ashton et al. (2006) with regard to fluvial and lacustrine settings in MIS 11. Behavioral preferences linked to landscape features, for example, the varying connectivity of lakes and rivers (Ashton et al., 2006), may be a further factor, although both types of landscape setting occur with and without hominin evidence.

Overall, late MIS 13 hominin site conditions (e.g., at Happisburgh 1, Waverley Wood, and Brooksby) are generally harsher than those of MIS 11c, with summer and, especially, winter temperatures lower than at present (see also Candy et al., 2015). These temperatures are reflected in boreal and some open ground vegetation, and may also be reflected in relatively small archaeological assemblages at selected sites (e.g., 199 flakes, flake tools, and cores at Happisburgh 1; Ashton et al., 2008b; Lewis et al., 2019), although larger artifact assemblages also occur (e.g., Boxgrove; Roberts and Parfitt, 1999; Pope et al., 2020). By contrast, MIS 11c hominin sites are associated with warmer conditions and peak interglacial woodland (e.g., La Celle, Barnham, and Swanscombe). The MIS 13 and 11 occupations may therefore highlight a contrast between hominin tolerances (MIS 13 sites) and hominin preferences (MIS 11c sites) during this period. However, the lack of a significant difference between the winter conditions at the British MIS 11 and MIS 13 sites (Fig. 7b), although the latter are more wide-ranging, suggests that any technological, behavioral, and/or social

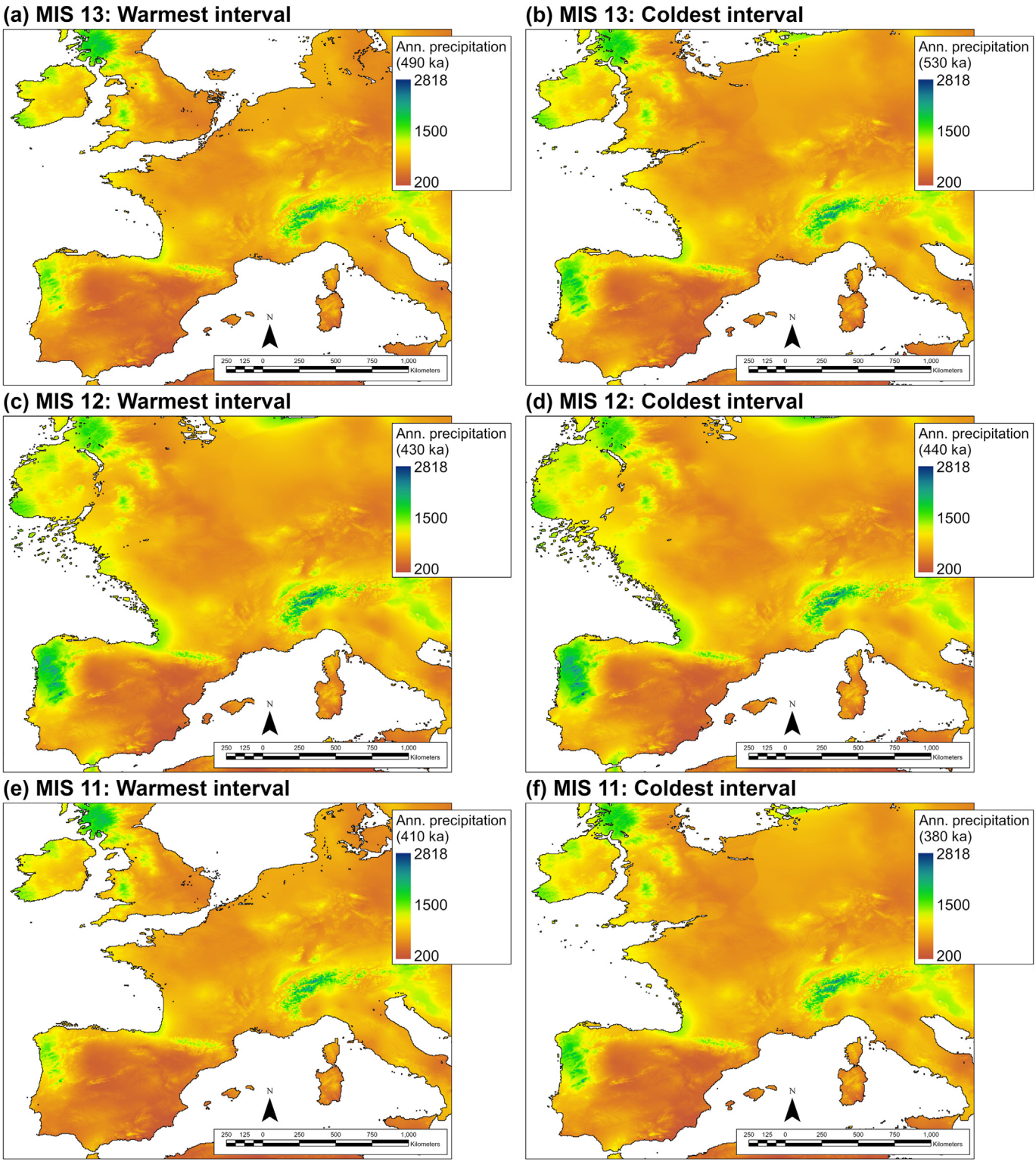

Figure 15. Reconstructed paleocoastlines and annual precipitation (mm; Bio12) estimates for the warmest (a, c, and e) and coldest intervals (b, d, and f) in MIS 13 (a and b), MIS 12 (c and d), and MIS 11 (e and f), using the 10 kyr-stepped outputs from Gamisch (2019). Color scale based on minimum (200 mm, brown) and maximum values (2818 mm, blue) across all six maps. Figure created in ArcGIS Pro v. 2.6.1 (map projection: WGS, 1984). Note that the Oscillayers mapping for the warmest MIS 13 interval (a) does not represent the Weald–Artois ridge. (For interpretation of the references to color in this figure legend, the reader is referred to the Web version of this article).2

solutions to the 'overwintering problem' (Roebroeks, 2001; Hosfield, 2016, 2020; MacDonald, 2018; Rodríguez et al., 2021) may have already been present by MIS 13.

While the hominin expansion into north-western Europe during late MIS 13 (Hosfield and Cole, 2018) therefore seems to have occurred against a backdrop of cooler conditions than those of MIS 11c, it also occurs toward the end of a period of generally sustained mild conditions spanning MIS 15–13 (Candy and Alonso-Garcia, 2018). These conditions may have facilitated repeated hominin expansions throughout that period (isotopic conditions in early and

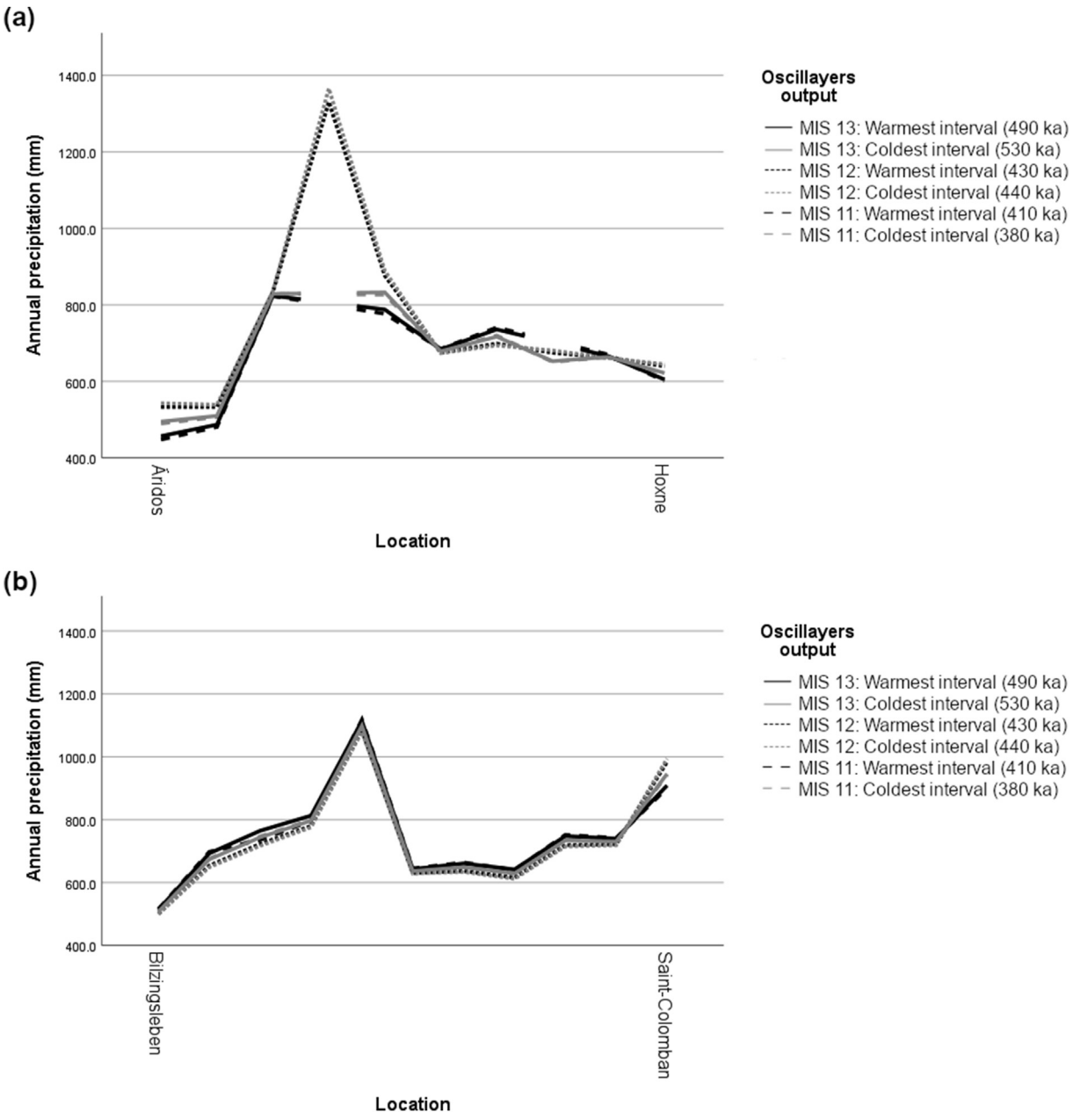

Figure 16. Annual precipitation values (mm; see also Fig. 15 and Table 9) along south-north transect (a) and east-west transect (b), for warmest and coldest intervals in MIS 13, MIS 12, and MIS 11, derived from Oscillayers outputs for the Bio12 variable (Gamisch, 2019). Solid lines: MIS 13; dotted lines: MIS 12; dashed lines: MIS 11; black lines: warmest interval within individual MIS; grey lines: coldest interval within individual MIS. Data gaps occur where sample transect points fall in maritime zones during specific periods.

late MIS 15 are at least comparable with late MIS 13 conditions), potentially reflected in the oldest artifact collections in the Bytham river landscape of eastern England (Moncel et al., 2015; Davis et al., 2017). A weaker latitudinal transect between north-west and south-west Europe in late MIS 13 may also be significant. This was previously suggested by Candy et al. (2015) and is potentially supported here by the 490 ka Oscillayers data, which estimates a MAT range of 5 °C for the south-north transect during the MIS 13 warmest interval (Table 6; compared to the 4 °C sea-surface temperature range reported by Candy et al., between 39°02′N, 10°40′W and 53°32′N, 20°17′W; Kandiano and Bauch, 2003; Rodrigues et al., 2011). The relatively small ranges in the minimum temperatures of the coldest month and mean temperatures of the coldest quarters along the south-north transect for the MIS 13 warm interval (4.3 °C and 3.7 °C, respectively; Table 7; SOM Table S2) may be a further factor in favor of range expansion in western Europe at this time, along with the relative stability in selected precipitation measures (e.g., precipitation of the wettest month and the wettest quarter; SOM Tables S12 and S13). The mean temperatures of the coldest quarter may be particularly significant (SOM Table S2), as they highlight the difference between the most extreme conditions, which may only have needed to be tolerated for a few days each year, and the general conditions associated with the coldest period of the year.

4.2. Marine Isotope Stages 13–11: Regional perspectives

South-western European conditions were clearly warmer overall (Fig. 20) in both MIS 11 (Ambrona, Áridos 1, Aroeira, and Trinchera Dolina 10.3) and MIS 12 (Caune de l'Arago and Sima de

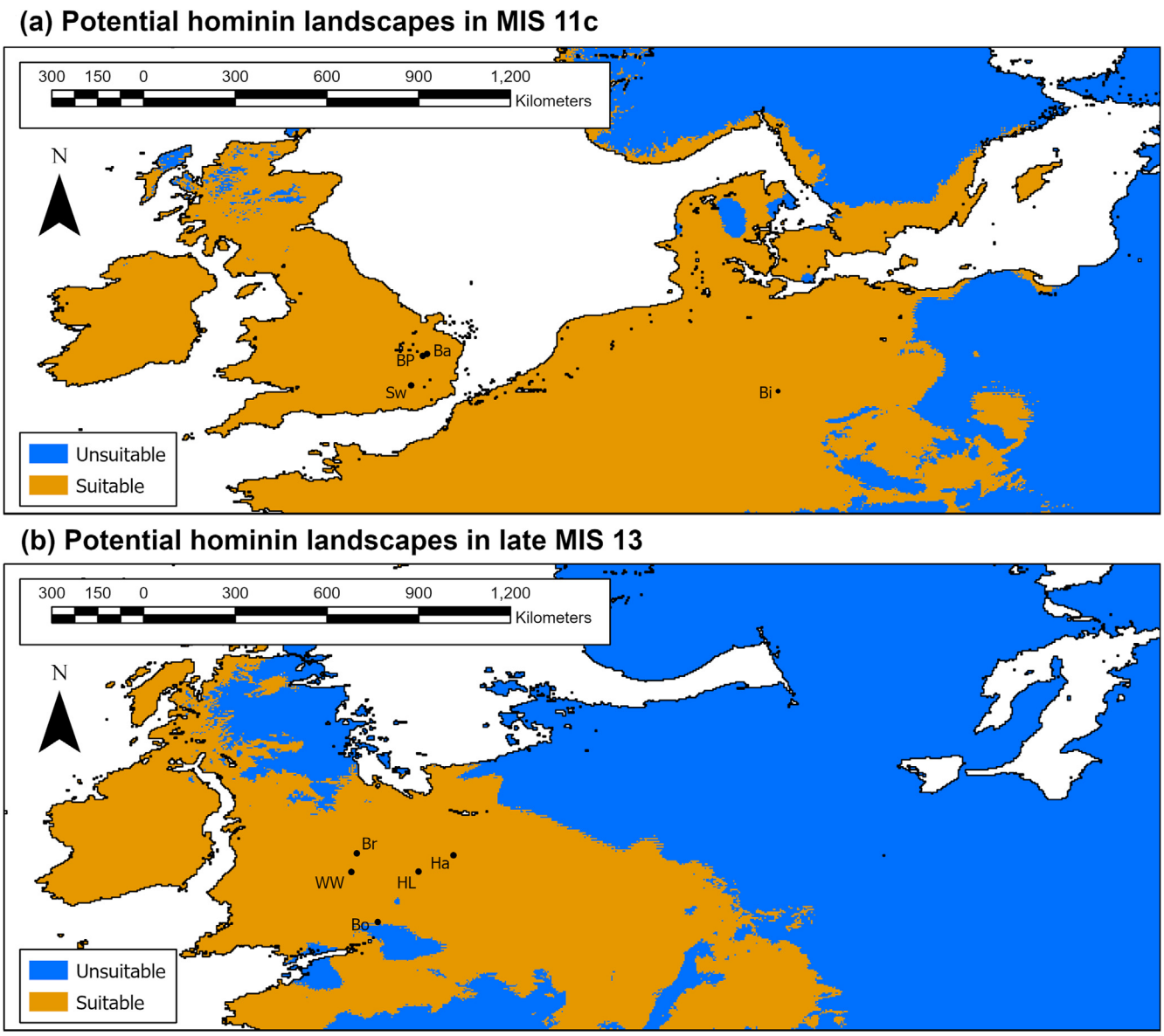

Figure 17. Predictive maps of potential hominin landscapes in north-western Europe for MIS 11c (a) and late MIS 13 (b), derived from Oscillayers outputs for 410 ka and 490 ka. Site-specific T_{min} and T_{max} temperature estimates for a) Ambrona, Áridos 1, Barnham (Ba), Beeches Pit (BP), Bilzingsleben (Bi), Gruta da Aroeira, Swanscombe (Lower Loam and Lower Middle Gravel; Sw), and Trinchera Dolina (TD-10.3; MIS 11), and b) Boxgrove (Bo), Brooksby (Br), Happisburgh 1 (Ha), High Lodge (HL), and Waverley Wood (WW; late MIS 13). See Figure 1 for the locations of Ambrona, Áridos 1, Gruta da Aroeira, and Trinchera Dolina (TD-10.3).

los Huesos), indicating a likely role for these areas as glacial refugia (Stewart et al., 2010) and potential population sources after periods of hominin extirpation in northern Europe. Marine Isotope Stage 12 occupations in western Europe are predominantly associated with the south-west, where conditions were relatively stable (López-García et al., 2021), in marked contrast to northern sites associated with MIS 12 (e.g., Ostend) or MIS 11 cold substages (e.g., Quinton Faunal Unit 2). However, it is also possible that the favorable MIS 12 conditions suggested at Sima de los Huesos reflect a temporary forest expansion during substage MIS 12b (López-García et al., 2021), emphasizing the scope for even more marked European de-populations during the coldest and driest, steppe-dominated stages of MIS 12 (Dennell et al., 2011; Rodríguez et al., 2011; MacDonald et al., 2012). The modeled precipitation values of the driest month and driest quarter in the Oscillayers data set (SOM Tables S5 and S6) also highlight specific water-finding challenges in the Iberian Peninsula, particularly during MIS 12.

Taking an east-west perspective there are overall similarities between fully temperate conditions in north-western and north-central Europe, at both hominin (e.g., between Bilzingsleben and Barnham/Swanscombe) and nonhominin sites (e.g., between Dethlingen/Bilshausen and Woodston/Quinton [Faunal Unit 1]; Tables 2 and 10), although summer conditions may have been warmer in the continental interior (e.g., at Bilzingsleben) compared to other north-western sites (e.g., Swanscombe). Summer temperatures do not appear to have been so high as to be problematic (the highest Bilzingsleben estimates are comparable to, for example, the estimates at Áridos 1 and Gruta da Aroeira), although access to freshwater and shade was presumably an important part of daily life. These temperature estimates suggest that the smaller

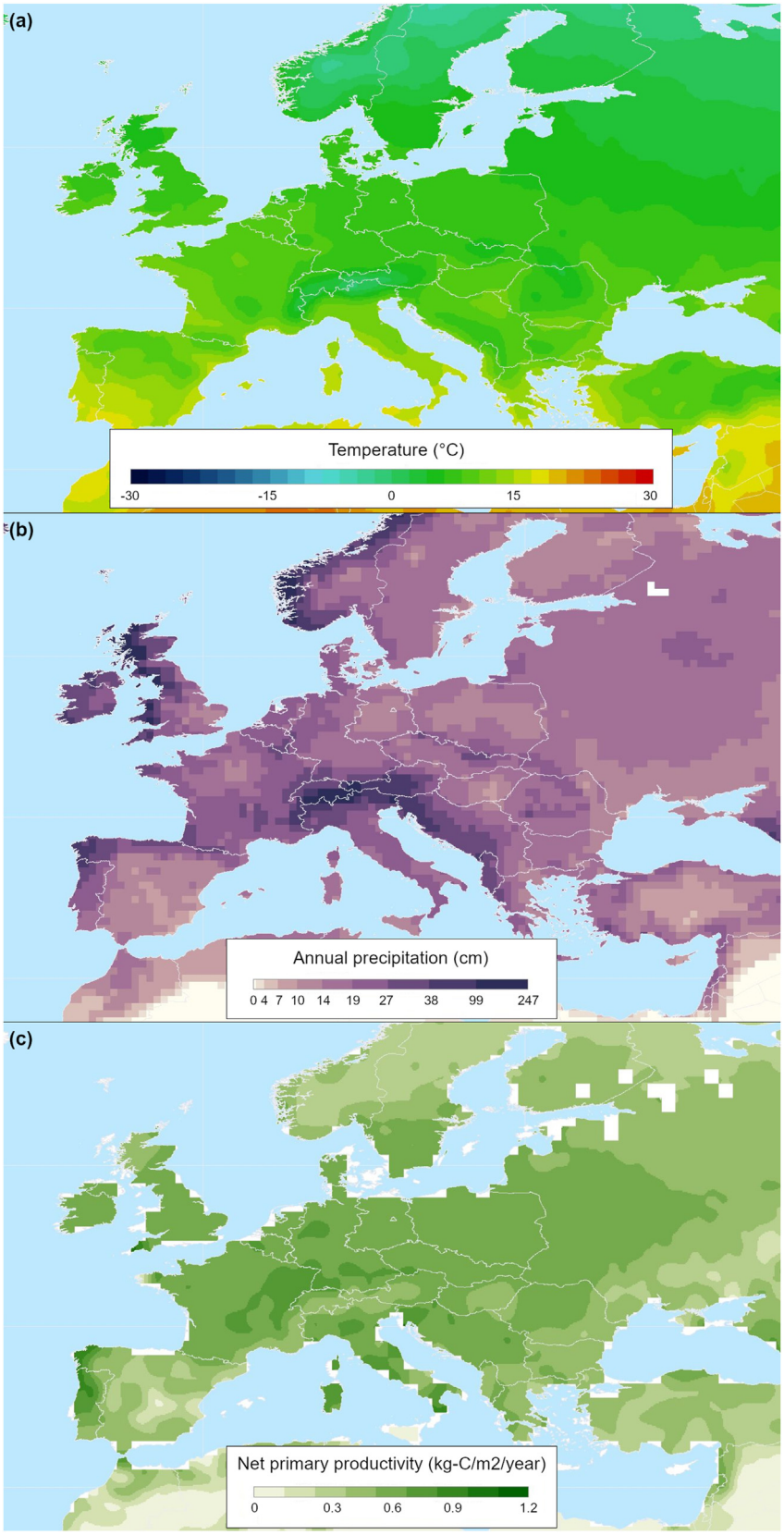

Figure 18. Modern European environmental variables: a) mean annual temperature (°C; source: CRU [Climate Research Unit, University of East Anglia] 0.5 Degree Dataset; color scale: −30 °C [dark blue] to +30 °C [red]); b) annual precipitation (cm/year; source: CRU, 0.5 Degree Dataset; color scale: 0 cm [white] to 247 cm [dark purple]); c) net primary productivity (kg-C/m2/year; sources: Foley et al., 1996; Kucharik et al., 2000; color scale: 0 [pale green] to 1.2 [dark green]). Note that modern European climatic patterns (a and b) broadly mirror the trends in MIS 13 and MIS 11, and site-specific estimates (Tables 2 and 6–9; Figs. 5 and 10–16), suggesting that modern ecosystem trends such as net primary productivity (c) may also have parallels in MIS 13–11. All images used by permission of The Center for Sustainability and the Global Environment (SAGE), Nelson Institute for Environmental Studies, University of Wisconsin–Madison. Figure legends re-drawn. (For interpretation of the references to color in this figure legend, the reader is referred to the Web version of this article).

Table 10
Paleoenvironmental reconstructions for selected western European MIS 13–11 sites (hominin—artifacts and/or fossils—and nonhominin). See Table 2 for paleoclimatic estimates for selected sites.

Sites	Paleoenvironment	References
MIS 13		
Bilshausen (beginning of warm stage)[a]	Pollen dominated by spruce, pine, alder, elm and birch.	Szymanek and Julien (2018)
Bilshausen (peak interglacial)[a]	Abundant hornbean and fir pollen.	Szymanek and Julien (2018)
Bilshausen (end of warm stage)[a]	Increase in pine and reduction in deciduous woodland.	Szymanek and Julien (2018)
Boxgrove (Unit 4b)[b]	Coastal mudflats, in a lagoonal-type environment, with occasional drying out and spread of grassland; temperate climate (not peak interglacial).	Parfitt (1999); Roberts (1999)
Boxgrove (Unit 4c and correlative units in Q1/B)[b]	Grassland, scrub, and mixed woodland, with spring-fed, shallow, permanent pools; possibly more continental climate than present.	Holman (1999); Parfitt (1999); Roberts (1999); Holmes et al. (2010)
Brooksby (Redland's Brooksby Channel)[b]	Large meandering river with floodplain pools and marshes, and local willow or alder woodland; flowing water throughout the year and permanently damp conditions.	Coope (2006)
Happisburgh 1 (Organic mud)[b]	Grassland floodplain, with reed swamp and sedges surrounding abandoned channels and pools, fringed by pine and birch woodland; cool-temperate climate; precipitation sufficient to maintain marshes throughout summer.	Coope (2006); Lewis et al. (2019)
High Lodge (Bed C1)[b]	Floodplain with pools and marshland (reed swamp); surrounding vegetation dominated by pine and spruce, with juniper and heathland plants; cool, slightly damp continental climate; relatively low summer rainfall.	Hunt (1992); Coope (2006)
Mathon (Brays Bed)[a]	Fairly fast-flowing river, fringed with grassy marshland and alder; surrounding woodland dominated by coniferous trees (e.g., pine, spruce, fir and larch), with scattered trees of oak, elm and hornbeam on drier ground; cool temperate climate.	Coope et al. (2002)
Miesenheim I[b]	Sparse pine-birch forests, final part of the warm stage.	Szymanek and Julien (2018)
Pools Farm Pit (Brandon Lower Organic Sands and Silts)	Fully temperate conditions; boreal forest vegetation.	Maddy et al. (1994)
Sidestrand (*Unio* Bed)[a]	Large body of slow-flowing freshwater, fringed by a mixture of marsh, shrub or woodland and extensive dry grassland habitats; temperate climate.	Preece et al. (2009)
Waverley Wood (Channel 2, Organic Mud)[b]	Sluggish river with oxbow lakes and marshland, grading into meadow-like habitats, with scattered stands of conifers and occasional deciduous trees beyond; cool temperate conditions (with hominin occupation likely associated with higher temperatures).	Coope (2006)
MIS 12		
Caune de l'Arago (G1 and G2)[b]	Cold, dry climatic conditions, with open environments (e.g. meadows).	López-García et al. (2021)
Caune de l'Arago (G3 and G4)[b]	Temperate, open-woodland environments, with associated Mediterranean and wetland faunas.	López-García et al. (2021)
Sima de los Huesos (LU 6)[b]	Open woodland landscape, with mild climatic conditions.	López-García et al. (2021)
MIS 11		
Ambrona (AS4/3)[b]	Warm temperate and humid; open dry and wet meadows and woodland areas (pine, with temperate elements, e.g., hazel).	Blain et al. (2015)
Áridos 1[b]	Warm and humid forest period; patchy landscape, with a mixture of dry meadows, scrubland and rocky habitats together with aquatic habitats.	Blain et al. (2014)
Barnham (Unit 5c; HoII)[b]	Large waterbody, varying between still and flowing, with a patchwork of marsh, open grassland, and deciduous woodland; warmer summers than present.	Holman (1998); Parfitt (1998a, 1998b); Ashton and Lewis (2012)
Beeches Pit (Bed 3b; HoIIb–c)[b]	Temperate climate; stagnant pools with calcareous grassland and surrounding open woodland.	Preece et al. (2007)
Beeches Pit (Bed 4; HoIIIb–IV)[b]	Fully temperate environment, with warmer summers and higher rainfall than present; shallow, spring-fed pools with deciduous woodland (initially closed, with subsequent opening of canopy).	Preece et al. (2007)
Beeches Pit (Bed 7)[b]	Cold, fluvial environment, with still or slow-flowing water.	Preece et al. (2007); Benardout (2015)
Bilzingsleben II[b]	Fully temperate, with subcontinental influences; mixed oak woodland and shrub associations, alternating with steppe meadows; annual precipitation from 600 to at least 850 mm.	Mania (1995); Mania and Mania (2003); Szymanek and Julien (2018)
Dethlingen, Hetendorf and Munster-Breloh (beginning of warm stage)[a]	Boreal forest (birch and pine).	Szymanek and Julien (2018)
Dethlingen, Hetendorf and Munster-Breloh (peak interglacial)[a]	Temperate mixed forests (boreal and atlantic taxa); mean annual precipitation: 600–650 mm.	Szymanek and Julien (2018)
Dethlingen, Hetendorf and Munster-Breloh (end of warm stage[a]	Gradual opening of forests and predominance of open environments.	Szymanek and Julien (2018)
Gruta da Aroeira[b]	Open woodland landscape and temperate conditions.	López-García et al. (2021)
Hoxne (Stratum D; HoIIIa)[a]	Lush water meadow and reed swamp/alder carr, with silting-up of the preceding interglacial lake (Stratum F and E).	Ashton et al. (2008a)
Hoxne (Stratum B2 and B1)[b]	Mixture of open landscape and forest; selected fish species (e.g., rudd) suggests relatively warm summer temperatures.	Ashton et al. (2008a)
Hoxne (Stratum A2 and A1)[b]	Fauna in A2 (possibly derived) suggests a temperate climate, but ice wedge casts (A2) and other periglacial structures (A1) suggest permafrost and cold climates.	Ashton et al. (2008a)
Kärlich Seeufer[b]	Lakeshore habitat, with interglacial boreal forest and fen vegetation immediately surrounding the site.	Szymanek and Julien (2018)
La Celle[b]	Closed forest environment, characterized by Mediterranean plants (e.g., figs, box, and hackberry) and thermophilous mammals (e.g., hippo and macaque); warm and wet interglacial optima.	Dabkowski et al. (2012)

(*continued on next page*)

Table 10 (*continued*)

Sites	Paleoenvironment	References
Marks Tey[a,c,d]	Lacustrine sequence spanning MIS 11c, including fully temperate conditions; open grassland and birch woodland (Ho I) > deciduous woodland (oak, elm, lime, alder, and hazel; Ho II and Ho III) > replacement of deciduous woodland by heath and grassland (Ho IV).	Turner (1970); Tye et al. (2016)
Quinton (Faunal Unit 1)[a,d]	Lacustrine environment in abandoned channel, with oak–alder forest (after initial birch-dominated woodland); temperate conditions, warmer than the present day.	Coope and Kenward (2007)
Quinton (Faunal Unit 2)[a]	Lacustrine environment in abandoned channel, with shrubland and birch–pine–fir tree stands; beetles suggest severe climatic deterioration to Arctic-like conditions (although not reflected in pollen).	Coope and Kenward (2007)
Quinton (Faunal Unit 3)[a,d]	Lacustrine environment in abandoned channel, with birch–pine woodland; cool-temperate beetle species indicate conditions slightly cooler than present day.	Coope and Kenward (2007)
Steinheim-an-der-Murr[b]	Warm, Mediterranean habitats; forests with open landscape.	Szymanek and Julien (2018)
Swanscombe (Lower Loam)[b]	Regional vegetation of mixed deciduous woodland (oak, with hazel), with areas of open, dry grassland on the river floodplain; mixture of flowing water and stagnant marshy conditions; temperate climate.	Hubbard (1996); Schreve (1996)
Swanscombe (Lower Middle Gravel)[b]	Wooded environment and warm, temperate conditions.	Hubbard (1996); Schreve (1996)
Trinchera Dolina (TD-10.3, Level T17)[b]	Warm, temperate environment, with landscape dominated by wet meadows and open woodland areas.	Blain et al. (2015)
Woodston[a,d]	Channel and estuary of large, slow-flowing river (freshwater, with tidal input); grass and marshland, with closed canopy deciduous woodland further away; early interglacial temperate conditions (HoII), with greater continentality than present.	Horton et al. (1992); Horne (2007)

[a] Nonhominin sites.
[b] Hominin sites.
[c] Occasional artifacts have been found around the margins of Marks Tey, but none have a firm context (Ashton et al., 2006).
[d] Comparable conditions are documented at multiple other British MIS 11 sites that also lack evidence of a hominin presence (Ashton et al., 2006, their table 1, and references therein).

hominin record in north-central Europe before ca. MIS 8 (Haidle and Pawlik, 2010; Romanowska, 2012) is not purely due to climatic challenges as characterized using T_{min} and T_{max}, although the apparent bias toward the Atlantic west in the European record may also reflect the higher temperature seasonality values (SOM Table S8) and annual temperature ranges (SOM Table S9; Fig. 20) in the continental interior. The potential impacts of major river systems, for example the Rhine, other topographic features, and the presence/absence of contiguous habitable environments (i.e., 'dispersal corridors') on hominin range expansions during periods of ameliorating climate (e.g., early MIS 11c and MIS 11a) should be a focus of future, model-based, research.

Broad, MIS-level comparisons between north-western (British), north-central (German), and south-western (Iberia and Southern France) hominin sites (Fig. 21) highlight the diverse range of conditions tolerated across MIS 13–11, but to some extent also overemphasize inter-regional differences at the expense of intra-regional variability. Different areas of western Europe are characterized by considerable internal variability, reflecting topography and other factors, as Blain et al. (2021) have emphasized for Iberia.

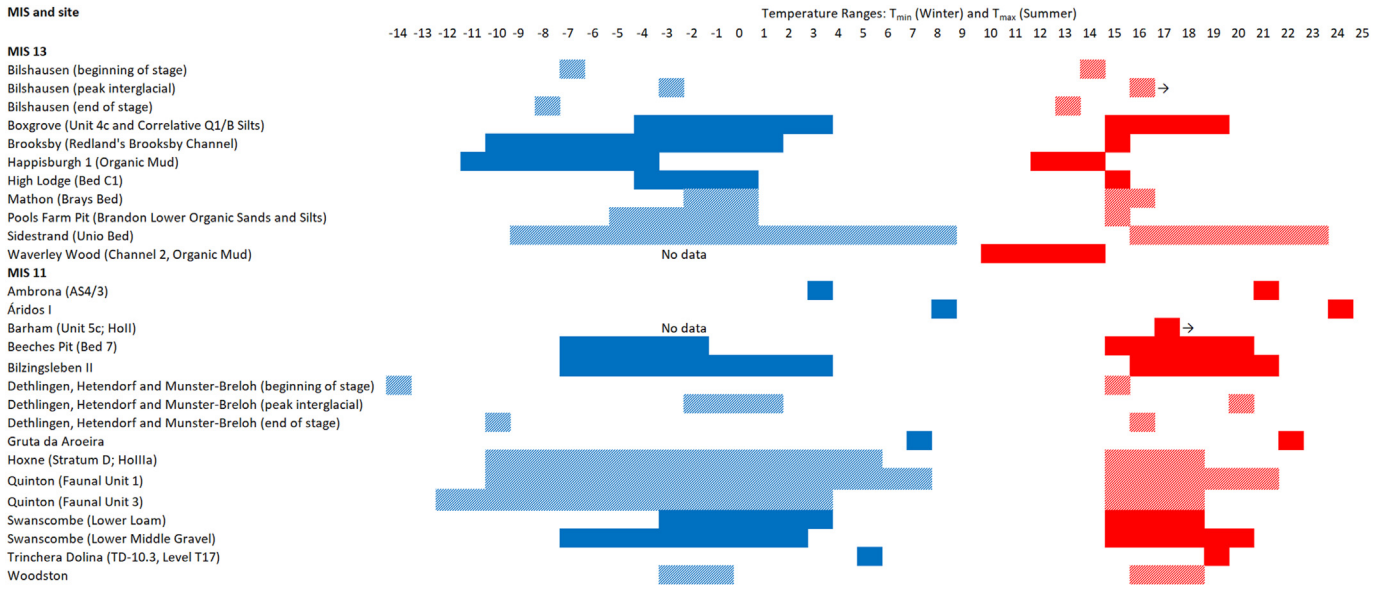

Figure 19. Winter (T_{min}; °C, blue) and summer (T_{max}; °C, red) temperature estimates for selected northern European MIS 13 and MIS 11 hominin (solid shading) and nonhominin sites (hatched shading). See Figure 1 for site locations. Note that the temperature bars for Bilzingsleben II represent the combined range of the molluscan/paleobotany and ostracod-based estimates (see Table 2 for details). Quinton (Faunal Unit 2) is not included as it represents a major cooling episode [T_{min}: (−27) − (−10)°C; T_{max}: (+9) − (+11)°C]. (For interpretation of the references to color in this figure legend, the reader is referred to the Web version of this article).

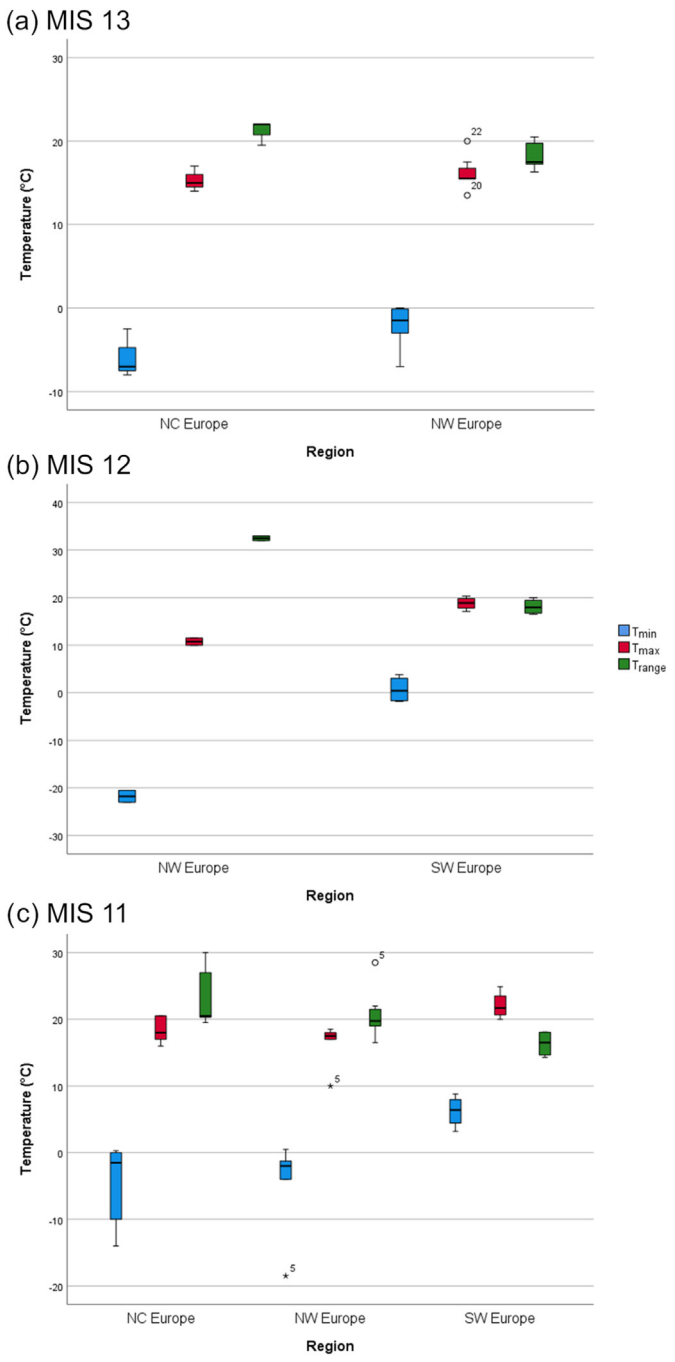

Figure 20. Boxplots of minimum temperature (T_{min}; °C, blue), maximum temperature (T_{max}; °C, red), and temperature range (T_{range}; °C, green) estimates for a) MIS 13, b) MIS 12, and c) MIS 11 hominin and nonhominin sites (combined) in north–central Europe (Germany), north-west Europe (Britain), and south-west Europe (southern France, Spain, and Portugal). Sample sizes: $n = 11$ (MIS 13; $n = 10$ for T_{min} and $_{Trange}$, as there was no T_{min} value for Waverley Wood), $n = 6$ (MIS 12), and $n = 18$ (MIS 11; n = 17 for T_{min} and $_{Trange}$, as there was no T_{min} value for Barnham). The potential outliers and extreme values are: Site 5 (MIS 11 plot): Quinton (Faunal Unit 2); Site 20 (MIS 13 plot): Happisburgh 1; Site 22 (MIS 13 plot): Sidestrand. See Table 2 for list of individual sites. Where two sets of temperature estimates are listed for the same site, that is, for Ostend [Arctic Bed] and Bilzingsleben II, both sets of estimates are included in these boxplots. The solid black line within each box represents the median. The box represents the interquartile range (IQR). The lower and upper whiskers represent values no more than 1.5 IQR below the first quartile and no more than 1.5 IQR above the third quartile, respectively. Potential outliers (circles) are between 1.5 and 3 IQR below the first quartile or above the third quartile. Extreme values (stars) are more than 3 IQR below the first quartile or above the third quartile. (For interpretation of the references to color in this figure legend, the reader is referred to the Web version of this article).

Such variability is also evident in the Oscillayers transects (Figs. 10, 12, 14 and 16). The Oscillayers critique by Brown et al. (2020) and the only moderately strong results of the correlation analysis reported in SOM S1 means that the paleoclimatic values and trends in the transects derived from Oscillayers (question 4) and the maps of potential hominin landscapes (question 5) should be considered as preliminary. Further studies are required, focusing on the development of new GCM-based models of Pleistocene paleoclimate, further testing of existing models (e.g., Oscillayers) against larger site-specific data-sets and/or other models, and further cross-comparisons and evaluations of the different methods for reconstructing paleotemperatures (as also called for by Farjon et al., 2020). Nonetheless, the statistically significant correlations between the site-specific paleotemperatures and the Oscillayers values (SOM S1), and the support from regional-scale, sea-surface temperature data (Candy et al., 2015), do suggest valuable insights in the regional-scale transects (question 4). Those transects suggest milder, wetter, and less seasonal climates in the west, raising the possibility that an Atlantic coastal zone focus, discussed by Cohen et al. (2012) with reference to the earliest occupations of north-western Europe, was also applicable during the MIS 13–11 interval. The sustained Lower Paleolithic occupations at Menez-Dregan 1 (MIS 13–11; Monnier et al., 2016) and Caune de l'Arago (Middle Complex; MIS 14–12; Falguères et al., 2015) appear significant in this regard, along with coastal/estuarine and lower river valley occupations such as Boxgrove, Happisburgh 1 and High Lodge (Lewis et al., 2019).

4.3. Revisiting the two hypotheses

Two hypotheses were proposed at the start of this paper with regard to the potential relationship between paleoclimatic conditions and the expanding hominin occupation record across MIS 13–11: 1) that the range of paleoclimatic conditions associated with hominin occupations expanded across MIS 13–11, suggesting that hominins expanded into and tolerated a wider range of climatic niches over time, and 2) that the range of paleoclimatic conditions associated with hominin occupations remained stable or narrowed across MIS 13–11, but that those conditions became available over a wider geographical extent and/or a longer chronological duration.

The British site-specific temperature estimates (Fig. 7) suggest that hominins occupied a similar, if slightly warmer, range of climatic niches in MIS 11c as in MIS 13 (Fig. 21), with greater similarity between the later MIS 11 sites and MIS 13 sites (e.g., the broadly comparable conditions in sites such as Beeches Pit [Bed 7] and Boxgrove and Happisburgh 1). These findings thus provide little support for the first hypothesis, and suggest limited changes in hominins' biocultural adaptations during this period. The global isotopic data sets indicate a longer period of warmer habitats during MIS 11c compared to MIS 13, although those conditions were clearly not continuous (e.g., the impacts of the NAP/OHO event), providing support for hypothesis two.

Although the late MIS 11 occupations at Hoxne offer some support for hypothesis one, the evidence from MIS 13 does not: artifacts are associated with varying climate regimes on pre-MIS 12 British sites (see also Ashton and Lewis, 2012), and the climatic and environmental records from those sites indicate that hominins occupied north-west Europe during non-peak as well as peak conditions in the early Middle Pleistocene and were subject to similar extremes of climate cycles as occurred after MIS 13 (see also Candy et al., 2011a). There is also limited evidence for dramatically different behavioral repertoires between MIS 13 and 11, with Acheulean behaviors characteristic of both periods (and in some

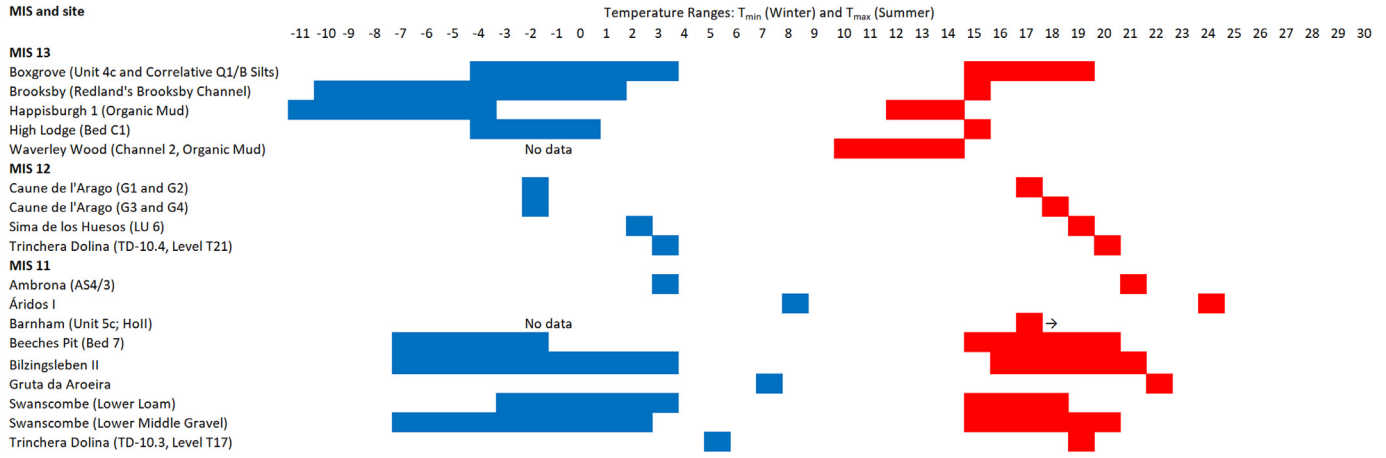

Figure 21. Winter (T_{min}; °C, blue) and summer (T_{max}; °C, red) temperature estimates for selected MIS 13, MIS 12, and MIS 11 western European hominin sites (see Table 2 for site details). Note the overall similarity of climatic conditions for MIS 13 and 11 sites (see also Fig. 1 for site locations and Fig. 20 for geographical variations in conditions), although with a shift toward slightly warmer conditions in MIS 11. The temperature bars for Bilzingsleben II represent the combined range of the molluscan/paleobotany and ostracod-based estimates (see Table 2 for details). (For interpretation of the references to color in this figure legend, the reader is referred to the Web version of this article).

cases prior to MIS 13; Moncel et al., 2015) and controlled fire technologies predominantly post-dating MIS 11 (Roebroeks and Villa, 2011; MacDonald et al., 2021).

Yet while it is difficult to demonstrate clear differences in conditions between MIS 13 and 11, the range of paleoclimatic conditions and habitats evident across the entire MIS 13–11 interval (e.g., from −11 °C at Happisburgh 1 to +24.9 °C at Áridos 1; Table 2) clearly indicates the expanding tolerances of Middle Pleistocene hominins relative to their European predecessors. They are in stark contrast to the much narrower range of conditions documented at the earliest European sites from the Early Pleistocene (e.g., Agustí et al., 2009, 2015; Messager et al., 2011; Leroy et al., 2011), and suggest a change before or at the very beginning of, rather than during, the MIS 13–11 interval. In this sense, the relative paleoclimatic stability across the MIS 15–13 interval (e.g., Candy and Alonso-Garcia, 2018) may have been of significance for western European hominin dispersals and progressive adaptations to a wider range of conditions, reflected in occupations such as the MIS 15 Bytham River sites (Ashton and Davis, 2021). On a broader Eurasian scale, Timmermann et al. (2022) have argued for the acquisition of new adaptive skills around 0.8–0.6 Ma by *H. heidelbergensis*, linked to an expanding geographical range and a positive migration-climate adaptation feedback.

However, the apparently limited evidence for change in the paleoenvironmental conditions on British sites between MIS 13 and 11 contrasts with recent studies from Iberia (Blain et al., 2021), which document a broadening of the hominin niche toward open, arid areas in the later Middle Pleistocene. This suggests that hominin preferences for, and adaptations to, paleoclimatic conditions may have varied regionally, as highlighted by Blain et al. (2021). This raises the possibility that a further aspect of 'Neanderthalization', namely changing habitat preferences and tolerances, also occurred in a piecemeal and mosaic manner, echoing the processes seen in later Middle Pleistocene hominin skeletal morphology (e.g., the accretion model for the emergence of Neanderthals; Hublin, 2009).

Overall, the evidence for expanding habitat tolerances and early 'Neanderthalization' in the European landscapes of MIS 13 and 11 is limited. The respective durations of favorable conditions in MIS 13 and 11c seem to be the best explanation for the expanding western European record of hominin activity in MIS 11 relative to MIS 13. The currently available western European data suggest a gradual rather than an abrupt change in hominin paleoclimatic preferences and tolerances across the MIS 13–11 interval. More fundamental changes are perhaps better sought in the MIS 15–13 era, associated with the earliest expanded occupations of southern Britain and northern France (Moncel et al., 2015), and subsequently, in MIS 9 and beyond, as western European hominins began to expand substantially beyond the Rhine (Haidle and Pawlik, 2010; Cohen et al., 2012; Szymanek and Julien, 2018).

5. Conclusions

Understanding the paleoclimatic and paleoenvironmental context of hominin occupations in western Europe in MIS 13–11 is dependent on a combination of continuous global (isotope) records, site-specific reconstructions, and regional models. Analysis of the currently available evidence suggests a series of conclusions. Overall, the breadth of paleoclimatic conditions on hominin sites from MIS 13 and 11 is in contrast to the earlier European record. The sustained mild conditions of MIS 15–13, and a relatively weak south-north temperature transect in late MIS 13, may have supported hominin dispersals in MIS 15–13. The cooler conditions of late MIS 13 suggest that key behavioral changes (i.e., the Acheulean 'behavioral package') were already in place during MIS 13, and may also indicate tolerated as opposed to preferred conditions. The general intraregional similarity of paleoclimatic conditions on hominin sites in MIS 13 and MIS 11 suggests that the expanded archaeological record of MIS 11 reflects the extended mild conditions of MIS 11c, rather than a widening of the hominin climatic niche. Moreover, the general intraregional similarities of paleoclimatic conditions on hominin and nonhominin sites in MIS 11 and, to some extent, MIS 13 suggest that the absence of hominin evidence on selected sites is due to sampling bias and taphonomic factors. Viewed at a regional scale the milder conditions in the west suggest that the Atlantic coastal zone played a role in hominin dispersals from south-west Europe during MIS 13 and MIS 11. Finally, the similarities between conditions in north-west and north-central Europe during MIS 11 suggest that the apparent delay in the widespread occupation of northern Europe east of the Rhine was not purely due to climatic factors.

However, there are also several outstanding issues which require improved methodologies, approaches, and data. Of particular note is the need for improved correlations between sites, regions, and global data sets, including comparisons between marine and terrestrial records. At the site-specific scale, there is also a need

for expanded data sets tracking rainfall fluctuations and temperatures throughout the year. Finally, increased testing of site-specific estimates against modeling data sets is required (e.g., as attempted in this paper for the Oscillayers data). All of the above will enhance our ability to characterize hominin presence/absences from a paleoenvironmental perspective, including their tolerances and preferences of climatic conditions, habitats, and landscape settings. Nonetheless, the currently available data from the MIS 13–11 interval offer a valuable perspective on the paleoclimatic context of hominin occupations, extirpations, dispersals, and contractions, during a critical phase of the European Lower Paleolithic.

Declaration of competing interest

The author declares that there is no conflict of interest.

Acknowledgments

Thank you to Paula García-Medrano and Nick Ashton, who invited me to present a paper at the 'Western European Acheulean Project' conference at the British Museum (October 2019). Thanks also to all the attendees for their questions, which have contributed to the ideas in this paper. Thanks to all the participants at the 'Coping with Climate: the legacy of *Homo heidelbergensis*' workshop (Brighton University, February 2017; funded by the AHRC: AH/N007514/1) and the 'MIS 13–11: A major transformation in the European Lower Palaeolithic?' session at UISPP (Paris, June 2018), the discussions at which also helped the development of this paper. Thank you to the Editor of JHE and the four anonymous reviewers, all of whose comments helped to focus the paper. All ideas and any remaining errors in the paper are of course my own. This research did not receive any specific grant from funding agencies in the public, commercial, or not-for-profit sectors.

Supplementary Online Material

Supplementary online material related to this article can be found at https://doi.org/10.1016/j.jhevol.2022.103213.

References

Agustí, J., Blain, H.A., Cuenca-Bescós, G., Bailon, S., 2009. Climate forcing of first hominid dispersal in Western Europe. J. Hum. Evol. 57, 815–821.
Agustí, J., Blain, H.A., Lozano-Fernández, I., Piñero, P., Oms, O., Furió, M., Blanco, A., López-García, J.M., Sala, R., 2015. Chronological and environmental context of the first hominin dispersal into Western Europe: The case of Barranco León (Guadix-Baza Basin, SE Spain). J. Hum. Evol. 87, 87–94.
Arsuaga, J.L., Martínez, I., Arnold, L., Aranburu, A., Gracia-Téllez, A., Sharp, W., Quam, R., Falguères, C., Pantoja-Pérez, A., Bischoff, J., 2014. Neandertal roots: Cranial and chronological evidence from Sima de los Huesos. Science 344, 1358–1363.
Ashton, N.M., 2015. Ecological niches, technological developments and physical adaptations of early humans in Europe: The handaxe-*heidelbergensis* hypothesis. In: Coward, F., Hosfield, R.T., Pope, M., Wenban-Smith, F.F. (Eds.), Settlement, Society and Cognition in Human Evolution: Landscapes in Mind. Cambridge University Press, Cambridge, pp. 138–153.
Ashton, N.M., 2016. The human occupation of Britain during the Hoxnian Interglacial. Quat. Int. 409, 41–53.
Ashton, N.M., Lewis, S.G., 2002. Deserted Britain: Declining populations in the British Late Middle Pleistocene. Antiquity 76, 388–396.
Ashton, N.M., Lewis, S.G., 2012. The environmental contexts of early human occupation of northwest Europe: The British Lower Palaeolithic record. Quat. Int. 271, 50–64.
Ashton, N., Davis, R., 2021. Cultural mosaics, social structure, and identity: The Acheulean threshold in Europe. J. Hum. Evol. 156, 103011.
Ashton, N.M., Cook, J., Lewis, S.G., Rose, J., 1992. High Lodge: Excavations by G. de G. Sieveking, 1962–68, and J. Cook, 1988. British Museum Press, London.
Ashton, N.M., Lewis, S.G., Parfitt, S.A., 1998. Excavations at the Lower Palaeolithic site at East Farm, Barnham, Suffolk 1989-94, British Museum Occasional Paper No. 125. British Museum Press, London.
Ashton, N.M., Lewis, S.G., Parfitt, S.A., White, M.J., 2006. Riparian landscapes and human habitat preferences during the Hoxnian (MIS 11) Interglacial. J. Quat. Sci. 21, 497–505.
Ashton, N.M., Lewis, S.G., Parfitt, S.A., Penkman, K.E., Coope, G.R., 2008a. New evidence for complex climate change in MIS 11 from Hoxne, Suffolk, UK. Quat. Sci. Rev. 27, 652–668.
Ashton, N.M., Parfitt, S.A., Lewis, S.G., Coope, G.R., Larkin, N., 2008b. Happisburgh Site 1 (TG388307). In: Candy, I., Lee, J.R., Harrison, A.M. (Eds.), The Quaternary of Northern East Anglia Field Guide. Quat. Res. Assoc., London, pp. 151–156.
Ashton, N.M., Lewis, S.G., Parfitt, S.A., Davis, R.J., Stringer, C., 2016. Handaxe and non-handaxe assemblages during Marine Isotope Stage 11 in northern Europe: Recent investigations at Barnham, Suffolk, UK. J. Quat. Sci. 31, 837–843.
Atkinson, T.C., Briffa, K.R., Coope, G.R., 1987. Seasonal temperatures in Britain during the past 22,000 years, reconstructed using beetle remains. Nature 325, 587–592.
Bassinot, F.C., Labeyrie, L.D., Vincent, E., Quidelleur, X., Shackleton, N.J., Lancelot, Y., 1994. The astronomical theory of climate and the age of the Brunhes-Matuyama magnetic reversal. Earth Planet Sci. Lett. 126, 91–108.
Bell, M., Walker, M.J.C., 2005. Late Quaternary Environmental Change: Physical and Human Perspectives, 2nd edition. Pearson-Prentice Hall, Harlow.
Benardout, G., 2015. Ostracod-based palaeotemperature reconstructions for MIS 11 human occupation at Beeches Pit, West Stow, Suffolk, UK. J. Archaeol. Sci. 54, 421–425.
Berger, A., 1988. Milankovitch theory and climate. Rev. Geophys. 26, 624–657.
Birks, H.J.B., Heiri, O., Seppä, H., Bjune, A.E., 2010. Strengths and weaknesses of quantitative climate reconstructions based on Late-Quaternary. Open Ecol. J. 3, 68–110.
Blain, H.-A., Santonja, M., Pérez-González, A., Panera, J., Rubio-Jara, S., 2014. Climate and environments during Marine Isotope Stage 11 in the central Iberian Peninsula: The herpetofaunal assemblage from the Acheulean site of Áridos-1, Madrid. Quat. Sci. Rev. 94, 7–21.
Blain, H.-A., Lozano-Fernández, I., Agustí, J., Bailon, S., Menéndez Granda, L., Espígares Ortiz, M.P., Ros-Montoya, S., Jiménez Arenas, J.M., Toro-Moyano, I., Martínez-Navarro, B., Sala, R., 2016. Refining upon the climatic background of the Early Pleistocene hominid settlement in western Europe: Barranco León and Fuente Nueva-3 (Guadix-Baza Basin, SE Spain). Quat. Sci. Rev. 144, 132–144.
Blain, H.-A., Lozano-Fernández, I., Ollé, A., Rodríguez, J., Santonja, M., Pérez-González, A., 2015. The continental record of Marine Isotope Stage 11 (Middle Pleistocene) on the Iberian Peninsula characterized by herpetofaunal assemblages. J. Quat. Sci. 30, 667–678.
Blain, H.-A., Fagoaga, A., Ruiz-Sánchez, F.J., García-Medrano, P., Ollé, A., Jiménez-Arenas, J.M., 2021. Coping with arid environments: A critical threshold for human expansion in Europe at the Marine Isotope Stage 12/11 transition? The case of the Iberian Peninsula. J. Hum. Evol. 153, 102950.
Boismier, W.A., Gamble, C., Coward, F., 2012. Neanderthals among mammoths: Excavations at Lynford Quarry, Norfolk UK. English Heritage Monographs, Swindon.
Brown, J.L., Hill, D.J., Dolan, A.M., Carnaval, A.C., Haywood, A.M., 2018. PaleoClim, high spatial resolution paleoclimate surfaces for global land areas. Sci. Data 5, 180254.
Brown, J.L., Hill, D.J., Haywood, A.M., 2020. A critical evaluation of the Oscillayers methods and datasets. Global Ecol. Biogeogr. 29, 1435–1442.
Bruner, E., Manzi, G., 2005. CT-based description and phyletic evaluation of the archaic human calvarium from Ceprano. Italy. Anat. Rec. 285, 643–657.
Candy, I., Alonso-Garcia, M., 2018. A 1 Ma sea surface temperature record from the North Atlantic and its implications for the early human occupation of Britain. Quat. Res. 90, 406–417.
Candy, I., Coope, G., Lee, J., Parfitt, S., Preece, R., Rose, J., Schreve, D., 2010. Pronounced warmth during early Middle Pleistocene interglacials: Investigating the Mid-Brunhes event in the British terrestrial sequence. Earth Sci. Rev. 103, 183–196.
Candy, I., Silva, B., Lee, J., 2011a. Climates of the early Middle Pleistocene in Britain: Environments of the earliest humans in Northern Europe. In: Ashton, N.M., Lewis, S.G., Stringer, C.B. (Eds.), The Ancient Human Occupation of Britain. Elsevier, Amsterdam, pp. 11–22.
Candy, I., Stephens, M., Hancock, J., Waghorne, R., 2011b. Palaeoenvironments of ancient humans in Britain: The application of oxygen and carbon isotopes to the reconstruction of Pleistocene environments. In: Ashton, N.M., Lewis, S.G., Stringer, C.B. (Eds.), The Ancient Human Occupation of Britain. Elsevier, Amsterdam, pp. 23–37.
Candy, I., Schreve, D.C., Sherriff, J., Tye, G.J., 2014. Marine Isotope Stage 11: Palaeoclimates, palaeoenvironments and its role as an analogue for the current interglacial. Earth Sci. Rev. 128, 18–51.
Candy, I., Schreve, D., White, T.S., 2015. MIS 13–12 in Britain and the North Atlantic: Understanding the palaeoclimatic context of the earliest Acheulean. J. Quat. Sci. 30, 593–609.
Cohen, K.M., MacDonald, K., Joordens, J.C., Roebroeks, W., Gibbard, P.L., 2012. The earliest occupation of north-west Europe: A coastal perspective. Quat. Int. 271, 70–83.
Conway, B., McNabb, J., Ashton, N.M., 1996. Excavations at Barnfield Pit, Swanscombe 1968–1972, Occasional Paper No. 94. British Museum, London.
Coope, G.R., 1993. Late-Glacial (Anglian) and Late-temperate (Hoxnian) Coleoptera. In: Singer, R., Gladfelter, B.G., Wymer, J.J. (Eds.), The Lower Palaeolithic Site at Hoxne, England. University Chicago Press, Chicago, pp. 156–162.

Coope, G.R., 2006. Insect faunas associated with Palaeolithic industries from five sites of pre-Anglian age in central England. Quat. Sci. Rev. 25, 1738–1754.
Coope, G.R., Kenward, H.K., 2007. Evidence from coleopteran assemblages for a short but intense cold interlude during the latter part of the MIS11 Interglacial from Quinton, West Midlands, UK. Quat. Sci. Rev. 26, 3276–3285.
Coope, G.R., Field, M.H., Gibbard, P.L., Greenwood, M., Richards, A.E., 2002. Palaeontology and biostratigraphy of Middle Pleistocene river sediments in the Mathon Member, at Mathon, Herefordshire, England. Proc. Geol. Assoc. 113, 237–258.
Dabkowski, J., Limondin-Lozouet, N., Antoine, P., Andrews, J., Marca-Bell, A., Robert, V., 2012. Climatic variations in MIS 11 recorded by stable isotopes and trace elements in a French tufa (La Celle, Seine Valley). J. Quat. Sci. 27, 790–799.
Daura, J., Sanz, M., Arsuaga, J.L., Hoffmann, D.L., Quam, R.M., Ortega, M.C., Santos, E., Gómez, S., Rubio, A., Villaescusa, L., Souto, P., Mauricio, J., Rodrigues, F., Ferreira, A., Godinho, P., Trinkaus, E., Zilhão, J., 2017. New Middle Pleistocene hominin cranium from Gruta da Aroeira (Portugal). Proc. Natl. Acad. Sci. USA 114, 3397–3402.
Davies, W., Gollop, P., 2003. The human presence in Europe during the Last Glacial period II: Climate tolerance and climate preferences of mid- and late glacial hominids. In: van Andel, T.H., Davies, W. (Eds.), Neanderthals and Modern Humans in the European Landscape during the Last Glaciation. McDonald Institute for Archaeological Research, Cambridge, pp. 131–146.
Davis, R., Ashton, N., 2019. Landscapes, environments and societies: The development of culture in Lower Palaeolithic Europe. J. Anthropol. Archaeol. 56, 101107.
Davis, R.J., Lewis, S.G., Ashton, N.M., Parfitt, S.A., Hatch, M.T., Hoare, P.G., 2017. The early Palaeolithic archaeology of the Breckland: Current understanding and directions for future research. J. Breckland Stud. 1, 28–44.
de Lombera-Hermida, A., Rodríguez-Álvarez, X.P., Mosquera, M., Ollé, A., García-Medrano, P., Pedergnana, A., Terradillos-Bernal, M., López-Ortega, E., Bargalló, A., Rodríguez-Hidalgo, A., 2020. The dawn of the Middle Paleolithic in Atapuerca: The lithic assemblage of TD10.1 from Gran Dolina. J. Hum. Evol. 145, 102812.
de Lumley, M.-A., 2015. L'homme de Tautavel. Un *Homo erectus* Européen évolué. *Homo erectus tautavelensis*. L'Anthropologie 119, 303–348.
de Lumley, H., Grégoire, S., Barsky, D., Batalla, G., Bailon, S., Belda, V., Briki, D., Byrne, L., Desclaux, E., El Guenouni, K., Fournier, A., Kacimi, S., Lacombat, F., de Lumley, M.-A., Moigne, A.-M., Moutoussamy, J., Paunescu, C., Perrenoud, C., Pois, V., Quiles, J., Rivals, F., Roger, T., Testu, A., 2004. Habitat et mode de vie des chasseurs paléolithiques de la Caune de l'Arago (600 000–400 000 ans). L'Anthropologie 108, 159–184.
Dennell, R.W., Martinón-Torres, M., Bermúdez de Castro, J.M., 2011. Hominin variability, climatic instability and population demography in Middle Pleistocene Europe. Quat. Sci. Rev. 30, 1511–1524.
Dibble, H.L., Abodolahzadeh, A., Aldeias, V., Goldberg, P., McPherron, S.P., Sandgathe, D.M., 2017. How did hominins adapt to ice age Europe without fire? Curr. Anthropol. 58, S278–S287.
EPICA-Community, Augustin, L., Barbante, C., Barnes, P.R.F., Marc Barnola, J., Bigler, M., Castellano, E., Cattani, O., Chappellaz, J., Dahl-Jensen, D., Delmonte, B., Dreyfus, G., Durand, G., Falourd, S., Fischer, H., Flückiger, J., Hansson, M.E., Huybrechts, P., Jugie, G., Johnsen, S.J., Jouzel, J., Kaufmann, P., Kipfstuhl, J., Lambert, F., Lipenkov, V.Y., Littot, G.C., Longinelli, A., Lorrain, R., Maggi, V., Masson-Delmotte, V., Miller, H., Mulvaney, R., Oerlemans, J., Oerter, H., Orombelli, G., Parrenin, F., Peel, D.A., Petit, J.-R., Raynaud, D., Ritz, C., Ruth, U., Schwander, J., Siegenthaler, U., Souchez, R., Stauffer, B., Peder Steffensen, J., Stenni, B., Stocker, T.F., Tabacco, I.E., Udisti, R., van de Wal, R.S.W., van den Broeke, M., Weiss, J., Wilhelms, F., Winther, J.-G., Wolff, E.W., Zucchelli, M., 2004. Eight glacial cycles from an Antarctic ice core. Nature 429, 623–628.
Falguères, C., Shao, Q., Han, F., Bahain, J.J., Richard, M., Perrenoud, C., Moigne, A.M., 2015. New ESR and U-series dating at Caune de l'Arago, France: A key-site for European Middle Pleistocene. Quat. Geochronol. 30, 547–553.
Farjon, A., Horne, D.J., Parfitt, S.A., Buckland, P.I., Lewis, M.D., 2020. Early Pleistocene conifer macrofossils from Happisburgh, Norfolk, UK, and their environmental implications for early hominin occupation. Quat. Sci. Rev. 232, 106115.
Foley, J.A., Prentice, I.C., Ramankutty, N., Levis, S., Pollard, D., Sitch, S., Haxeltine, A., 1996. An integrated biosphere model of land surface processes, terrestrial carbon balance and vegetation dynamics. Global Biogeochem. Cycles 10, 603–628.
Gamble, C.S., 1986. The Palaeolithic Settlement of Europe. Cambridge University Press, Cambridge.
Gamisch, A., 2019. Oscillayers: A dataset for the study of climatic oscillations over Plio-Pleistocene time-scales at high spatial-temporal resolution. Global Ecol. Biogeogr. 28, 1552–1560.
Gamisch, A., 2020. A reply to the 'critical evaluation of the Oscillayers methods and dataset'. Global Ecol. Biogeogr. 29, 1443–1448.
Gibbard, P.L., Aalto, M.M., Beales, P.W., 1977. A Hoxnian interglacial site at Fishers Green, Stevenage, Hertfordshire. New Phytol. 78, 505–523.
Gupta, S., Collier, J.S., Garcia-Moreno, D., Oggioni, F., Trentesaux, A., Vanneste, K., De Batist, M., Camelbeeck, T., Potter, G., Van Vliet-Lanoë, B., Arthur, J.C.R., 2017. Two-stage opening of the Dover Strait and the origin of island Britain. Nat. Commun. 8, 15101.
Haidle, M.N., Pawlik, A.F., 2010. The earliest settlement of Germany: Is there anything out there? Quat. Int. 223, 143–153.
Hansen, J., Sato, M., Russell, G., Kharecha, P., 2013. Climate sensitivity, sea level and atmospheric carbon dioxide. Phil. Trans. R. Soc. Lond. 371, 20120294.
Hardy, B.L., 2010. Climatic variability and plant food distribution in Pleistocene Europe: Implications for Neanderthal diet and subsistence. Quat. Sci. Rev. 29, 662–679.
Haywood, A.M., Hill, D.J., Dolan, A.M., Otto-Bliesner, B.L., Bragg, F., Chan, W.L., Chandler, M.A., Contoux, C., Dowsett, H.J., Jost, A., Kamae, Y., 2013. Large-scale features of Pliocene climate: Results from the Pliocene Model Intercomparison Project. Clim. Past 9, 191–209.
Holman, J.A., 1998. The herpetofauna. The interglacial mammalian fauna from Barnham. In: Ashton, N.M., Lewis, S.G., Parfitt, S.A. (Eds.), Excavations at the Lower Palaeolithic Site at East Farm, Barnham, Suffolk 1989–94. The British Museum, London, pp. 101–106.
Holman, J.A., 1999. Herpetofauna. In: Roberts, M.B., Parfitt, S.A. (Eds.), Boxgrove: A Middle Pleistocene Hominid Site at Eartham Quarry, Boxgrove, West Sussex. English Heritage, London, pp. 181–187.
Holmes, J.A., Atkinson, T., Fiona Darbyshire, D.P., Horne, D.J., Joordens, J., Roberts, M.B., Sinka, K.J., Whittaker, J.E., 2010. Middle Pleistocene climate and hydrological environment at the Boxgrove hominin site (West Sussex, UK) from ostracod records. Quat. Sci. Rev. 29, 1515–1527.
Horne, D.J., 2007. A Mutual Temperature Range method for Quaternary palaeoclimatic analysis using European nonmarine Ostracoda. Quat. Sci. Rev. 26, 1398–1415.
Horton, A., Keen, D.H., Field, M.H., Robinson, J.E., Coope, G.R., Currant, A.P., Graham, D.K., Green, C.P., Phillips, L.M., 1992. The Hoxnian interglacial deposits at Woodston, Peterborough. Philos. Trans. R. Soc. Lond. B Biol. Sci. 338, 131–164.
Hosfield, R., 2016. Walking in a winter wonderland? Strategies for Early and Middle Pleistocene survival in midlatitude Europe. Curr. Anthropol. 57, 653–682.
Hosfield, R., 2020. The Earliest Europeans – A Year in the Life: Seasonal survival strategies in the Lower Palaeolithic. Oxbow Books, Oxford.
Hosfield, R., Cole, J., 2018. Early hominins in north-west Europe: A punctuated long chronology? Quat. Sci. Rev. 190, 148–160.
Howell, F.C., Freeman, L.G., 1982. Ambrona: An early Stone Age site on the Spanish Meseta. L.S.B. Leakey Foundation News 22, 11–13.
Hubbard, R., 1996. The palynological studies from the Waechter excavations. In: Conway, B., McNabb, J., Ashton, N.M. (Eds.), Excavations at Barnfield Pit, Swanscombe, 1968-72. British Museum Occasional Paper No. 94, London, pp. 191–200.
Hublin, J.J., 2009. The origin of Neandertals. Proc. Natl. Acad. Sci. USA 106, 16022–16027.
Hunt, C.O., 1992. Pollen and algal microfossils from the High Lodge clayey-silts. In: Ashton, N.M., Cook, J., Lewis, S.G., Rose, J. (Eds.), High Lodge: Excavations by G. de G. Sieveking, 1962–68, and J. Cook, 1988. British Museum Press, London, pp. 109–115.
Imbrie, J., Hays, J.D., Martinson, D.G., McIntyre, A., Mix, A.C., Morley, J.J., Pisias, N.G., Prell, W.L., Shackleton, N.J., 1984. The orbital theory of Pleistocene climate: Support from a revised chronology of the marine $\delta^{18}O$ record. In: Berger, A., Imbrie, J., Hays, J., Kukla, G., Saltzman, B. (Eds.), Milankovitch and Climate: Part 1. Plenum Reidel, Dordrecht, pp. 269–305.
Iovita, R., Tuvi-Arad, I., Moncel, M.-H., Despriee, J., Voinchet, P., Bahain, J.-J., 2017. High handaxe symmetry at the beginning of the European Acheulian: The data from la Noira (France) in context. PLoS One 12, e0177063.
Jouzel, J., Masson-Delmotte, V., Cattani, O., Dreyfus, G., Falourd, S., Hoffmann, G., Minster, B., Nouet, J., Barnola, J.M., Chappellaz, J., Fischer, H., Gallet, J.C., Johnsen, S., Leuenberger, M., Loulergue, L., Luethi, D., Oerter, H., Parrenin, F., Raisbeck, G., Raynaud, D., Schilt, A., Schwander, J., Selmo, E., Souchez, R., Spahni, R., Stauffer, B., Steffensen, J.P., Stenni, B., Stocker, T.F., Tison, J.L., Werner, M., Wolff, E.W., 2007. Orbital and millennial antarctic climate variability over the past 800,000 Years. Science 317, 793–796.
Kandiano, E.S., Bauch, H.A., 2003. Surface ocean temperatures in the north-east Atlantic during the last 500,000 years: Evidence from foraminiferal census data. Terra Nova 15, 265–271.
Kelly, R.L., 1983. Hunter-Gatherer mobility strategies. J. Anthropol. Res. 39, 277–306.
Kucharik, C.J., Foley, J.A., Delire, C., Fisher, V.A., Coe, M.T., Lenters, J.D., Young-Molling, C., Ramankutty, N., Norman, J.M., Gower, S.T., 2000. Testing the performance of a dynamic global ecosystem model: Water balance, carbon balance, and vegetation structure. Global Biogeochem. Cycles 14, 795–825.
Kühl, N., Gobet, E., 2010. Climatic evolution during the Middle Pleistocene warm period of Bilshausen, Germany, compared to the Holocene. Quat. Sci. Rev. 29, 3736–3749.
Lamotte, A., Tuffreau, A., 2016. Acheulean of the Somme basin (France): Assessment of lithic changes during MIS 12 to 9. Quat. Int. 409, 54–72.
Leroy, S.A., Arpe, K., Mikolajewicz, U., 2011. Vegetation context and climatic limits of the Early Pleistocene hominin dispersal in Europe. Quat. Sci. Rev. 30 (11–12), 1448–1463.
Lewis, S.G., Ashton, N.M., Field, M.H., Hoare, P.G., Kamermans, H., Knul, M., Mücher, H.J., Parfitt, S.A., Roebroeks, W., Sier, M.J., 2019. Human occupation of northern Europe in MIS 13: Happisburgh Site 1 (Norfolk, UK) and its European context. Quat. Sci. Rev. 211, 34–58.
Limondin-Lozouet, N., Nicoud, E., Antoine, P., Auguste, P., Bahain, J.-J., Dabkowski, J., Dupéron, J., Dupéron, M., Falguères, C., Ghaleb, B., Jolly-Saad, M.-C., Mercier, N., 2010. Oldest evidence of Acheulean occupation in the Upper Seine valley (France) from an MIS 11 tufa at La Celle. Quat. Int. 223–224, 299–311.
Limondin-Lozouet, N., Antoine, P., Bahain, J.J., Cliquet, D., Coutard, S., Dabkowski, J., Ghaleb, B., Locht, J.L., Nicoud, E., Voinchet, P., 2015. North-West European MIS 11 malacological successions: A framework for the timing of Acheulean settlements. J. Quat. Sci. 30, 702–712.

Lisiecki, L.E., Raymo, M.E., 2005. A Pliocene-Pleistocene stack of 57 globally distributed benthic $\delta^{18}O$ records. Paleoceanography 20. https://doi.org/10.1029/2004PA001071.
López-García, J.M., Cuenca-Bescós, G., Galindo-Pellicena, M.Á., Luzi, E., Berto, C., Lebreton, L., Desclaux, E., 2021. Rodents as indicators of the climatic conditions during the Middle Pleistocene in the southwestern Mediterranean region: Implications for the environment in which hominins lived. J. Hum. Evol. 150, 102911.
MacDonald, K., 2018. Fire-free hominin strategies for coping with cool winter temperatures in North-Western Europe from before 800,000 to circa 400,000 years ago. PaleoAnthropology 7, 7–26.
MacDonald, K., Martinón-Torres, M., Dennell, R.W., Bermúdez de Castro, J.M., 2012. Discontinuity in the record for hominin occupation in south-western Europe: Implications for occupation of the middle latitudes of Europe. Quat. Int. 271, 84–97.
MacDonald, K., Scherjon, F., van Veen, E., Vaesen, K., Roebroeks, W., 2021. Middle Pleistocene fire use: The first signal of widespread cultural diffusion in human evolution. Proc. Natl. Acad. Sci. USA 118 e2101108118.
Maddy, D., Coope, G.R., Gibbard, P.L., Green, C.P., Lewis, S.G., 1994. Reappraisal of Middle Pleistocene fluvial deposits near Brandon, Warwickshire and their significance for the Wolston glacial sequence. J. Geol. Soc. London 151, 221–233.
Mania, D., 1995. The earliest occupation of Europe: The Elbe-Saale region (Germany). In: Roebroeks, W., van Kolfschoten, T. (Eds.), The Earliest Occupation of Europe. Proceedings of the European Science Foundation Workshop at Tautavel (France) 1993. Leiden University Press and European Science Foundation, Leiden, pp. 85–102.
Mania, D., Mai, D.-H., 2001. Molluskenfaunen und-floren im Elbe-Saalegebiet während des mittleren Eiszeitalters. Praehist. Thuringica 6/7, 3–25.
Mania, D., Mania, U., 2003. Bilzingsleben — *Homo erectus*, his culture and his environment. The most important results of research. In: Burdukiewicz, J.M., Ronen, A. (Eds.), Lower Palaeolithic Small Tools in Europe and the Levant. BAR, Oxford, pp. 29–48.
Mania, D., Mania, U., 2005. The natural and socio-cultural environment of *Homo erectus* at Bilzingsleben, Germany. In: Gamble, C.S., Porr, M. (Eds.), The Hominid Individual in Context: Archaeological Investigations of Lower and Middle Palaeolithic Landscapes, Locales and Artefacts. Routledge, London, pp. 98–114.
Manzi, G., Magri, D., Milli, S., Palombo, M.R., Margari, V., Celiberti, V., Barbieri, M., Barbieri, M., Melis, R.T., Rubini, M., 2010. The new chronology of the Ceprano calvarium (Italy). J. Hum. Evol. 59, 580–585.
Martinón-Torres, M., Bermúdez de Castro, J.M., Gómez-Robles, A., Prado-Simón, L., Arsuaga, J.L., 2012. Morphological description and comparison of the dental remains from Atapuerca – Sima de los Huesos site (Spain). J. Hum. Evol. 62, 7–58.
McNabb, J., 2007. The British Lower Palaeolithic: Stones in Contention. Routledge, Abingdon.
McNabb, J., 2020. Problems and pitfalls in understanding the Clactonian. In: Groucutt, H. (Ed.), Culture History and Convergent Evolution. Springer, Cham, pp. 29–53.
Messager, E., Lebreton, V., Marquer, L., Russo-Ermolli, E., Orain, R., Renault-Miskovsky, J., Lordkipanidze, D., Despriée, J., Peretto, C., Arzarello, M., 2011. Palaeoenvironments of early hominins in temperate and Mediterranean Eurasia: New palaeobotanical data from Palaeolithic key-sites and synchronous natural sequences. Quat. Sci. Rev. 30 (11–12), 1439–1447.
Meyer, M., Fu, Q., Aximu-Petri, A., Glocke, I., Nickel, B., Arsuaga, J.-L., Martínez, I., Gracia, A., Carbonell, E., Pääbo, S., 2014. Amitochondrial genome sequence of a hominin from Sima de los Huesos. Nature 505, 403–406.
Moncel, M.-H., Moigne, A.-M., Sam, Y., Combier, J., Ashton, N., Díez, C., Monnier, G., Rolland, N., Sala Ramos, R., Szmidt, C.C., 2011. The emergence of Neanderthal technical behavior: New evidence from Orgnac 3 (Level 1, MIS 8), southeastern France. Curr. Anthropol. 52, 37–75.
Moncel, M.-H., Ashton, N.M., Lamotte, A., Tuffreau, A., Cliquet, D., Despriée, J., 2015. The early Acheulian of north-western Europe. J. Anthropol. Archaeol. 40, 302–331.
Moncel, M.-H., Ashton, N., Arzarello, M., Fontana, F., Lamotte, A., Scott, B., Muttillo, B., Berruti, G., Nenzioni, G., Tuffreau, A., 2020. Early Levallois core technology between marine isotope stage 12 and 9 in Western Europe. J. Hum. Evol. 139, 102735.
Monnier, J.-L., Ravon, A.-L., Hinguant, S., Hallégouët, B., Gaillard, C., Laforge, M., 2016. Menez-Dregan 1 (Plouhinec, Finistère, France): Un site d'habitat du Paléolithique inférieur en grotte marine. Stratigraphie, structures de combustion, industries riches en galets aménagés. L'Anthropologie 120, 237–262.
Moreno, D., Falguères, C., Pérez-González, A., Voinchet, P., Ghaleb, B., Despriée, J., Bahain, J.J., Sala, R., Carbonell, E., de Castro, J.M.B., Arsuaga, J.L., 2015. New radiometric dates on the lowest stratigraphical section (TD1 to TD6) of Gran Dolina site (Atapuerca, Spain). Quat. Geochronol. 30, 535–540.
Mounier, A., Marchal, F., Condemi, S., 2009. Is *Homo heidelbergensis* a distinct species? New insight on the Mauer mandible. J. Hum. Evol. 56, 219–246.
Muller, R.A., MacDonald, G.J., 1997. Glacial cycles and astronomical forcing. Science 277, 215–218.
Müller, W., Pasda, C., 2011. Site formation and faunal remains of the Middle Pleistocene site Bilzingsleben. Quartar 58, 1–27.
Ocobock, C., Lacy, S., Niclou, A., 2021. Between a rock and a cold place: Neanderthal biocultural cold adaptations. Evol. Anthropol. 30, 262–279.
Parfitt, S.A., 1998a. The interglacial mammalian fauna from Barnham. In: Ashton, N.M., Lewis, S.G., Parfitt, S.A. (Eds.), Excavations at the Lower Palaeolithic Site at East Farm, Barnham, Suffolk 1989–94. British Museum, London, pp. 111–147.
Parfitt, S.A., 1998b. Palaeoecological summary of Unit 5c. In: Ashton, N.M., Lewis, S.G., Parfitt, S.A. (Eds.), Excavations at the Lower Palaeolithic Site at East Farm, Barnham, Suffolk 1989–94. British Museum, London, pp. 167–172.
Parfitt, S.A., 1999. Mammalia. In: Roberts, M.B., Parfitt, S.A. (Eds.), Boxgrove: A Middle Pleistocene Hominid Site at Eartham Quarry, Boxgrove, West Sussex. English Heritage, London, pp. 197–290.
Parfitt, S.A., Roberts, M.B., 1999. Human modification of faunal remains. In: Roberts, M.B., Parfitt, S.A. (Eds.), Boxgrove: A Middle Pleistocene Hominid Site at Eartham Quarry, Boxgrove, West Sussex. English Heritage, London, pp. 398–419.
Parfitt, S.A., Ashton, N.M., Lewis, S.G., Abel, R.L., Coope, G.R., Field, M.H., Gale, R., Hoare, P.G., Larkin, N.R., Lewis, M.D., Karloukovski, V., Maher, B.A., Peglar, S.M., Preece, R.C., Whittaker, J.E., Stringer, C.B., 2010. Early Pleistocene human occupation at the edge of the boreal zone in northwest Europe. Nature 466, 229–233.
Pol, K., Debret, M., Masson-Delmotte, V., Capron, E., Cattani, O., Dreyfus, G., Falourd, S., Johnsen, S., Jouzel, J., Landais, A., 2011. Links between MIS 11 millennial to sub-millennial climate variability and long term trends as revealed by new high resolution EPICA Dome C deuterium data – a comparison with the Holocene. Clim. Past 7, 437–450.
Pope, M., Parfitt, S., Roberts, M.B., 2020. The Horse Butchery Site 2020: A High-Resolution Record of Lower Palaeolithic Hominin Behaviour at Boxgrove, UK. SpoilHeap Publications, London.
Preece, R., Parfitt, S., Bridgland, D., Lewis, S., Rowe, P., Atkinson, T., Candy, I., Debenham, N., Penkman, K., Rhodes, E., 2007. Terrestrial environments during MIS 11: Evidence from the Palaeolithic site at West Stow, Suffolk, UK. Quat. Sci. Rev. 26, 1236–1300.
Preece, R.C., Parfitt, S.A., Coope, G.R., Penkman, K.E.H., Ponel, P., Whittaker, J.E., 2009. Biostratigraphic and aminostratigraphic constraints on the age of the Middle Pleistocene glacial succession in north Norfolk, UK. J. Quat. Sci. 24, 557–580.
Prossinger, H., Seidler, H., Wicke, L., Weaver, D., Recheis, W., Stringer, C., Müller, G.B., 2003. Electronic removal of encrustations inside the Steinheim cranium reveals paranasal sinus features and deformations, and provides a revised endocranial volume estimate. Anat. Rec. 273, 132–142.
Rightmire, G.P., 1997. Deep roots for the Neanderthals. Nature 389, 917–918.
Rightmire, G.P., 1998. Human evolution in the Middle Pleistocene: The role of *Homo heidelbergensis*. Evol. Anthropol. 6, 218–227.
Rightmire, G.P., 2008. *Homo* in the Middle Pleistocene: Hypodigms, variation, and species recognition. Evol. Anthropol. 17, 8–21.
Roberts, M.B., 1999. Geological summary. In: Roberts, M.B., Parfitt, S.A. (Eds.), Boxgrove: A Middle Pleistocene Hominid Site at Eartham Quarry, Boxgrove, West Sussex. English Heritage, London, pp. 149–155.
Roberts, M.B., Parfitt, S.A., 1999. Boxgrove: A Middle Pleistocene hominid site at Eartham Quarry, Boxgrove, West Sussex. English Heritage, London.
Rodrigues, T., Voelker, A.H.L., Grimalt, J.O., Abrantes, F., Naughton, F., 2011. Iberian Margin sea surface temperature during MIS 15 to 9 (580–300 ka): Glacial suborbital variability versus interglacial stability. Paleoceanography 26, PA1204.
Rodríguez, J., Burjachs, F., Cuenca-Bescós, G., García, N., Van der Made, J., Pérez González, A., Blain, H.A., Expósito, I., López-García, J.M., García Antón, M., Allué, E., Cáceres, I., Huguet, R., Mosquera, M., Ollé, A., Rosell, J., Parés, J.M., Rodríguez, X.P., Díez, C., Rofes, J., Sala, R., Saladié, P., Vallverdú, J., Bennasar, M.L., Blasco, R., Bermúdez de Castro, J.M., Carbonell, E., 2011. One million years of cultural evolution in a stable environment at Atapuerca (Burgos, Spain). Quat. Sci. Rev. 30, 1396–1412.
Rodríguez, J., Willmes, C., Mateos, A., 2021. Shivering in the Pleistocene. Human adaptations to cold exposure in Western Europe from MIS 14 to MIS 11. J. Hum. Evol. 153, 102966.
Rodriguez-Hidalgo, A., Saladié, P., Olle, A., Arsuaga, J.L., de Castro, J.M.B., Carbonell, E., 2017. Human predatory behavior and the social implications of communal hunting based on evidence from the TD10.2 bison bone bed at Gran Dolina (Atapuerca, Spain). J. Hum. Evol. 105, 89–122.
Roebroeks, W., 2001. Hominid behaviour and the earliest occupation of Europe: An exploration. J. Hum. Evol. 41, 437–461.
Roebroeks, W., Villa, P., 2011. On the earliest evidence for habitual use of fire in Europe. Proc. Natl. Acad. Sci. USA 108, 5209–5214.
Roksandic, M., Radović, P., Lindal, J., 2018. Revising the hypodigm of *Homo heidelbergensis*: A view from the Eastern Mediterranean. Quat. Int. 466, 66–81.
Romanowska, I., 2012. Ex oriente lux: A re-evaluation of the Lower Palaeolithic of central and eastern Europe. In: Ruebens, K., Romanowska, I., Bynoe, R. (Eds.), Unravelling the Palaeolithic: 10 Years of Research at the Centre for the Archaeology of Human Origins. BAR, Oxford, pp. 1–12.
Rubio-Jara, S., Panera, J., 2019. Unravelling an essential archive for the European Pleistocene. The human occupation in the Manzanares valley (Madrid, Spain) throughout nearly 800,000 years. Quat. Int. 520, 5–22.
Rubio-Jara, S., Panera, J., Rodríguez-de-Tembleque, J., Santonja, M., Pérez-González, A., 2016. Large flake Acheulean in the middle of Tagus basin (Spain): Middle stretch of the river Tagus valley and lower stretches of the rivers Jarama and Manzanares valleys. Quat. Int. 411, 349–366.
Saladié, P., Rodríguez-Hidalgo, A., Marín, J., i Poch, J.V., Carbonell, E., 2018. The top of the Gran Dolina (Atapuerca, Spain) sequence: A zooarchaeological and occupational perspective. Quat. Sci. Rev. 195, 48–71.

Santonja, M., Villa, P., 2006. The Acheulian of Western Europe. In: Goren-Inbar, N., Sharon, G. (Eds.), Axe Age: Acheulian Tool-Making from Quarry to Discard. Equinox, London, pp. 429–478.
Schreve, D.C., 1996. The mammalian fauna from the Waechter excavations, Barnfield Pit, Swanscombe. In: Conway, B., McNabb, J., Ashton, N.M. (Eds.), Excavations at Barnfield Pit, Swanscombe, 1968-1972. British Museum Occasional Paper No. 94, London, pp. 149–162.
Schreve, D., Candy, I., 2010. Interglacial climates: Advances in our understanding of warm climate episodes. Prog. Phys. Geogr. 34, 845–856.
Sherriff, J.E., Schreve, D.C., Candy, I., Palmer, A.P., White, T.S., 2021. Environments of the climatic optimum of MIS 11 in Britain: Evidence from the tufa sequence at Hitchin, southeast England. J. Quat. Sci. 36, 508–525.
Singarayer, J.S., Valdes, P.J., 2010. High-latitude climate sensitivity to ice-sheet forcing over the last 120 kyr. Quat. Sci. Rev. 29, 43–55.
Singer, R., Wymer, J.J., Gladfelter, B.G., 1973. Excavation of the Clactonian industry at the Golf Course, Clacton-on-Sea, Essex. Proc. Prehist. Soc. 39, 6–74.
Singer, R., Gladfelter, B.G., Wymer, J.J., 1993. The Lower Palaeolithic site at Hoxne, England. Chicago University Press, Chicago.
Sloan, L.C., Rea, D.K., 1996. Atmospheric carbon dioxide and early Eocene climate: A general circulation modelling sensitivity study. Palaeogeogr. Palaeoclimatol. Palaeoecol. 119, 275–292.
Spahni, R., Chappellaz, J., Stocker, T.F., Loulergue, L., Hausammann, G., Kawamura, K., Flückiger, J., Schwander, J., Raynaud, D., Masson-Delmotte, V., 2005. Atmospheric methane and nitrous oxide of the late Pleistocene from Antarctic ice cores. Science 310, 1317–1321.
Stewart, J.R., Lister, A.M., Barnes, I., Dale, L., 2010. Refugia revisited: individualistic responses of species in space and time. Proc. Royal Soc. B 277, 661–671.
Stringer, C., 2012. The status of *Homo heidelbergensis* (Schoetensack 1908). Evol. Anthropol. 21, 101–107.
Stringer, C.B., Hublin, J.J., 1999. New age estimates for the Swanscombe hominid, and their significance for human evolution. J. Hum. Evol. 37, 873–877.
Szymanek, M., Julien, M.-A., 2018. Early and Middle Pleistocene climate-environment conditions in Central Europe and the hominin settlement record. Quat. Sci. Rev. 198, 56–75.
Thoma, A., 1972. Cranial capacity, taxonomical and phylogenetical status of Vértesszölös man. J. Hum. Evol. 1, 511–512.
Timmermann, A., Yun, K.S., Raia, P., Ruan, J., Mondanaro, A., Zeller, E., Zollikofer, C., Ponce de León, M., Lemmon, D., Willeit, M., Ganopolski, A., 2022. Climate effects on archaic human habitats and species successions. Nature 604, 495–501.
Tuffreau, A., Antoine, P., 1995. The earliest occupation of Europe: Continental northwestern Europe. In: Roebroeks, W., van Kolfschoten, T. (Eds.), The Earliest Occupation of Europe: Proceedings of the European Science Foundation Workshop at Tautavel (France), 1993. Leiden University Press, Leiden, pp. 147–163.
Turner, C., 1970. The Middle Pleistocene deposits at Marks Tey, Essex. Philos. Trans. R. Soc. Lond. B Biol. Sci. 257, 373–437.
Turner, E., 1999. Lithic artefacts and animal bones in floodplain deposits at Miesenheim I (Central Rhineland, Germany). In: Gaudzinski, S., Turner, E. (Eds.), The Role of Early Humans in the Accumulation of European Lower and Middle Palaeolithic Bone Assemblages. Habelt, Bonn, pp. 103–119.
Tye, G.J., Sherriff, J., Candy, I., Coxon, P., Palmer, A., McClymont, E.L., Schreve, D.C., 2016. The $\delta^{18}O$ stratigraphy of the Hoxnian lacustrine sequence at Marks Tey, Essex, UK: Implications for the climatic structure of MIS 11 in Britain. J. Quat. Sci. 31, 75–92.
Tzedakis, P.C., Hooghiemstra, H., Pälike, H., 2006. The last 1.35 million years at Tenaghi Philippon: Revised chronostratigraphy and long-term vegetation trends. Quat. Sci. Rev. 25, 3416–3430.
Villa, P., 1990. Torralba and Aridos: Elephant exploitation in Middle Pleistocene Spain. J. Hum. Evol. 19, 299–309.
White, M.J., 2000. The Clactonian question: On the interpretation of core-and-flake assemblages in the British Lower Palaeolithic. J. World Prehist. 14, 1–63.
White, M.J., 2006. Things to do in Doggerland when you're dead: Surviving OIS3 at the northwestern-most fringe of Middle Palaeolithic Europe. World Archaeol. 38, 547–575.
White, M., Ashton, N., 2003. Lower Palaeolithic core technology and the origins of the Levallois method in north-western Europe. Curr. Anthropol. 44, 598–609.
White, M.J., Pettitt, P.B., 2011. The British Late Middle Palaeolithic: An interpretative synthesis of Neanderthal occupation at the northwestern edge of the Pleistocene world. J. World Prehist. 24, 25–97.
White, T.S., Preece, R.C., Whittaker, J.E., 2013. Molluscan and ostracod successions from Dierden's Pit, Swanscombe: Insights into the fluvial history, sea-level record and human occupation of the Hoxnian Thames. Quat. Sci. Rev. 70, 73–90.
Whittow, J., 2000. The Penguin Dictionary of Physical Geography, 2nd edition. Penguin Books, London.
Woodward, J., 2014. The Ice Age: A Very Short Introduction. Oxford University Press, Oxford.
WorldClim, 2020. Global climate and weather data. https://www.worldclim.org/data/index.html. (Accessed 16 March 2022).
Wymer, J.J., 1999. The Lower Palaeolithic Occupation of Britain. Wessex Archaeology and English Heritage, Salisbury.
Wymer, J.J., Lewis, S.G., Bridgland, D.R., 1991. Warren Hill, Mildenhall, Suffolk (TL 744743). In: Lewis, S.G., Whiteman, C.A., Bridgland, D.R. (Eds.), Central East Anglia and the Fen Basin: Field Guide. Quat. Res. Association, London, pp. 50–58.
Zellweger, F., Braunisch, V., Morsdorf, F., Baltensweiler, A., Abegg, M., Roth, T., Bugmann, H., Bollmann, K., 2015. Disentangling the effects of climate, topography, soil and vegetation on stand-scale species richness in temperate forests. For. Ecol. Manag. 349, 36–44.